UNIVERSITY OF SOUTHAMPTON

Faculty of Earth and Life Sciences
School of Ocean and Earth Sciences

Beyond Global Mean Warming: Pathways Towards Multiple Climate Targets

DOI: 10.1002/0470841559.ch1

by

Sandy Avrutin

MMet

ORCiD: 0000-0002-3064-2712

A thesis for the degree of
Doctor of Philosophy

December 2023

University of Southampton

Abstract

Faculty of Earth and Life Sciences
School of Ocean and Earth Sciences

Doctor of Philosophy

Beyond Global Mean Warming: Pathways Towards Multiple Climate Targets

by Sandy Avrutin

Climate change is a defining issue of the 21st century, impacting weather patterns, sea levels, crop production, ecosystem function and human health. Currently the global aim to limit climate change is framed by an aim to limit warming, specifically by reducing anthropogenic CO_2 emissions because these are the main driver of warming. As such, remaining carbon budgets (RCBs) are defined by exploiting the near-linear relationship between cumulative CO_2 emissions and warming. This is arguably an incomplete solution. Firstly, although the relationship between warming and cumulative emissions is near-linear, there is uncertainty in the constant of proportionality. There are also aspects of climate change that are not necessarily addressed by limiting global mean warming. These include ocean acidification, which is caused by ocean absorption of CO_2 but not linked to warming, and sea level rise, which is caused by warming but has uncertainty and pathway dependence that is not addressed in policy that aims to limit only warming. This thesis explores how other impacts of climate change (beyond global mean warming) can be used to frame RCBs. This is done with a reduced-complexity Earth systems model with a semi-empirical method for calculating sea level rise. In Chapter 2, an RCB is defined using both warming and surface ocean acidification targets. In Chapter 3, the impact on uncertainty of allowing ice melt to vary nonlinearly with warming is explored. In Chapter 4, the model is used to quantify how much CO_2 must be removed from the atmosphere to reduce the commitment to sea level rise to zero. Using a reduced-complexity model is computationally cheap, so a large ensemble can be used to assess parametric (related to model parameters) uncertainty in climate projections. When warming and acidification are used together to frame an RCB, uncertainty in the RCB is reduced because the upper end of the uncertainty distribution is lowered. Uncertainty is increased by considering a nonlinear relationship between warming and ice melt, the level of carbon emissions we must remove from the atmosphere to prevent future sea level rise is better constrained than the most recent RCB estimate.

Contents

List of Figures

List of Tables

Declaration of Authorship

I declare that this thesis and the work presented in it is my own and has been generated by me as the result of my own original research.

I confirm that:

1. This work was done wholly or mainly while in candidature for a research degree at this University;
2. Where any part of this thesis has previously been submitted for a degree or any other qualification at this University or any other institution, this has been clearly stated;
3. Where I have consulted the published work of others, this is always clearly attributed;
4. Where I have quoted from the work of others, the source is always given. With the exception of such quotations, this thesis is entirely my own work;
5. I have acknowledged all main sources of help;
6. Where the thesis is based on work done by myself jointly with others, I have made clear exactly what was done by others and what I have contributed myself;
7. Parts of this work have been published as: S. Avrutin, P. Goodwin, and T.H.G. Ezard. Assessing the remaining carbon budget through the lens of policy-driven acidification and temperature targets. *Climatic Change*, 2023, in press

Signed:..... Date:.....

Acknowledgements

Thanks firstly to Dr Philip Goodwin, because without years of guidance and advice (and the WASP model in the first place) none of this would have been nearly as easy or fun. Also to Profs Ivan D Haigh, Robert J Nicholls and Thomas H G Ezard, for interesting and motivating discussions. All of you helped me to become a scientist. Also also to my examiners, Profs Gavin Foster and Jason Lowe, for reading this whole thing (sorry/you're welcome), and to Prof. Paul Wilson for making sure this thesis was always going to happen.

Next to a non-exhaustive and not prioritised list of people: Javi, Rhi, Pablo, Nathan, Estacey, Kaveri, Deborah, Spencer, Lewis, Matina, Joe, Jon, Ellen, Tasha and anyone else I've ever had lunch with at NOC. All of you helped me to become a human.

To my family.

Especially my dad, who spent 3 years asking if I'd published my first chapter yet; my mum, who ignited my interest in physics (and her finger) with a concave mirror; and my brother, who reminds me that the whole world can be home

Chapter 1

Introduction

1.1 Climate Change: A Global Problem

Climate change is a defining issue of the 21st century which causes damage to ecosystems, reduces habitable areas (including those habitable by humans) and exacerbates inequality.

In 2022, global carbon concentration reached 417.2ppm: almost double the preindustrial concentration of 278ppm (Friedlingstein et al. (2022)). This acts to warm the planet via the greenhouse effect. Although there is non-CO_2 related radiative forcing which also contributes to warming, the biggest single contributor to the increase in radiative forcing is CO_2, so the focus of this thesis is CO_2 emissions. Global surface air temperature (GMST) has increased by a median value 1.09°C, with a likely (66%) range of 0.95 to 1.20 °C since the preindustrial period (1850-1900) (Gulev et al. (2021)). This warming has impacted climate modes and therefore dominant weather patterns, increasing the likelihood of extreme hot and cold events. The warming atmosphere and oceans is causing glaciers, ice caps and ice sheets to melt. Melting ice and thermal expansion caused by increasing global mean temperatures has been causing sea level to rise at a faster rate than at any time over the past three millenia, leading to a likely range of sea-level rise of 0.15 to 0.25m between 1901 and 2018 (Fox-Kemper et al. (2021)). Rising seas contribute to, and are expected to continue to contribute to, increased flood risk, salinisation of groundwater and erosion of coastlines. This has severe implications for coastal ecosystems, as well as coastal populations. The impact of this will be felt worldwide, as global population and development is denser on coastlines (Neumann et al. (2015)).

sea-level rise is one contributor to coastal flood events, alongside tides, storms and storm surges, and wave set-up. Although relative sea-level rise (the changing position of the sea relative to the coast) plays more of a direct role than global mean sea-level

rise and includes climate change-independent factors such as land subsidence, the two are not completely unrelated. As global mean sea-level rises, its contribution towards coastal flooding will increase (e.g. Hermans et al. (2023)) putting large populations at risk, with 250 million people estimated to be living on land below annual flood levels, and 1 billion less than 10m above high tide lines (Kulp and Strauss (2019)). Studies assessing the impacts of historical sea-level rise are low in number due to a lack of relevant datasets, but Treu et al. (2023) have begun to address this gap and facilitate impact attribution studies by creating a reconstruction of hourly and monthly coastal water levels, and a corresponding dataset with the trend in long-term sea level removed. The expected impacts as sea levels continue to rise have been examined in more detail. Kirezci et al. (2023) estimated that by 2100 following RCP8.5, 146 million people may be impacted by flooding annually (up from 34 million in 2015) if no adaptation measures are put in place. If adaptation measures are increased at a rate commensurate with the rate of sea-level rise, this number could be reduced to 119 million. In terms of the economic damage this flooding causes, they estimated annual damage of 2.9% of GDP with no adaptation, and 1.1% with adaptation that keeps up with sea level change (in both cases, with sea-level rise following SSP3-8.5). In both cases, this is an increase from 0.3% of GDP today. Although this is a relatively small percentage, it is worth noting that because this is damage from coastal flooding, the cost will be borne by countries with (longer) coastlines, and disproportionately by countries without the resources to build flood defences. The increase in population at risk from rising seas will in turn give rise to changing migration patterns as coastal areas become less dependable places to live.

Separate to warming, the absorption of carbon dioxide from the atmosphere into the ocean causes ocean acidification. Since the preindustrial era, global mean ocean pH has decreased by 0.11 units (as of 2000), and is lower than it has been over the past 25k years (Gulev et al. (2021)). The latest IPCC report stated that surface ocean pH has been declining at a very likely (95% confidence) rate of 0.016 to 0.020 per decade in the subtropics and 0.002 to 0.026 per decade in subpolar and polar zones since the 1980s (Canadell et al. (2021)). By 2100, global pH is projected to decrease further by 0.3-0.4 units following SSP585 (low mitigation - Kwiatkowski et al. (2020)).

Ocean acidification is caused by gas exchange at the surface, but IPCC AR6 states with high confidence that CO_2 absorbed by the upper ocean is being ventilated into the interior (Canadell et al. (2021)). The impacts of acidification on species and ecosystems are therefore being felt throughout the ocean column. Acidification threatens organisms both through disruption to metabolic physiology, and through reducing the saturation state of calcium carbonate, which modulates the ability of calcifying organisms to grow. In combination with warming, acidification notably threatens corals (especially warm-water corals) and the species and ecosystems dependent on them. This has an important effect on marine ecology, as Fisher et al. (2015) estimate

that tropical corals provide a habitat for at least 25% of marine species. Cornwall et al. (2021) estimated that globally, by 2100, no reefs will be accreting carbonate at a rate matching sea-level rise following a partially mitigated RCP4.5 scenario, or the low mitigation RCP8.5 scenario (while RCP8.5 is not considered a likely future scenario, its intended use was to be able to explore a low-likelihood, high-impact scenario (Riahi et al. (2011))). This will dangerously limit their ability to photosynthesise, because light attenuates through water. Although they found this decline in accretion rate was mainly driven by bleaching events, already damaged corals (due to prolonged heat or acidification) were found to be more sensitive. Damage to coral reefs will have knock-on effects on economies and livelihoods; corals provide billions of dollars of goods and services (Burke et al. (2011), which mainly benefit developing countries Moberg and Folke (1999). This means the impacts of ocean acidification may contribute towards increasing global inequity.

1.2 Global Mean Warming Targets: an Incomplete Solution

1.2.1 Global Mean Warming as a Climate Target

In light of the urgent existential threat posed by a changing climate, global scale efforts to mitigate greenhouse gas emissions are taking place. The current focus in political climate change mitigation discourse is limiting warming to well below 2°C, and as close as possible to 1.5°C. These warming targets have been discussed widely enough that they are generally accepted to be recommended by "science". However, when the target was agreed upon by the international community at the 2009 climate conference in Copenhagen, no research had been published with the explicit aim of quantifying that 2°C represents a meaningful limit in the climate system, or is a safe amount of warming (Knutti et al. (2016)). Although explicit research had not been conducted in the context of recommending 2°C as a meaningful climate target, 2°C has existed in climate science literature since the 1970s (Gao et al. (2017)). Early estimates of the equilibrium climate sensitivity (the equilibrium response to a doubling in atmospheric CO_2) were 2°C (e.g. Manabe and Wetherald (1967)), and 2°C or a doubling of atmospheric CO_2 was subsequently used in cost-benefit analyses (e.g. Nordhaus (1977); Nordhaus (1991)). The first mention of 2°C as a climate target was by the European Union in 1996, although there was no reason provided for this choice of target (Gao et al. (2017)); Cointe et al. (2011) maintain that there is no clear origin for 2°C to have been employed as a target. The introduction of 1.5°C to climate discourse was relatively quicker, and the additional target was ratified in 2015 at COP21 (although it had existed in discourse since COP15 in 2009). The main proponents of this addition were representatives from Small Island Developing States at risk of serious impacts from sea-level rise, who pushed for more stringent and effective

climate policy (Ourbak and Magnan (2018)). This target originated purely on the political side; the impacts of, and potential pathways towards, 1.5°C were unexplored in a scientific context. Research into the 1.5°C target was sparked in response to the target being ratified (Cointe and Guillemot (2023)).

One important question following the introduction of this new warming target was whether it actually constituted an improvement on the existing 2°C goal - that is, are the climate impacts associated with 1.5°C any less than those associated with 2°C. Despite their differing, obscure and somewhat arbitrary origins, these two targets have since been found to represent distinct impacts on the climate system and human health. In terms of warming, an increase in global mean temperature of 1.5°C leads to a climate state consistent with the upper bound of modern day natural variability, whereas 2°C marks a shift in regime (Schleussner et al. (2016)). This line of research was complemented by examining the observational record, where differences in hot and cold extremes have been found between the 1960-1979 and 1991-2010 periods, the difference in average temperature of which was just about 0.5°C (Schleussner et al. (2017)). The rate of sea-level rise is also impacted, with a 30% reduction in the median rate of sea-level rise at the end of the century between a 2°C trajectory and a 1.5°C trajectory (Schleussner et al. (2016)). The difference in absolute sea-level rise between the two targets by 2150 avoids inundation of land currently home to around 5 million people (Rasmussen et al. (2018)), including 60,000 in small island developing states. The difference in ecological impacts of acidification are more difficult to define, because although it is possible to distinguish the level of ocean acidification associated with each warming target (see Figure 2.1), separating the impacts of acidification and warming is difficult (Hoegh-Guldberg et al. (2018)).

A second question that arose in the wake of 1.5°C being introduced as a target was whether the carbon emissions pathway required to reach this target was distinct from established pathways towards 2°C. It is not a given that the pathways towards distinct warming targets are also distinct, due to the uncertain warming response to emissions: CMIP6 projections of warming following SSPs 126, 245 and 370 overlap significantly in the mid-term (c2050), and are not fully distinct even by the end of the century (Lee et al. (2021)). However, the two targets are separated enough that remaining carbon budgets towards the 1.5°C and 2°C targets have not been found to overlap. Goodwin et al. (2018a) found the likely range (17-83%) for the remaining carbon budgets to be 195-205 PgC for 1.5°C, and 395-405PgC for 2°C, and Goodwin et al. (2018b) presented carbon emissions pathways towards each target with fully distinct likely ranges after 2050.

Perhaps ironically, considering how central the 1.5°C target is in climate science and climate change discourse, it is increasingly unlikely that this warming target will be met. The gap between current intention and what is necessary to limit warming to 1.5°C is too large; the gap between intention and action is just as notable. The idea that

1.5°C may be overly optimistic as a climate target prompts consideration as to whether there are other targets that may prevent damage in the long term, that are still achievable by feasible action in the short to medium term. For example, Li. et al (2020) found that using sea-level rise as a climate target, rather than the amount of warming consistent with that amount of sea-level rise, leads to a less stringent amount of necessary emissions reductions. This is a particularly salient thought when it comes to the 1.5°C target, because its conception was fuelled by the need to avoid the impacts of sea-level rise associated with 2°C.

Whether the targets of 1.5°C and 2°C are feasible or not, global mean warming is now embedded into the political and public consciousness as a definitive metric of climate change. Indeed, it is useful in that context because it scales linearly with cumulative emissions (e.g. Allen et al. (2009)) so translates well into emissions targets. However in a scientific context, it seems more arbitrary and incomplete. Global mean warming is difficult to measure and has uncertain real-world implications at any specific location on Earth due to the multiple ways that the same level of global mean warming can be realised (Seneviratne et al. (2018)). Discussing global mean warming (or any other global mean quantity) in a meaningful sense also requires common understanding of the timeframe over which we must average data in order to avoid natural climate variability obscuring anthropogenic climate change signals. It also requires common understanding of a reference period from which warming (or any quantity) is measured. Further, although global mean warming has been shown to scale linearly with cumulative emissions, the magnitude of this scaling is not well constrained - so the associated emissions target is subject to uncertainty. Efforts have been made in other studies to consider emissions targets that are consistent with more meaningful climate metrics, such as regional temperature and precipitation extremes (Seneviratne et al. (2016)). The benefit of considering regional extremes is clear - they do not require an established baseline, and are meaningful metrics for each region being considered. They can also be scaled with global mean warming and therefore with cumulative emissions. The result of this method was a lower amount of allowable emissions, implying that the emissions targets associated with just global mean warming may be a 'necessary but not sufficient' condition to avoid unmanageable climate change on a regional basis.

This result highlights a further risk of considering just global mean warming as the standard metric of climate change, and therefore the quantity we must aim to limit: keeping global mean warming to a predefined minimum is not necessarily enough to prevent dangerous change to the climate system. The UNFCCC definition of the climate system incorporates the atmosphere, hydrosphere, cryosphere, biosphere, and all its interactions. Keeping global mean warming to 1.5°C does not necessarily mean that all of these elements are protected from dangerous change. This is partly because of the uncertainty in the relationship between cumulative emissions and warming,

which means that processes like ocean acidification, which are related to emissions but not warming, are not intentionally addressed. We must also consider impacts of warming that are pathway dependent and/or subject to lag, like sea-level rise. There are many pathways and many timeframes for limiting warming to 1.5 or 2°C, and not all of these provide adequate surety that sea-level rise will remain manageable. Notably, most pathways towards the 1.5°C target reach the target by overshooting and then relying on negative emissions to return to the acceptable amount of warming. Overshoot has implications for parts of the climate system that do not exhibit the same path independence as global mean warming, such as sea level (e.g. Mengel et al. (2018)) and, especially for high levels of overshoot, the carbon cycle (Tokarska et al. (2019)).

1.2.2 Ocean Acidification is Not Necessarily Addressed by Limiting Warming

The ocean is a significant carbon sink in the climate system. As of 2019, it was estimated that it was absorbing between 16 and 30% of yearly anthropogenic carbon emissions (Friedlingstein et al. (2019)). Although this is beneficial in terms of preventing the global warming and pollution issues that would arise from all carbon emissions remaining in the atmosphere, it presents a concurrent problem to global warming that is receiving less attention in the media and in policy. CO_2 absorbed by the ocean leads to ocean acidification, which threatens ocean biodiversity and the human systems that are dependent on this to thrive.

Once CO_2 is dissolved in seawater, it reacts with the water to form carbonic acid H_2CO_3:

$$CO_2(aq) + H_2O \rightleftharpoons H_2CO_3$$

And dissociates into bicarbonate HCO_3^-:

$$H_2CO_3 \rightleftharpoons HCO_3^- + H^+$$

And carbonate CO_3^{2-}:

$$HCO_3^- + H_2O \rightleftharpoons CO_3^{2-} + H^+$$

The effect of adding extra CO_2 to seawater is to increase the concentration of H^+ (thus decreasing pH, which is $-log([H^+])$), H_2CO_3 and HCO_3^-, and to decrease the concentration of CO_3^{2-} (Fabry et al. (2008); Kleypas et al. (1999)). The reduced concentration of CO_3^{2-}, in turn, reduces the levels of carbonate ions, which are necessary for calcifying organisms such as corals, molluscs and crustaceans. The main modulator of the impacts felt by calcifying organisms is the saturation state (Ω) of

calcium carbonate ($CaCO_3$), which is given by

$$\Omega = \frac{[Ca^{2+}][CO_3^{2-}]}{K^*_{sp}}$$

Where K^*_{sp} is the solubility product for aragonite or calcite. In order for most calcifying organisms to grow skeletons and shells, they require surrounding waters to be saturated with respect to calcitic or aragonitic $CaCO_3$: Ω_{arag}, Ω_{calc} >1.0. Kleypas et al. (1999) found that corals require $\Omega_{arag} > 3.4$ to grow.

The key point to be taken from the fact that acidification is linked to carbon rather than to warming, is that limiting warming is necessary but not sufficient to limit acidification. This is due to uncertainty in the transient climate sensitivity to emissions (TCRE), which has a likely range of 1.0 to 2.3 K EgC^{-1} in IPCC AR6, 2021 (Forster et al. (2021)). This means that limiting warming to 1.5°C is consistent with a total allowable emissions limit ranging from 650 to 1500 PgC (since preindustrial), which could lead to a range of acidification or around 0.02pH units (see Figure 2.1), and this range increases for larger amounts of warming.

1.2.3 sea-level rise is Not Necessarily Addressed by Limiting Warming

Global mean sea-level rise has three main contributors: thermal expansion, ice melt and landwater storage. The single biggest source between 1901 and 2018 is glacial ice melt, with a 67.2 (likely range 41.8 to 92.6) mm contribution. Other land ice contributions (the Greenland and Antarctic ice sheets respectively) stand at 40.0 (27.2 to 3.5) mm and 6.7 (-4.0 to 17.4) mm respectively (Fox-Kemper et al. (2021)) (see Figure 1.1). The contribution from Antarctica is much lower because warming in the southern high latitudes is so far slower than in the northern high latitudes, and its contribution may even be negative due to the contribution of increased snowfall to the surface mass balance as humidity in Antarctica increases (Edwards et al. (2021)). The next biggest contributor to sea-level rise after glacial melt is thermal expansion. Between 1901 and 2018, thermal expansion contributed 63.2 (47.0-79.4) mm to global mean sea-level rise (Fox-Kemper et al. (2021)). The final contributor to global mean sea level change is changing land-water storage, which contributed -12.9 (-45.8 to 20.0) mm between 1901 and 2018. This is treated as scenario-independent in projections of sea-level rise in IPCC reports (most recently in AR6, Fox-Kemper et al. (2021)). While some of the contributors to land-water storage are independent of the radiative forcing component of scenarios (for example changing land use and populations), this assumption is less realistic when considering shared socioeconomic pathways (SSPs) which are not just pathways of radiative forcing, but include a societal component that accounts for changing land use and population dynamics.

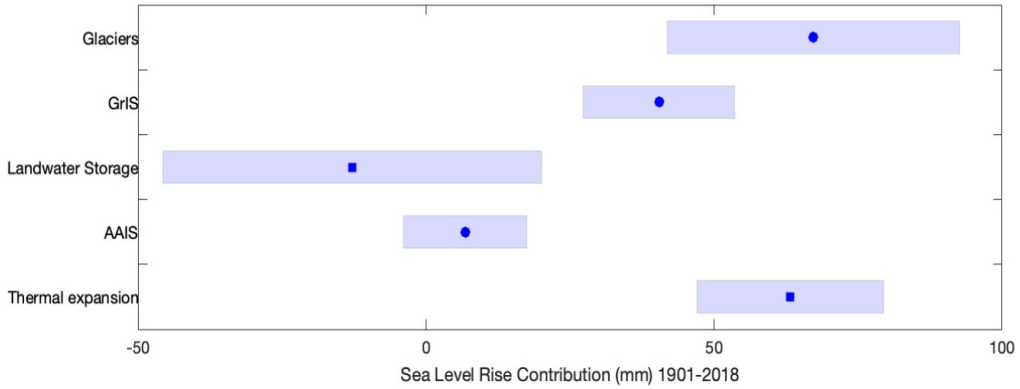

FIGURE 1.1: Observed contributions of individual sea-level rise contributors from IPCC AR6 (Fox-Kemper et al. (2021)) Shaded box = 5-95% range, points in the middle mark the median. Peripheral glacier contributions are included in the respective ice sheet contributions.

Beyond 2100, the contribution of Antarctica is expected to overtake both glaciers and the Greenland ice sheet as self-sustaining feedbacks like marine ice sheet instability (MISI, which describes a self-sustaining retreat of the grounding line of an ice sheet along a retrograde slope until or unless the grounding line is re-pinned by some change in the topography) begin to take place, and as the contribution from glaciers plateaus as they start to disappear. However, because the nature of these feedbacks and other variables that impact ice melt are uncertain and difficult to model, the future contribution of Antarctica is a source of significant uncertainty in sea-level rise projections. The uncertainty of Antarctica, and ice melt in general, will be revisited in Section 1.3.2.1 and in more detail in Chapter 3.

Unlike warming, sea-level rise is dependent on the pathway of emissions. Different emissions pathways leading to the same cumulative emissions by the end of a time period will have different impacts on sea level; unlike warming, which simply scales to cumulative emissions (Matthews et al. (2009)). The pathway dependence of sea-level rise also impacts the rate of sea-level rise at the end of a given emissions pathway (Li et al. (2020)), which is arguably just as important a consideration as absolute sea-level rise, because it dictates the urgency of any given adaptation plan. Li et al. (2020) described the impact on sea-level rise of two different emissions pathways - one with a higher rate followed by a slower rate, one where emissions start slow and speed up. The first pathway would result in a larger absolute sea-level rise by the end of the timeframe being considered, and the latter would result in less sea-level rise but a faster rate to contend with in the future. Given that the rate of sea-level rise impacts the ease of adaptation, the latter pathway would likely be associated with higher adaptation costs down the line. The difference in sea level stories here, and the resultant impact on economy, is noticeable - however both of these pathways lead to the same cumulative emissions and therefore the same warming. This demonstrates

how warming targets are not necessarily enough to keep sea-level rise at a manageable magnitude and rate.

Compounding the issue of sea-level rise is the fact that its contributing processes are subject to time lag. Limiting, and eventually ceasing, warming and emissions is not sufficient to limit sea-level rise, which will continue for millennia and continue to present problems long after warming is (ideally) no longer a threat. Nauels et al. (2019) estimated that warming up to 2016 has already committed the world to 0.7-1.1m of sea-level rise by 2300, and the emissions pledges made in the wake of the Paris Agreement increase this commitment to 0.8-1.4m. The timescales of sea level equilibration mean that even this estimate does not tell the whole story, as sea level will continue to rise far beyond 2300. Levermann et al. (2013) calculated a millennial sensitivity of sea-level rise to warming of around 2.3m/K. Taking this value and a current global mean warming of 1.1°C (Gulev et al. (2021)), this commits us to a millennial-scale commitment of 2.53m of sea-level rise.

1.3 Modelling for Climate Targets

1.3.1 Climate Sensitivity and Reduced Complexity Modelling

Climate models need to be able to simulate the climate response to emissions. There are different metrics to quantify the sensitivity of warming to emissions. The Equilibrium Climate Sensitivity (ECS) is defined as the final amount of warming once the Earth's energy budget has stabilised following an abrupt doubling of CO_2, assuming no feedbacks associated with ice sheets. The Transient Climate Sensitivity (TCR) is the amount of warming at the point when atmospheric CO_2 is doubled following a 1% increase per year trajectory. The Transient Climate Response to Emissions (TCRE) is the ratio total warming to cumulative CO_2 emissions. To quantify the ECS or TCR, there are processes on multiple spatial and temporal scales that must be accounted for. Some of these can be directly resolved in complex (process based) models, however many must be parameterised. Because process-based models are computationally expensive, each parameterised process can only be assigned order(1) parameter value, which is tuned until the model is able to represent a functional Earth system. However the Earth system is driven by many processes acting on a large range of spatial and temporal scales, so projections of the future remain unresolved and are subject to uncertainty. This, in turn, leads to uncertainty in pathways towards warming targets.

Estimates of TCR and ECS can be constrained further by combining process understanding from models, historical observations, emergent constraints and (in the case of ECS) evidence from palaeoclimate records (Forster et al. (2021)). Due to the

definition of the TCR (that it is transient) there is less palaeo-evidence available to constrain estimates, because the palaeoclimate record is too low-resolution to examine transient climate change. Sherwood et al. (2020) found that by combining these lines of evidence, the ECS can be constrained to a likely (66%) range of 2.6-3.9°C. The IPCC AR6 combined assessment of climate sensitivity from the above lines of evidence placed the likely range of ECS at 2.5 to 4.0°C, and the likely range of TCR at 1.4 to 2.2°C (Forster et al. (2021)).

Reduced-complexity models (or RCMs) can be used to avoid the issue of computational expense in climate modelling. Often, the reduced complexity of RCMs stems from outputting globally and annually averaged data (Nicholls et al. (2021)). While this provides a more spatially and temporally limited outlook on changing climate, the computational cheapness of this method means that RCMs can be used to assess uncertainties at more points in the cause-effect chain than more complex Earth-system models (ESMs). As such, RCMs can be used to embrace and explore the issue of uncertainty rather than attempting to reduce it, and present a complementary method to complex ESMs. This allows for a better impression of how uncertainty impacts our understanding of how to go about mitigating climate change by reducing emissions. Nicholls et al. (2021) conducted a model intercomparison project (RCMIP, in this case phase 2) assessing the extent to which reduced-complexity models are able to probabilistically reproduce specific earth system response metrics from specialised studies, including the ECS, TCR and TCRE. Table 1.1 shows the percentage difference between the magnitude of the multi-model median for these three metrics of all models used in the study, and the data used as the benchmark. For most of the metrics assessed in the study (including ones not shown on Table 1.1), they found that the RCMs were able to capture the median better than the likely (33-66%) and the very likely (5-95%) ranges, apart from the TCR where the upper ranges are also well captured, and the TCRE where the lower ranges are captured better. The discrepancies in skill in capturing each metric considered in this table arose from the different nature of the studies used as benchmark: Sherwood et al. (2020) used multiple lines of evidence for their assessment of ECS, Tokarska et al. (2020) used CMIP6 ESMs constrained with observations of past warming for their assessment of TCR, and Arora et al. (2020) used unconstrained CMIP6 ESMs.

		Multimodel Median of Magnitude of Relative Differences				
Assessed Metric	Study as Benchmark	5%	17%	50%	83%	95%
ECS	Sherwood et al. (2020)	16%	15%	12%	14%	20%
TCR	Tokarska et al. (2020)	38%	18%	7%	4%	7%
TCRE	Arora et al. (2020)	9%	11%	20%	19%	20%

TABLE 1.1: The percentage difference between the magnitude of the multi-model median for these three metrics of all models used by Nicholls et al. (2021), and the data used as the benchmark

Statistical emulators are another computationally cheap method to explore uncertainty in climate. The idea of a statistical emulator is to create a statistical relationship between the inputs of a model (e.g. carbon concentration or warming) and its outputs. They do this by creating a prior ensemble of simulations of the Earth system, with parameter values that are randomly selected from a prior distribution of possible values. The simulations that are able to recreate the constraining data are then selected for the posterior distribution, which is used for analysis. This method means that statistical emulators are not physically motivated and do not resolve individual processes like carbon cycling, meaning they are computationally cheap; so the use of statistical emulators to explore climate sensitivity to forcing allows further exploration of the parameter space than process-based models. However, the reduced complexity of statistical emulators mean that they tend to represent a constant climate state, which means that their estimates of climate sensitivity (or other quantities) are better interpreted as a measure of the historical period than a true estimate of the state of the climate (Forster et al. 2021). Statistical emulators have also been used to constrain the ECS and TCR, although they have been found to be sensitive to the choice of constraining dataset and the prior distribution of parameters (Forster et al. (2021), Lewis (2013)). The semi-empirical method of modelling climate is similar in principle to emulators, but rather than constraining a relationship between force and effect with a more complex model, semi-empirical models are calibrated using observational data. In practice, 'emulator' is often used to describe any reduced complexity and/or non-physical models, regardless of whether they are calibrated using model outputs or observational data.

1.3.2 sea-level rise as a Potential Climate Target

1.3.2.1 Uncertainty in Understanding and Projections

A large contributor to uncertainty in projections of future global mean sea-level rise is the contribution of land ice, especially the Antarctic and Greenland ice sheets (AIS and GrIS) which act on longer timescales than glaciers and ice caps.

Mass loss from the AIS is dominated by dynamic thinning (the acceleration of glacier flow away from the centre of the ice sheet), especially around the West Antarctic Ice Sheet (WAIS). The dominant cause of this is the loss of buttressing from ice shelves (Oppenheimer et al. (2019)) which provide support to grounded ice but do not contribute to sea-level rise because they are already floating. Because the main cause of dynamic thinning is the loss of support from floating ice shelves which is caused by basal melt, mass loss is modulated by ocean heat content. This is in turn modulated by ENSO patterns (Cai et al. (2023)) as well as being subject to the long-term signal of climate change. For example, Jacobs et al. (2011) found that deepwater temperatures

in Pine Island had increased between the years 1994 and 2009, and stronger circulation patterns led to increase ice melt, leading to a cavity in the Pine Island Glacier ice shelf that allowed the warming deepwater to reach the grounding line of the ice sheet. Dutrieux et al. (2014) found that variations in the oceanic melting of Pine Island Glacier could be partly attributed to atmospheric forcing, particularly in 2012 due to a strong La Nina event. The size and relative remoteness of the AIS mean that so far it has reacted slowly to warming and its contribution to sea-level rise has remained small, although it has the potential to contribute far more to sea-level rise as warming continues. However, the future of the AIS contribution to sea-level rise remains deeply uncertain (Fox-Kemper et al. (2021)).

One significant reason for deep uncertainty is related to marine ice sheet instability (MISI). Bulthuis et al. (2019) made a probabilistic assessment of different uncertainties the impact projections of AIS melt, and found that the sensitivity of projections to parametric uncertainty (uncertainty related to model parameterisations) increases as the atmosphere and oceans continue to warm. They found MISI to be the most significant controlling factor of the AIS contribution to sea-level rise, especially from the WAIS which is more sensitive. The onset of MISI was found to be avoided in RCP2.6, unavoidable in RCP8.5, and subject to parametric uncertainty in RCPs 4.5 and 6.0. Robel et al. (2019) examined the impact of MISI on uncertainty in projected sea-level rise, and found that it causes an upward skew in the severity of projections - faster rates of sea-level rise were more likely than slower rates with MISI accounted for, and the distribution of rate of rise was more symmetrical when MISI is not a significant contributor.

The Pine Island Glacier and the Thwaites Glacier are believed to be vulnerable to MISI-like retreat. Favier et al. (2014) projected a 3.5-10.0mm contribution to eustatic sea level over the next 20 years from Pine Island Glacier, and Rignot et al. (2014) noted a 31 km retreat of the glacier at its centre with no major topography that would prevent further retreat of the grounding line. Although Rignot et al. (2014) found retreat of the Thwaites glacier to be more spatially varied, they found that the grounding line is retreating along a consistently retrograde slope. On top of this, buttressing from ice shelves is also unlikely (Parizek et al. (2013)). Ritz et al. (2015) examined the potential sea-level rise from Antarctica by constraining a process-based model using observations of melt from the entire Amundsen Sea Embayment (which covers both the Thwaites and the Pine Island Glacier, among others). They found that, in an ensemble of simulations where melt from the Amundsen Sea Embayment was accurately recreated, the sea-level rise contribution from Antarctica was up to 30 cm by 2100 and 72 cm by 2200 (95%). Although there is observational evidence of rapid retreat of susceptible glaciers, whether or not MISI is currently occurring is difficult to ascertain because it requires time-consuming modelling experiments (e.g. Garbe et al. (2020)), and no conclusive results have been reached (Rosier et al. (2021)).

Under low warming scenarios and in the near term, the contribution from the Antarctic ice melt is largely expected to come from the WAIS. Only under high warming is the East Antarctic Ice Sheet (EAIS) contribution expected to become larger (Bamber et al. (2022) - see Figure 1.2 adapted from their paper). Grinsted et al. (2022) calculated the transient sea level sensitivity for the WAIS and EAIS (TSLS, defined as the ratio of sea level rate in m/century to century-averaged warming) and found that there was no clear relationship for the WAIS, and a small negative relationship for the EAIS over the 21st century under any scenario. The constant transient sensitivity across scenarios for the WAIS implies that no thresholds have been crossed, indicating that no MISI-like behaviour is caused before 2100. The slightly negative relationship for the EAIS implies that change is largely dominated by surface mass balance, which increases due to increased precipitation caused by warmer (and therefore wetter) atmospheric conditions. Defining a TSLS in this way is also useful for comparison of model outputs and data to test the ability of models to represent the Earth system, and calculating a TSLS based on structured expert judgement can provide insight into the mismatch between common understanding of the system versus the ability to model it. The implications of this will be discussed further in Chapter 3.

Another, more controversial source of uncertainty in projections of SLR from Antarctica is Marine Ice Cliff Instability (MICI) which describes the brittle fracture of ice cliffs over a critical height of 90m (Bassis and Walker (2012); Clerc et al. (2019)). This has been found to contribute to deep uncertainty in ice melt projections from Antarctica (Li et al. (2023); DeConto and Pollard (2016)). However, there is no direct evidence of MICI occurring, other than a lack of cliff faces over the critical height of 90m (Bassis and Walker (2012)). Attempts to model palaeo-sea level with and without MICI have yielded mixed results, with DeConto and Pollard (2016) finding they are able to simulate Pliocene and Last Interglacial SLR with MICI included in their model setup, but Edwards et al. (2019) emulating the model of DeConto and Pollard and finding that MICI did not necessarily have to be included to be able to recreate past SLR. Li et al. (2023) found that structural differences in the climate-ocean models that are used to force ice sheet models can cause a wide spread in the equilibrium state of the AIS, which impacts whether or not MICI occurs. This means that there is deep uncertainty regarding whether MICI has occurred, whether it will occur on human timescales, and how much more sea-level rise it will cause.

The uncertainty in the future land ice contribution to SLR, and the role the AIS plays in this, was examined by Edwards et al. (2021), who found that for a middle of the road SSP scenario such as SSP 245, the land-ice contribution to sea level ranged by around 25 cm, or up to 40 cm in a risk-averse model configuration (one with a more pessimistic set of assumptions regarding ice melt from Antarctica). The difference caused by making the standard versus risk-averse assumptions was impactful enough that the high-end scenario in the standard projections and the low-end scenario in the

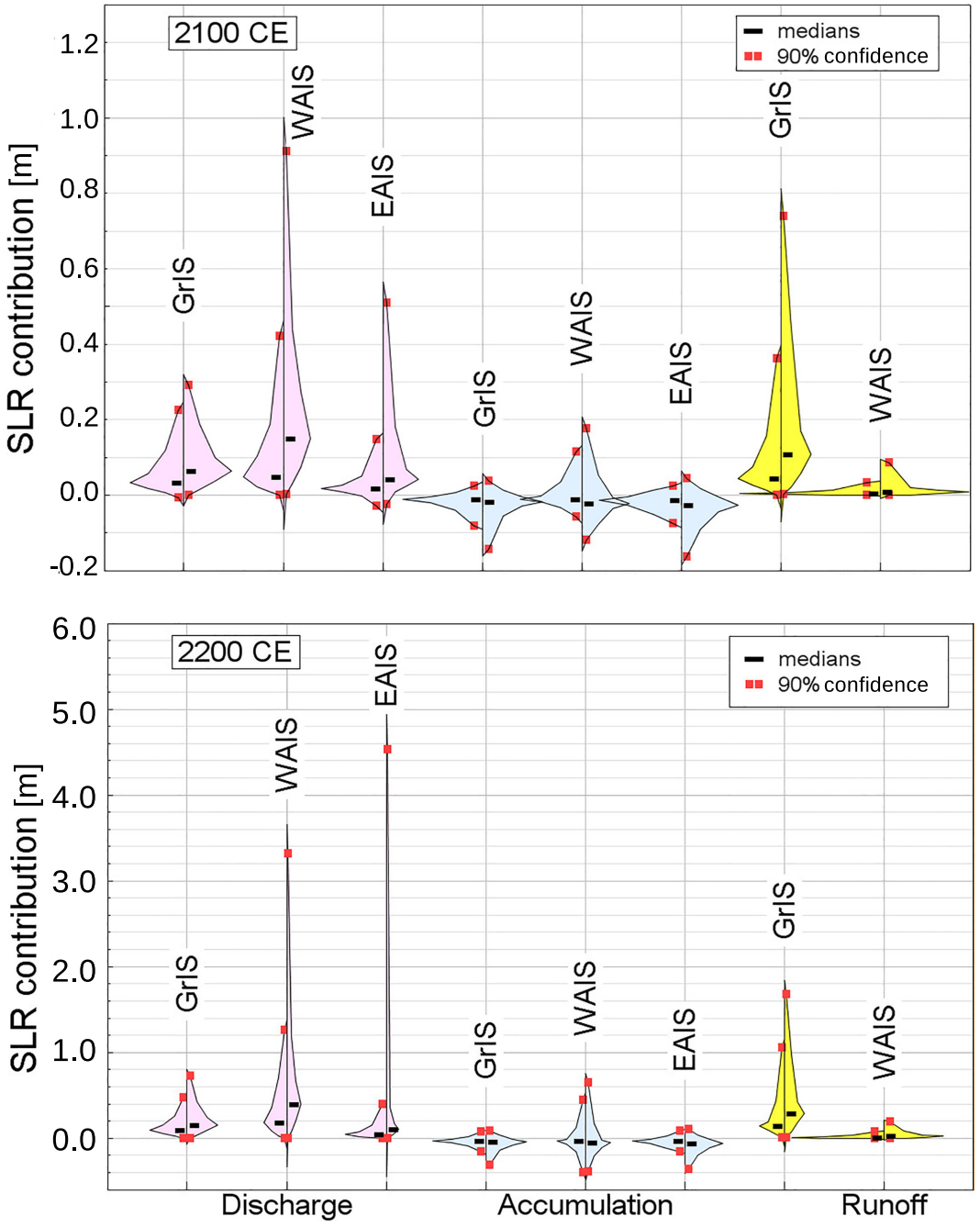

FIGURE 1.2: Projections of discharge, accumulation and runoff from the GrIS and WAIS and EAIS in 2100 (top) and 2200 (bottom) in a low warming (2°C by 2100, left side) scenario and a high warming (5°C by 2100, right side) scenario. Adapted from Bamber et al. (2022)

risk-averse projections overlapped. The change in the range of sea-level rise for the 'risk-averse' Antarctica projections reflects the specific uncertainty of the reaction of the AIS to a warming world. IPCC AR6 (Fox-Kemper et al. (2021)) also has two sets of projections for the sea-level rise contribution from the AIS, one omitting MICI and one taking it into account. Without MICI, the projected sea-level rise by 2100 (likely range in brackets) is 0.11 (0.03-0.27)m following SSP126, and 0.12 (0.03-0.34)m following SSP585. With MICI, the projections for SSP126 and 585 are 0.08 (0.06 to 0.12) and 0.34 (0.19 to 0.53)m, respectively. It is worth noting that the projections with MICI included are presented with low confidence, whereas those without MICI are presented with medium confidence.

Although the current contribution of the AIS is small and there is uncertainty about its transient response, the long-term commitment from the AIS as a result of 21st century warming is large. Lowry et al. (2021) found that although it was difficult to separate the sea level signals of different warming scenarios in the 21st century, there was no overlap in the likely range between scenarios by 2300 when forcing is held constant at the 2100 value, demonstrating that warming over the 21^{st} century has significant long-term implications. They projected a median contribution to sea level of 1.0 m for RCP2.6 and 2.75 for RCP8.5 by 2300. Chambers et al. (2022) extend this type of analysis further, stopping forcing in 2100 and continuing to project Antarctic change until the year 3000. For 'unabated warming' scenarios including RCP8.5 and SSP585, they found a median of 3.5m by year 3000, and up to 5.3m in the most sensitive experiment. Most of this melt came from the WAIS, which sustained considerably more loss than the EAIS. In low emissions scenarios (RCP2.6 and SSP126), the WAIS was not found to collapse, and the median sea-level rise from Antarctica was 0.24m by year 3000. Golledge et al. (2015) also found WAIS collapse following 1.5-2.0°C warming, which is exceeded in all scenarios except RCP2.6/SSP126.

Between 1992-2018, mass loss from the GrIS has been caused in almost equal proportions by changing surface mass balance and increasing discharge from marine-terminating outlet glaciers (dynamic thinning - e.g.Shepherd et al. (2020); Brough et al. (2023)). More recently, mass loss from the GrIS has been dominated by changes in surface mass balance (the difference between accumulation and melt) Mouginot et al. (2019), which is dominated by atmospheric forcing. This is expected to continue to be the dominant cause of melt with high confidence (Fox-Kemper et al. (2021)). Bevis et al. (2019) found that accelerations and decelerations in ice melt from the GrIS corresponded with North Atlantic Oscillation (NAO) phase, where a negative phase means warmer summer and reduced snowfall, causing a more negative mass balance (i.e., more melt/less accumulation from precipitation). The sensitivity to atmospheric forcing means that mass loss from Greenland is subject to strong interannual variability, and this is a source of uncertainty when projecting mass loss and sea-level rise from the GrIS. Atmospheric forcing, surface processes, submarine

melt, calving and ice dynamics on the GrIS are all subject to deep uncertainty (Fox-Kemper et al. (2021)). As well as this, the response of different glaciers in the ice sheet to each forcing is different due to glacier-specific properties such as the geometry of the bed and fjord (Brough et al. (2023). Hofer et al. (2019) found that two significant controls over projections of sea-level rise from the GrIS were cloud microphysics and circulation anomalies, with differences in cloud properties in an RCM causing larger differences in high-emissions scenarios than the difference between the high and low emissions scenario.

Ocean warming has been found to influence the calving rate and thinning of marine-terminating glaciers on the GrIS. IPCC AR6 (Fox-Kemper et al. (2021)) reported high confidence that warming water and increased surface runoff both lead to increased submarine melt, leading to increased ice discharge. However, there is only medium confidence that warmer waters contributed to increasing mass loss from the GrIS. The reaction of glaciers to warming water was found to be variable between glaciers by Brough et al. (2023). South of 69°N, glacier retreat was more consistent and attributed to warming oceans. North of 69°N, glaciers were less influenced by warming oceans and more by glacier-specific qualities, leading to less spatially consistent change in the North of Greenland. In general, the impact of ocean warming is projected to decrease in any scenario as the ice sheet retreats and the amount of contact that glaciers have with the warming ocean decreases (Fürst et al. (2015)). The impact of albedo is known to dominate surface mass balance changes on the GrIS, but albedo is modulated by small-scale processes that are poorly resolved in models (Bamber et al. (2022)), for example impurities like dust and soot (e.g. Dumont et al. (2014); Raoult et al. (2023)), and increasing snow grain size due to warming air temperature (e.g. Box et al. (2012)). There is debate as to which of these factors has the largest impact on albedo, and therefore which is responsible for more melt. Lewis et al. (2021) found that snow grain size had a larger impact on albedo than impurities in the snow, with increasing grain size caused by warmer weather, more insolation and fewer storms - all of which are associated with atmospheric blocking (high pressure) over Greenland. Ryan et al. (2018) found that the albedo of the dark zone in Greenland (a dark patch of ice along the western side of the ice sheet) is largely controlled by surface impurities (73%), including dust, soot and algae. This speeds up melting along the western edge of the GrIS, increasing its contribution to sea-level rise.

Despite uncertainty in the future of ice melt from the GrIS, Edwards et al. (2021) found a much clearer relationship between warming and sea-level rise from the GrIS than they do for the AIS (in the less risk-averse set of projections) due to the stronger warming signal in Northern high latitudes, and the higher dependence of the GrIS on atmospheric warming than oceanic warming. Their likely range of projections for the GrIS contribution to sea-level rise was smaller than the likely range for the contribution from the AIS. IPCC AR6 (Fox-Kemper et al. (2021)) project a sea-level rise

equivalent from the GrIS of 0.06 (0.01 to 0.10)m (likely range) with a 90% range of –0.02 to 0.15m for SSP126, and 0.13 (0.09 to 0.18) with a 90% range of 0.05 to 0.23m, through the use of emulators calibrated using ISMIP6. Uncertainty in GrIS projections is also introduced from CMIP5 models that do not resolve changes in circulation over Greenland that have been occurring since the late 20th century (Hanna et al. (2018); Delhasse et al. (2018)). Using CMIP6 models rather than CMIP5 can change projections of sea-level rise from the GrIS (Hofer et al. (2020)), but not significantly enough that the projections of AR6 represented a significant change from the projections of AR5 (Church et al. (2013)) or SROCC (Oppenheimer et al. 2019). Recently, the committed sea-level rise from the GrIS has been a point of concern. Box et al. (2022) predicted that historical warming commits us to at least 27 cm of SLR by the time the ice sheet has reached equilibrium, regardless of concentration pathway going forward. Nias et al. (2023) found a committed sea-level rise over the 21st century of 33.5 mm (3.35 cm). These two results together imply a large amount of sea-level rise from the GrIS can be expected on multi-centennial timescales.

1.3.2.2 Semi-Empirical sea-level rise Modelling

Semi-empirical modelling of sea-level rise can be a useful tool to examine uncertainty in sea-level rise further, because it is computationally cheap. There was initially a large disparity between semi-empirical and process-based modelling, with semi-empirical projections exceeding processed-based projections by 2-3 times (Orlić and Pasarić (2013)). One significant reason for this disparity was the initial grouping of all processes that contribute to sea-level rise into one parameter (e.g. Rahmstorf (2007)). The projections from this method were considerably higher than projections from process-based models (up to 2m by the end of 2100). Considering the two main contributors to sea-level rise (ice melt and thermosteric expansion) are unlikely to be able to contribute 2m together, this projection is potentially physically unrealistic (Lowe and Gregory (2010)) This method does not represent that processes act at different magnitudes on different timescales. It therefore omits the different evolutions of thermosteric sea-level rise and the contribution of ice melt, significantly overestimating the future thermosteric contribution and underestimating that of melting ice. Goodwin et al (2017) addressed this issue by representing the thermosteric and ice-melt components of sea-level rise in two different terms in a semi-empirical model, such that thermosteric rise was a process-based calculation using ocean heat content, and ice-melt was linearly related to warming via a single constant. Using this method, the different timescales of thermosteric expansion and ice melt could now be accounted for. The assumption that the ice melt contribution to global mean sea-level rise scales linearly with warming will be revisited in Chapter 3 of this thesis.

Emulators and semi-empirical models can both be used to aid understanding of uncertainty by examining the behaviour of sea-level rise in a more complex model in detail (Edwards et al. (2019)), making projections of sea-level rise (Nauels et al. (2017)) or examining past sea level (Grinsted et al. (2010)), or by exploring the relationship between sea-level rise and forcing (Grinsted and Hesselbjerg Christensen (2021)). Edwards et al. (2019) emulated the process-based model used in DeConto and Pollard (2016) to re-examine the projections created using that model, and especially to consider the impact of including the Marine Ice Cliff Instability feedback (MICI), and whether it was necessary to recreate past sea level. The details of MICI and its implications for past and future sea-level rise will be discussed in more detail in Chapter 3 of this thesis. Grinsted and Hesselbjerg Christensen (2021) used a semi-empirical model to assess the relationship between century-averaged warming and the rate of sea-level rise and define the transient sensitivity of sea-level rise to warming, which (when defined using observations) is a useful constraint for sea-level rise modelling. This analysis was used to compare projections from the CMIP6 suite to observations and structured expert judgement to examine discrepancies between the three (Grinsted et al. (2022)).

Jackson et al. (2018) compared 21st century sea-level rise in line with the Paris Agreement targets from process-based and semi-empirical models, and found that the mean and variance of sea level in 2100 were both larger in semi-empirical models. The difference in the median and spread in projections was mainly due to the difference in ice melt contributions. For their study, the process-based ice melt contribution to sea-level rise was calculated following relationships derived by Fettweis et al. (2013) and Vries et al. (2014), whereas the semi-empirical contribution was calculated by subtracting process-based estimations of land-storage, steric rise and glacial output from a semi-empirical model created by Grinsted et al. (2010). The contribution to the variance in sea level from the Greenland ice sheet was found to be considerably bigger in the semi-empirical projections and both Greenland and Antarctica contributed consistently throughout the time period. In the process-based result, the variance from each ice sheet grew throughout the 21st century, and the variance from Antarctica was considerably larger than in the semi-empirical projections. The larger contribution to variance from the AIS in process-based models indicates uncertainty surrounding processes that are not active in the observational data used to calibrate the semi-empirical model.

Luo and Lin (2023) used semi-empirical techniques to link meltwater from individual glaciers in both Greenland and Antarctica to forcing from oceanic warming, as a way of reducing the computational complexity needed for process-based models without losing sight of the different natures and sensitivities of each glacier to ocean forcing. The method could also continue to be used to sample uncertainty as models or observational datasets get updated at little computational expense. However, the

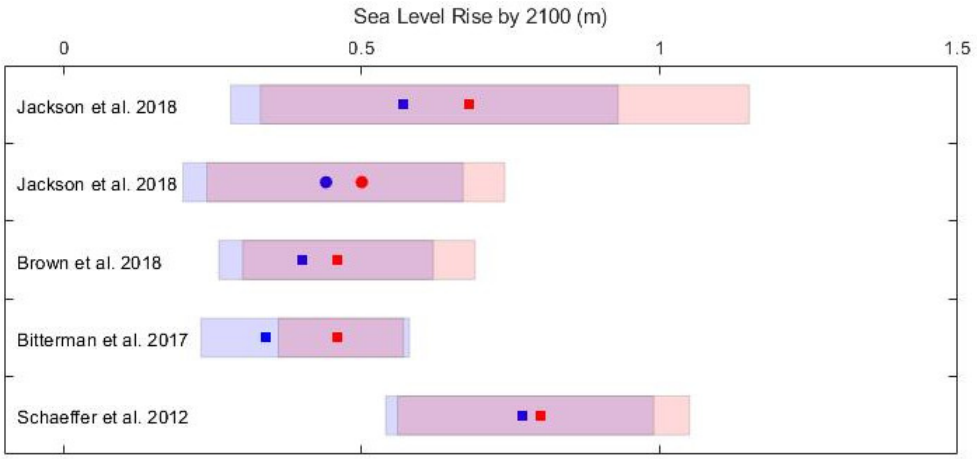

FIGURE 1.3: Projections of sea-level rise to 2100 following trajectories towards 1.5C (blue) and 2.0C (red), from Schaeffer et al. (2012); Brown et al. (2018); Bittermann et al. (2017); Jackson et al. (2018). Shaded box = 5-95% range, points in the middle mark the median. Squares indicate a study using semi-empirical methods, circles indicate process-based.

method does not directly capture the impact of changes in atmospheric forcing, for example solar radiation or wind; although these may have an impact on ocean heat which would be captured in the method.

1.3.2.3 Projections of sea-level rise Following Paris Targets

The warming targets of the Paris Agreement were influenced in large part by representatives of Small Island Nations who are at direct risk of sea-level rise. It therefore makes sense to consider the amount of sea-level rise projected following these targets, and especially to consider the difference between the projections for each target. This can be used to make some judgement on how effective the reduction of the warming target from 2.0°C to 1.5°C is. Figure 1.3 shows projected sea-level rise by 2100 relative to the 1986-2005 baseline, following trajectories towards each Paris Agreement target. It is worth noting that 2100 is a relatively close time horizon in terms of sea-level rise due to the long timescales of ice melt and thermal expansion, so these projections will continue to increase, and are likely to diverge, beyond 2100. In each set of projections there is still a significant overlap in absolute sea-level rise in 2100, but the median value for the 1.5°C scenario is generally distinctly lower than that of the 2.0°C scenario. There is a noticeable amount of disagreement between the various semi-empirical methods, which can arise from differences in model formulation and calibration, and differences in warming/emissions pathways used.

The method of choosing pathways towards the Paris Agreement warming targets can make inter-study comparison difficult, because there are no standardised pathways

towards them. Different methods to develop these targets include selecting model runs from the CMIP5 suite that stabilise at each target with some degree of probability (e.g. Jackson et al. (2018)), or by creating idealised pathways that stabilise at a given warming target with some degree of probability (e.g. Bittermann et al. (2017); Brown et al. (2018)). As well as the method of choosing temperature pathways, the chosen degree of probability of staying within a given target will also have implications for the amount of sea-level rise projected in a study. One consideration when defining warming pathways to examine future sea-level rise in this manner is that warming is not pathway dependent, but sea-level rise is. This presents a complication when considering pathways towards optimistic warming targets, as they will involve some element of peak and decline in emissions, if not overshoot and then negative emissions (carbon dioxide removal, CDR). Mengel et al. (2018) find that the pathway dependent nature of sea-level rise means that every five-year delay in peaking emissions before declining them leads to an extra 0.2m of sea-level rise in the long term.

1.3.2.4 Communicating and Managing sea-level rise

It is known that sea level will continue to rise even if emissions halt immediately, so there should be just as much of a focus on adaptation to sea-level rise as there is to mitigation. Knowing how much sea-level rise to prepare for is essential for adaptation planning, and therefore sea-level rise projections are of great interest to regional policy and decision makers. sea-level rise projections are generally communicated as a likelihood range and a median value. When it comes to managing sea-level rise, for example by building increased flood defences, the high-end of this range is useful so that planners are prepared for, or at least aware of, a 'worst-case' scenario. For this reason, a likely range (17-83%) of sea-level rise is not always sufficient, and stakeholders are often interested in the very likely (5-95%) range (e.g. Hinkel et al. (2019)).

The manner that uncertainty in sea-level rise is communicated to, and dealt with by, decision makers and local authorities matters here. Stammer et al. (2019) and van de Wal et al. (2022) emphasise the importance of making a distinction between general scientific endeavours and so-called 'actionable science' which is designed to support decision makers and stakeholders. They specify the need for new research to be reviewed carefully before being incorporated into planning or guidance, to avoid a situation where every new piece of research has (potentially unnecessary or conflicting) repercussions on planning efforts. Stammer et al. (2019) provide a framework to facilitate discussion of a high-end projection for sea-level rise that draws on multiple lines of evidence and provides clear and consistent messaging for practitioners. van de Wal et al. (2022) built on this, to develop high-end projections that are suitable for practitioners. They note an important distinction between what

the aim is in most scientific studies of sea-level rise (precise estimates of likelihood) and what is most important for practitioners (that the evidence is credible, relevant to their needs, and legitimate).

Mitigating global mean sea-level rise is an especially long-term endeavour, due to the long timescales of its two biggest contributors (ice melt and thermal expansion). Because this means that the benefits of acting to mitigate sea-level rise will not be fully evident in the near future, it is perhaps more practical in a political sense to focus on mitigating warming, which in turn mitigates sea-level rise. As such, many studies that consider mitigation of sea-level rise do so by considering the damage avoided by faster or more stringent mitigation of warming, as compared to the damage inflicted by failing to mitigate warming sufficiently (e.g. Brown et al. (2018); Nicholls et al. (2018); Mengel et al. (2016)). For outlines of studies that do address the explicit aim to limit sea-level rise, see Section 1.4.

1.3.3 Acidification as a Potential Climate Target

1.3.3.1 Projecting Acidification

Projections of (surface) ocean acidification in IPCC AR6 are presented with high confidence (Lee et al. (2021)), owing to the well-constrained relationship between emissions and surface acidification. Projections of acidification from the CMIP6 models are higher than those from the CMIP5 suite (Canadell et al. (2021)), but this is attributed to higher atmospheric carbon concentration in equivalent SSP/RCP scenarios, rather than changing understanding of carbon absorption in the surface ocean (Kwiatkowski et al. (2020); Lee et al. (2021)). There is more uncertainty regarding future acidification at depth, due to uncertainty in how warming will impact ocean circulation and therefore downwelling, which in turn modulates how the deep ocean acidifies. Further, although surface acidification can be undone by carbon dioxide removal from the atmosphere, seasonal cycles in carbonate chemistry take longer to recover (Jiang et al. (2023)). Carbon Dioxide Removal (CDR) will also have minimal effect on acidification at depth, which is modulated by the strength of ocean overturning rather than by gas exchange at the surface. Because of this, acidification at depth is only reversible on the same timescale as overturning, which is much longer than the timescale of gas exchange at the surface (milennia rather than years). Mathesius et al. (2015) found that the legacy of carbon emissions in the deep ocean was still felt at the end of their model simulations in 2700, which matches with the 10^3-year timescale of ocean overturning circulations. They attributed this lag to reduced overturning and increased stratification due to the ocean warming at the surface, which would effectively isolate the deep ocean and prevent any changes that happened from the top down from reversing. This inertia leading to a committed

amount of acidification at depth is further reason that limiting acidification is something that should be explicitly aimed for, rather than limiting acidification as a by-product of limiting warming. The lack of reversibility here also lends itself to the argument that CDR is not a complete solution: we must work towards reducing emissions in the first place.

1.3.3.2 Aragonite Saturation

A large part of the concern over ocean acidification is due to the impact it has on aragonite saturation. While carbon can be removed from the atmosphere via negative emission technologies, the impact it has on the ocean has been shown to be slower to reverse. Joos and Frölicher (2011) examined the impact of the inertia in the ocean carbon cycle on projections of aragonite saturation (Ω_{arag}) until 2500, using three scenarios: one where emissions stop in 2000, and two where emissions stop in 2100 after following a high- and low-emissions trajectory. They found that the global-average Ω_{arag} begins to recover quickly after emissions stop, but did not reach its values from the beginning of the experiment even after at least 400 years of equilibration. From the pre-industrial global mean of 3.7, saturation reached 3.2 in 2500 following a pathway where emissions stopped in 2000, 2.7 after a low-emissions scenario that stops in 2100, and 2.2 in a high-emissions scenario that stops in 2100. To put this result in context, two relevant saturation states are 1 (the boundary between undersaturation and oversaturation) which is a threshold for calcifying organisms at high latitude, and 3.4 which is the lowest saturation state at which corals can comfortably survive Kleypas et al. (1999).

Ocean biogeochemistry is impacted by more than atmospheric CO_2 alone, so changes to ocean biogeochemistry are not spatially uniform. Oceans at high latitude are acidifying faster due to colder temperatures aiding gas exchange between the atmosphere and the surface ocean. This is particularly an issue in the Arctic Ocean (Terhaar et al. (2020)). Regional carbonate chemistry and acidification are not only related to carbon emissions, but to local processes such as circulation, temperature changes, carbon cycling and biological processes (Hurd et al. (2018)). This means that long term trends are superimposed on climate modes such as ENSO, which has been found to alter carbon uptake in the Pacific ocean (Vaittinada Ayar et al. (2022)). There are competing effects in each phase of ENSO (with temperature-related solubility contrasting with the strength of upwelling modulating nutrients and dissolved inorganic carbon, DIC). With all of these accounted for, the main modulating process is the modulation of DIC by upwelling strength (Vaittinada Ayar et al. (2022)). Lovenduski et al. (2015) examined natural variations in the saturation of carbonate ions ($[CO_3^{2-}]$) by running an Earth systems model at a constant (preindustrial) atmospheric carbon concentration, so the only variation in climate is caused by

unforced variability in atmosphere and ocean state. $[CO_3^{2-}]$is the primary source of variation in aragonite saturation, so examining variation in $[CO_3^{2-}]$ provides a basis of understanding how aragonite saturation can vary naturally. They found close relationships between $[CO_3^{2-}]$ and the Pacific Decadal Oscillation in the North Pacific and ENSO in the tropical Pacific, and a weaker relationship between $[CO_3^{2-}]$ and the North Atlantic Oscillation and Atlantic Multidecadal Oscillation in the North Atlantic.

1.3.3.3 Communicating and Managing Ocean Acidification

There are a number of ways in which environmental policy can target ocean acidification, on scales ranging from community-based action to international policy. Billé et al. (2013) categorise these into four groups: responses that aim to prevent ocean acidification; those that work to strengthen ecosystem resilience; those that adapt human activities and those that repair damage that has already been done. The scope of this thesis fits within the first category: preventing ocean acidification. Within this category, specific responses include limiting carbon concentration, reducing local factors that contribute to ocean acidification, reducing the risk of methane clathrate release and solar radiation management - although there is uncertainty here in the magnitude and direction of its impact on ocean acidification (Williamson and Turley (2012)). In reviewing the management and policy options for addressing ocean acidification, Billé et al. (2013) conclude that while there is sufficient legal basis for action, there are significant barriers to implementing policy here.

The barriers to implementing acidification-specific policy mean that although a number of multilateral environmental agreements exist that have the intention to manage ocean acidification, by 2019 there was no unifying treaty focused on reducing ocean acidification on a global scale (Harrould-Kolieb (2019)). Rather than pushing for more policy frameworks to be put in place, Harrould-Kolieb (2019) proposed that a more practical solution would be to assess how existing policy frameworks can be used to address ocean acidification. One example of this is the policy frameworks of the UNFCCC that set CO_2 reduction goals, where ocean acidification could be taken into account when determining the scale of emissions reductions. Although they argue that a focus on emissions reductions may limit the potential of what policy could be put in place, the counter-argument here is that CO_2 reductions are already a familiar goal to practitioners, so would require less change in outlook in this sense.

Harrould-Kolieb (2016) also argued that it is within the UNFCCC to limit carbon emissions with the explicit aim of managing ocean acidification - however, this is not currently present in any significant way. There is minimal mention of limiting ocean acidification in the UNFCCC itself, but there is potential for acidification to be a motivating factor in the individual Nationally Determined Contributions (NDCs) of a signatory to the Paris Agreement. Gallo et al. (2017) found that this was still low, with

only 14 out of 161 NDCs addressing ocean acidification in their NDCs, and most of these NDCs came from small island developing states. Using existing policy frameworks to address ocean acidification (rather than creating whole new structures) has been recommended on a national as well as global scale. Hull (2014) noted that policy in the US relating to ocean acidification focussed more on collecting data relating to ocean acidification rather than acting to combat it, and recommended that policymakers use the Clean Water Act as a vessel to introduce policy that actively addresses the problem. Although not mentioned in the UNFCCC, avoiding acidification is an explicit aim of the United Nations Convention on Biological Diversity (UN CBD), which was first published in 2010. However regardless of whether and where explicit mention of combating ocean acidification exists, it remains the case that the most prominent climate discourse and policy centres on warming goals. Cooley et al. (2019) suggest that one solution to protecting oceans and ecosystem services is to implement deliberate acidification targets, and this is an idea that will be explored in Chapter 2.

1.4 Multiple or Alternative Climate Targets

There are many limitations to taking global mean warming as the single metric of climate change that we aim to limit. One has already been discussed in Section 1.2.1 and 1.2.2: that warming and cumulative emissions scale near-linearly, but this relationship is uncertain. Another issue is that the focus on warming easily fuels the impression that CDR is a fix for if/when a warming target is overshot. However, although removing carbon from the atmosphere can undo excess warming, there are other aspects of the Earth system which are subject to more inertia. Ocean circulation and sea-level rise will recover on much slower timescales, and other aspects of the Earth system may also be subject to hysteresis or asymmetrical behaviour that means that much more cooling is necessary to return to their preindustrial state. This hysteresis in the Earth system has been found to be not only pathway-dependent, but to increase nonlinearly as the assumed ECS increases for Earth-system responses such as surface air temperature, upper ocean heat content, ocean oxygenation and ocean pH (Jeltsch-Thömmes et al. (2020)). This further intensifies the problem of uncertainty in the equilibrium warming response of the climate to carbon emissions.

In terms of global mean sea-level rise, there are two processes that must be considered: thermosteric rise and ice melt. Ehlert and Zickfeld (2018) examined the behaviour of thermosteric sea-level rise under CDR scenarios and found that if carbon concentration increases by 1% a year, then decreases at the same rate back to preindustrial, thermosteric sea level will not return to its preindustrial state until 1000 years after the preindustrial concentration of atmospheric CO_2 has been restored. Boucher et al. (2012) and Boucher et al. (2012) also concluded that thermosteric

sea-level rise would only restored in the event of rapid reduction of radiative forcing. In terms of ice melt, the AIS was found by Garbe et al. (2020) to have several temperature thresholds where a certain amount of sea-level rise becomes irreversible: at 2°C warming, they projected partial collapse of the WAIS due to MISI; and 6-9°C they projected 70% ice mass loss, and at 10°C, a virtually ice-free Antarctic. They also projected that the WAIS will not start to recover until temperatures are 1°C lower than preindustrial, indicating hysteresis in ice regrowth, and that the pattern of ice thickness will not recover to be the same as it was before ice melt. There is also irreversibility with regards to ocean acidification, as ocean circulation will transport acidified waters to greater depth and prevent gas exchange with the atmosphere, essentially 'trapping' the acidified water (Joos and Frölicher (2011)). As ocean circulation is projected to slow with warming and take centuries to recover, ocean acidification at depth is subject to inertia on the same timescales as ocean circulation. However, the rest of this thesis will focus on surface ocean acidification, where this form of inertia is less relevant. On top of irreversibility of changes in deep-ocean carbonate chemistry due to ocean circulation, the response of carbon cycling in the ocean as carbon is removed from the system varies over time, as different feedbacks relating to the solubility and biological pumps act and react on different timescales (Keller et al. (2018)). This presence of inertia in the Earth system should be an impetus to work towards actively limiting dangerous change in more areas than just global mean warming. Even if warming is the only metric considered, Zickfeld et al. (2013) found that global mean temperature is still higher than preindustrial, after atmoshperic CO_2 is ramped down to preindustrial concentration over 100 years and held at that value for another 900. This was understood to be because of thermal inertia in the climate system, as well as a small amount of forcing from non-CO_2 actors, which were held at a small positive value even as CO_2 was ramped down. Boucher et al. (2012) found that when atmoshperic CO_2 concentration is reduced to zero, air temperatures over the ocean are subject to more time lag than air temperatures over land, and this lag increases the more warming is allowed to occur before CO_2 removal is initiated.

Calibrating carbon emissions to adhere to a single climate target may also lead to a deceptively large carbon budget. Steinacher and Joos (2016) considered carbon budgets towards multiple climate targets (steric sea-level rise, aragonite saturation state, soil carbon loss on croplands and net primary production on land), and found that the carbon budget for more than one climate target together was less than the carbon budget even for the most restrictive single target of the group considered, due to interdependence between the climate targets. The implication of this is that if we wish to avoid dangerous change across the entire climate system, we need to mitigate more than a single warming target may indicate. One benefit of using global mean warming as a climate target is the simple scaling of warming with cumulative emissions. However, this form of relationship is not unique to warming. Steinacher

et al. (2013) find a linear transient relationship between cumulative emissions with surface ocean pH, sea surface temperature and surface air temperature. Although they found steric sea-level rise to be more pathway dependent, Grinsted and Hesselbjerg Christensen (2021) defined a transient sea level sensitivity to warming that was linear over the observational period. This means there is some basis for defining a carbon budget framed using climate targets other than warming.

Although the relationship between sea-level rise and warming/cumulative emissions is somewhat pathway dependent, there are still various ways to consider how we can use sea-level rise as the frame for climate targets, and the implications of this for future carbon emissions. One of the more simple illustrative methods is to consider the temperature at which the rate of sea-level rise is zero (i.e., the point at which we are no longer committed to sea-level rise). Grinsted and Hesselbjerg Christensen (2021) find this to be -1.1°C - roughly the amount of warming that we have experienced since the beginning of the industrial age (Gulev et al. (2021)). This has dramatic implications in terms of the amount of cooling/emissions reductions necessary to undo the impact that industrialisation has had on sea levels, and therefore the importance of taking adaptation as seriously as mitigation when it comes to sea-level rise. Foster and Rohling (2013) came to a similar conclusion by examining the relationship on equilibrium timescales between atmospheric CO_2 and sea level, stating that to avoid significant sea-level rise in the long term, atmospheric CO_2 should be returned to preindustrial levels or similar. Li et al. (2020) found that steering emissions directly towards a sea-level rise target consistent with a given warming target, rather than a warming target consistent with the same amount of sea-level rise, allows for more carbon emissions yet limits sea-level rise more effectively in the long term.

1.5 Completing the Narrative: Thesis Aims, Objectives and Novelty

The aim of this thesis is to establish carbon emissions pathways that are consistent with climate goals beyond global mean warming. Chapter 2 will consider adaptive mitigation pathways and remaining carbon budgets for combined warming and acidification targets. Chapter 3 will examine the nonlinear relationship between warming and ice melt and how this can be represented in a climate emulator, as an intermediary step before Chapter 4. Chapter 4 will then address adaptive mitigation pathways that stabilise the sea-level rise commitment.

Each of these chapters has a different motivation and benefits. Considering ocean acidification and warming in combination will reduce the uncertainty of the remaining carbon budget, due to the better constrained relationship between carbon emissions and surface ocean acidification (compared to cumulative emissions and

warming). It is also a potential mechanism to address ocean acidification through pre-existing structures to limit warming to a politically motivated target. Including nonlinearities in the relationship between warming and the ice-melt contribution to sea-level rise allows for an in-depth examination of the impact of nonlinear ice behaviour on sea-level rise, because a climate emulator is computationally cheap so can efficiently explore a wide parameter space. The projections of sea-level rise will run to 2300, consistent with AR6 projections and giving a picture of the scale of sea-level rise in a longer term view than studies that project until 2100. The work in Chapter 4 will fill the gap left by a lack of studies addressing how future sea level can be stabilised. Steinacher et al. (2013) calculated remaining carbon budgets framed with sea level targets, however they only considered steric rise. Grinsted and Hesselbjerg Christensen (2021) and Foster and Rohling (2013) have both conducted studies that illuminated the scale of action needed to stabilise sea level. Grinsted and Hesselbjerg Christensen (2021) defined the transient sea level sensitivity to century-averaged warming, and Clark et al. (2018) define the transient sensitivity of sea-level rise to cumulative emissions (given that warming and cumulative emissions scale near-linearly, these methods both hold). Clark et al. (2018) posit that this relationship can be used to inform carbon budgets consistent with manageable sea-level rise. However, this author could find no peer reviewed study that has used this concept to create emissions pathways towards minimising sea level commitment.

1.5.1 Scientific Questions

For the next three chapters, the respective scientific question is as follows:

1. How does the remaining carbon budget change if we consider not just global mean warming, but global mean surface ocean acidification?
2. How do observed nonlinearities in the relationship between warming and ice melt impact future sea-level rise?
3. How much carbon removal would it take to stabilise the commitment to sea-level rise?

1.6 Methods

1.6.1 The WASP Model

The main tool for this thesis is the Warming, Acidification and Sea-level Projector (WASP) model (Goodwin (2016)). The WASP model is a reduced-complexity ESM,

with the atmosphere-ocean-terrestrial system represented by 8 boxes (5 ocean, 2 terrestrial and 1 atmosphere). For Chapter 2, a different version of WASP is used than in Chapters 3 and 4.

For Chapter 2, the model has 19 parameters that describe the climate response to radiative forcing from CO_2, other greenhouse gases and aerosols, and the exchange of carbon and heat between the 8 boxes. These parameters are varied randomly within a prescribed range according to Goodwin et al. (2018b) - see Table A.1 and A.2. In Chapters 3 and 4, the model has 28 varied parameters, listed in Table A.3 and A.4. Because the model is computationally highly efficient (5.4×10^8 simulated years per CPU hour, run on a 2.0 GHz Intel Skylake processor), it is possible to create large ensembles and efficiently and thoroughly explore a wide parameter space. the variation of parameters being the source of variation between simulations, so the uncertainty explored here is parametric uncertainty, not process uncertainty. The model is run using the University of Southampton supercomputer, IRIDIS. Chapter 2 uses IRIDIS 4, and Chapters 3 and 4 use IRIDIS 5. In all chapters, the model runs from 1750 to 2300. In Chapters 3 and 4, the period from 1750 to 1850 is used as a spin-up period, and data from 1850 to 2300 is used for analysis.

The WASP model is calibrated using a history matching protocol, which means that an initial very large prior ensemble is generated with Earth system parameters randomly varied within feasible bounds, and a posterior ensemble is created using those simulations from the prior ensemble that are consistent with the observational period. The Earth system parameters that are varied between simulations are slightly different between Chapter 2 and Chapters 3 and 4, and are outlined in Table A.1 and A.2, and Table A.3 and A.4, respectively. For Chapter 2, simulations are allowed into the posterior ensemble if they lie within the 90% range of at least 8 out of 9 of the historical observation checks outlined in Table 2.1. For Chapters 3 and 4, a Bayesian history matching protocol is implemented where simulations in the posterior ensemble are assigned a weighting based on how well they are able to recreate the historical observations outlined in Table 3.1 (see Figure 1.4). To do this, a likelihood function for each observable on Table 3.1 is defined as the probability of a simulated value (x_k) of that observable 'k' (given the known background information I and that the climate system parameter $X = X'$) as it lies on a gaussian distribution with a mean and standard deviation of μ_k and σ_k (according to Table A.3):

$$P\left(\{obs\}_k \,|X = X', I\right) = e^{\frac{-(\mu_k - x_k)}{2\sigma_k^2}} \tag{1.1}$$

A cost function is then defined as all of the likelihood functions for each observable 'k' multiplied together, and the simulation is weighted according to the cost function. To increase efficiency, if the cost function is below a given value, not every simulation with that value of cost function is used in the posterior. Instead, for a cost function

order 10^n and a minimum cost function order 10^m, one simulation in every $(m - n)$ simulations is used in the posterior ensemble, and given a weighting of 1.

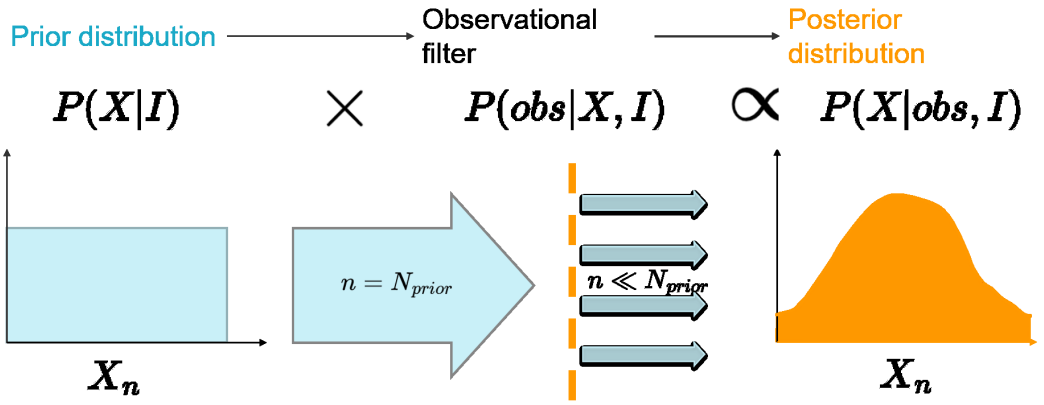

FIGURE 1.4: A schematic of the Bayesian history matching protocol implemented in the version of WASP used in Chapters 3 and 4.

1.7 The Adjusting Mitigation Pathways Algorithm

The WASP model can be run either to follow idealised carbon pathways (e.g. 1% increase in CO_2 per year; abrupt doubling or quadrupling); to follow Shared Socioeconomic Pathways (SSP) scenarios, or create Adjusting Mitigation Pathways towards a given warming target. The algorithm to create these pathways (the AMP algorithm) will be adapted in Chapters 2 and 4 to stabilise at a different type of target, but the following section will describe how this algorithm works in its original form.

The key principle that the AMP algorithm exploits is the near-linear and pathway-independent relationship between cumulative emissions and global mean warming. Every 10 years, the algorithm will calculate how much carbon can be emitted ($I_{remaining}$) before reaching the set warming target (ΔT_{target}):

$$I_{remaining} = \left[\Delta T_{target} - \Delta T_{obs}\right] / \left[\frac{\Delta X}{\Delta T}\right]\Bigg|_{obs} \tag{1.2}$$

Where $\frac{\Delta X}{\Delta T}\Big|_{obs}$ is essentially the model-calculated value for the TCRE, which results from the parameters in the model that describe the climate response to radiative forcing. The TCRE is assumed to be constant on short (10-year) timescales, and is calculated every 10 years at time t_n, using decadal-averaged values for warming and taking the period 2003-2012 as a baseline:

$$\frac{\Delta X}{\Delta T}\Bigg|_{obs} = \frac{\overline{T}(t = t_n - 11 \rightarrow t_n - 1) - \overline{T}(t = 2003 \rightarrow 2012)}{I_{em}(t = t_n - 5) - I_{em}(2008)} \tag{1.3}$$

The time period taken for warming averages ends one year before the emissions rate is adjusted, to simulate time taken for policy changes and implementation. From here, the algorithm then calculates an emissions rate (EmRate) that will linearly reduce this carbon budget to 0, starting at time t, such that

$$C_{Rate}(t) = C_{Rate}(t_n)\left(1 - \frac{t - t_n}{t_{C=0}}\right) \tag{1.4}$$

Until $t - t_n = t_{C=0}$. Because the algorithm assumes a linear reduction in emissions, $t_{C=0}$ (the time at which all carbon has been used up) can be calculated as $t_{C=0} = 2I_{remaining}(t_n)/C_{rate}(t_n)$. As the 'observed' warming and emissions in the WASP model are continuously recalculated, this entire process (calculating $I_{remaining}$ and C_{Rate}) is repeated every 10 years, to allow for changes in the model estimate of the TCRE. Figure 1.5 shows this in a flow chart.

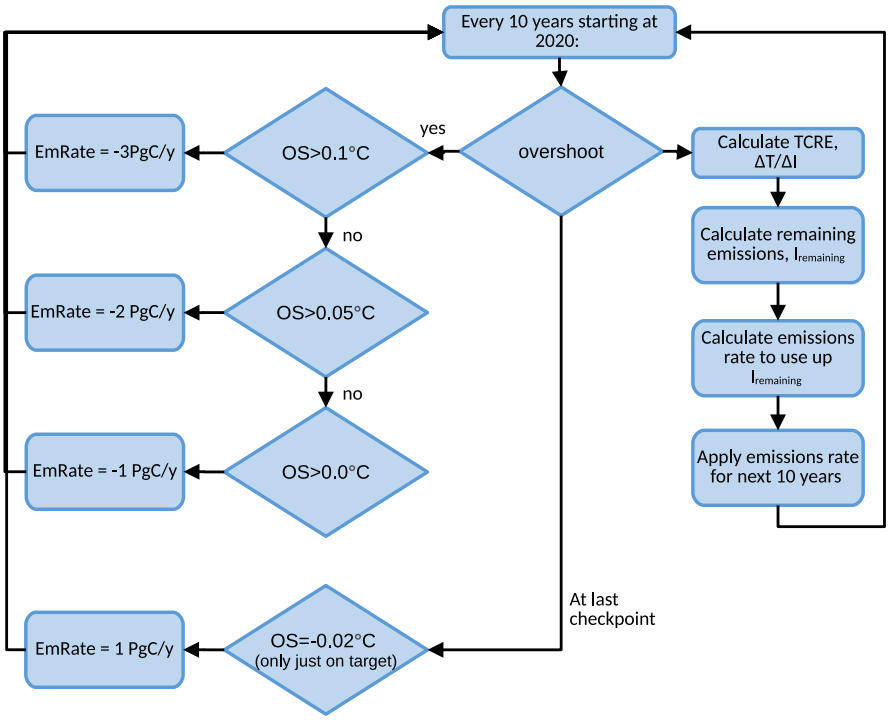

FIGURE 1.5: A flowchart showing the process of the AMP algorithm, including the protocol for if the warming target is overshot.

It is important to note that this algorithm only considers carbon emissions, so radiative forcing from non-CO_2 greenhouse gases is not regulated by emissions reductions calculated by the AMP algorithm. When the algorithm is implemented, the assumption is that radiative forcing from non-CO_2 greenhouse gases follows RCP2.6, assuming that if effort is put into mitigating CO_2 emissions, the same effort is put into mitigating non-CO_2 gases. This may not be the case in practice, and while this

assumption makes little difference if the warming target is low (1.5°C), the impact of the assumption is greater as the warming target increases to 2°C (Goodwin et al. 2018). A recent study by Terhaar et al. (2022) examined adaptive emissions pathways using similar principles to the AMP algorithm, but considering CO_2 equivalent forcing including multiple non-CO_2 agents. This allowed the budget to be broken down into these different agents rather than making assumptions about how non-CO_2 GHGs evolve in the future.

The AMP algorithm (and indeed the algorithm of Terhaar et al. (2022)) creates mitigation pathways towards a given (usually politically-motivated) warming target. However, mitigating emissions with the sole purpose of limiting warming may mean letting other impacts of carbon emissions and climate change become too much of a hazard. The mitigation pathways made using this algorithm are therefore not necessarily sufficient to prevent dangerous change across the climate system. The aim of this thesis is to explore the impact on emissions pathways of considering climate targets other than global mean warming.

Chapter 2

Defining the Remaining Carbon Budget Through the Lens of Policy-Driven Acidification Targets

This chapter is a paper that was first submitted to Climatic Change on 25-10-2022, and was accepted on 13-07-2023.

Formal analysis and investigation: Sandy Avrutin; Methodology: Sandy Avrutin, Philip Goodwin; Write up: lead by Sandy Avrutin, with comments by Philip Goodwin and Thomas H.G. Ezard; Original conceptualisation: Based on idea from INSPIRE studentship advert placed by supervising team. Supervision: Philip Goodwin and Thomas H.G. Ezard

2.1 Abstract

Basing a remaining carbon budget on warming targets is subject to uncertainty due to uncertainty in the relationship between carbon emissions and warming. Framing emissions targets using a warming target therefore may not prevent dangerous change throughout the entire Earth system. Here, we use a climate emulator to constrain a remaining carbon budget that is more representative of the entire Earth system by using a combination of both warming and ocean acidification targets. The warming targets considered are 1.5 and 2°C; the acidification targets are -0.17 and -0.21 pH units, informed by aragonite saturation states where coral growth begins to be compromised. The aim of the dual targets is to prevent not only damage associated with warming, but damage to corals associated with atmospheric carbon and ocean acidification. We find that considering acidification targets in conjunction with warming targets narrows the uncertainty in the remaining carbon budget, especially in

situations where the acidification target is more stringent than, or of similar stringency to, the warming target. Considering a strict combination of the two more stringent targets (both targets of 1.5°C warming and -0.17 acidification must be met), the carbon budget ranges from -74.0 to 129.8PgC. This reduces uncertainty in the carbon budget by 29% (from 286.2PgC to 203.8PgC). This reduction comes from reducing the high-end estimate of the remaining carbon budget derived from just a warming target. Assuming an emissions rate held constant since 2021 (which is a conservative assumption), the budget towards both targets will be spent by 2023 or 2029.

2.2 Introduction

Climate change is one of the defining issues of the 21st century. The Paris Agreement has been politically adopted by 196 parties and commits countries to an effort to "limit global warming to well below 2 [°C], preferably to 1.5°C, compared to pre-industrial levels". Therefore, a central aim in climate science is to establish carbon emissions pathways or budgets that are consistent with these warming goals. The concept of a remaining carbon budget (RCB – the allowable carbon emissions remaining before a given climate target is met) is particularly meaningful in this context, as it allows for easy communication between the science and policy spheres regarding the impact of emissions on a complex system (Messner et al. (2010); Rogelj et al. (2019)). Conventionally, the RCB is defined with respect to a single target of global mean warming (Rogelj et al. (2016); Rogelj et al. (2018)). This is possible because the relationship between cumulative emissions and global mean warming is approximately linear (Allen et al. (2009); Matthews et al. (2009); Zickfeld et al. (2009)), due to opposing ocean uptake of heat and carbon (Solomon et al. (2009); Goodwin et al. (2015)). Exploiting this linear relationship allows for the simple calculation of a RCB towards a warming target.

Although calculating the RCB towards a warming target is a useful starting point, it has weaknesses. There is uncertainty in the value of the RCB due to uncertainty in the constant of proportionality (the transient response to climate change, TCRE), and uncertainty in non-CO_2 related warming. Uncertainty in the TCRE (with a likely range of 1.0 to 2.3 K EgC^{-1} (1000 to 2300 K PgC^{-1}) in IPCC AR6, 2021 (Forster et al. (2021)) leads to a remaining carbon budget (RCB) of 80 to 250PgC. Political or sociological uncertainties increase this range even further (Rogelj et al. (2016)). Uncertainty in the TCRE stems from corrections that must be made for feedbacks that are not well-represented in Earth-system models, and for the zero-emissions commitment (ZEC). One Earth-system feedback that was not included in AR5 assessments of the TCRE was permafrost feedbacks, which were since found to increase estimates of the TCRE by 15% (MacDougall and Friedlingstein (2015)). These feedbacks (apart from methane and tropospheric ozone, which are accounted for in

calculations of the non-CO_2 contribution) are estimated to add up to 7±27 PgC/K, and are assessed with low confidence in the IPCC AR6 (Canadell et al. (2021)). A further source of uncertainty in calculations of the RCB is correcting for non-CO_2 contributors to warming (e.g. aerosols, and non-CO_2 greenhouse gases), which in AR6 was estimated to contribute 0.1 to 0.2°C to TCRE estimates (Canadell et al. (2021)).

As well as this, the UNFCCC definition of the climate system is 'the totality of the atmosphere, hydrosphere, biosphere and geosphere and their interactions' (UNFCCC, 1992). The stated aim of avoiding dangerous climate change therefore, by definition, includes the protection of sustainable oceans, food production and ecosystems. Following this logic, the uncertainty associated with carbon emission pathways towards a 1.5°C temperature change could mean carbon emissions that are on track with the Paris goals, but that would still cause dangerous change to the climate system as a whole (Steinacher et al. (2013)), with carbon-associated changes predicted to ocean acidity and net primary production on land. Further, even if warming is restricted to 1.5°C, at least 90% of all reef areas will be at risk of long-term degradation due to both ocean warming and ocean acidification caused by CO_2 uptake (Schleussner et al. (2016)). In particular, the reef-building coral *Siderastrea sidera* has been found to react negatively to warming and acidification (the impacts of both stressors being worse than the impacts of just one), with acidification impacting calcification and skeletal morphology (Horvath et al. (2016)). As well as warm water corals, species in high latitude oceans face negative impacts from acidification, with seasonal aragonite undersaturation predicted in the Southern Ocean at 450ppm (McNeil and Matear (2008)). Hauri et al. (2016) find that by 2060, surface aragonite undersaturation events will impact 30% of the Southern Ocean following RCP8.5, increasing to more than 70% by 2100. Undersaturation harms the growth of calcifying plankton (for example *Limanica helicina* (McNeil and Matear (2008)), which has potential knock-on effects for the wider ecosystem.

An ensemble of simulations from a climate emulator (WASP: Goodwin (2016)), using scenarios that restore to either defined warming or defined acidification, finds that the resultant acidification from following warming targets broadly consistent with the range of warming mentioned in the Paris Agreement (from 1.5 to 2.1°C of warming) is between -0.135pH (less acidification) and -0.2pH (more acidification). Figure 2.1a shows the full range of achieved pH from pathways that stabilise at different warming targets. The variation across the ensemble is due to the uncertainty in the relationship between a given amount of warming and the associated carbon emissions, leading to uncertainty in how much acidification occurs.

Some previous studies have examined ways to create more a representative RCB, including by using targets based on regional extreme temperatures and precipitation (Seneviratne et al. (2016)). The relationship is not 1:1 and varies spatially, which has the effect of lowering the RCB by differing amounts depending on which region is

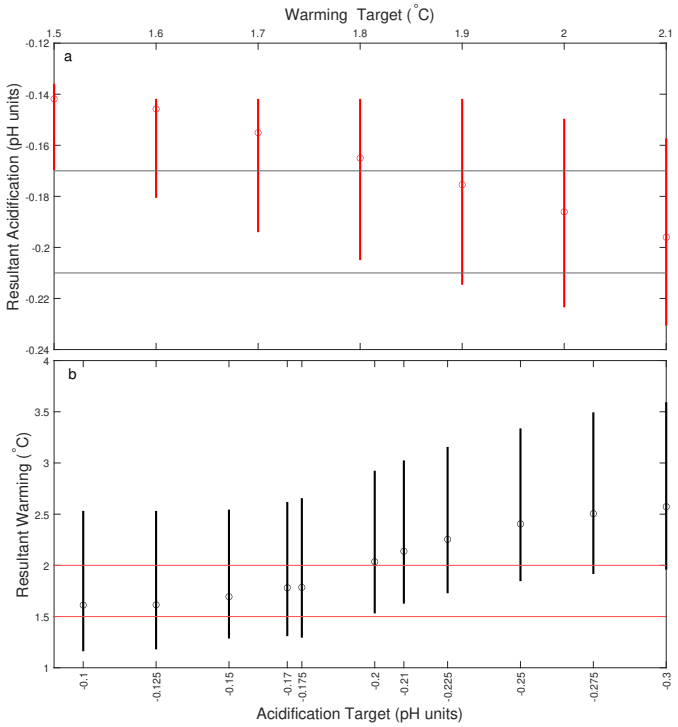

FIGURE 2.1: a- The resultant surface ocean acidification from emissions pathways consistent with warming targets within a range of 1.5 and 2.1°C. b- The resultant warming from acidity targets ranging from -0.3 to -0.1

being considered. This method does avoid undesirable outcomes related to global mean warming but does not address issues that are related to carbon emissions and not to warming (for example, ocean acidification). The practice of scaling local temperature or precipitation extremes to global mean temperatures is also subject to limitations related to uncertainty in the scaling process, model biases and issues to do with exploring scaling on a local or regional basis. Many of these issues do not apply in the case of this study because the scale is global, and we are exploiting a well-constrained relationship (i.e., between atmospheric carbon and ocean acidity). Other studies have examined the RCB under combinations of climate targets, rather than solely (scaled) global mean warming (Steinacher et al. (2013)). This is a manageable way to reduce the likelihood of dangerous change to multiple aspects of the climate system, and, like the study by Seneviratne et al. (2016), the use of combinations of climate targets reduces the allowable carbon emissions remaining before these targets are met. The study by Steinacher et al. (2013) is carried out using a set of illustrative targets relating to atmospheric warming, steric sea-level rise, ocean aragonite saturation and terrestrial productivity. They find that the RCB is lower for combined targets than for the most restrictive single target in the set, especially in the long term, due to interdependence between the targets.

Here, we extend an algorithm for generating emissions pathways to reach

warming-only targets (Goodwin et al. (2018a)) to include an additional ocean acidification target, and explore the impact on the RCB of incorporating another climate target. Acidification is used as the accompanying climate target for a few reasons. Firstly, it has been identified as a key issue that impacts many aspects of the ocean ecosystem. Ocean acidification caused by anthropogenic carbon emissions is already causing damage to coral reefs (Kleypas et al. (1999); Hughes et al. (2003); Bruno and Selig (2007)), and these impacts are projected to increase as acidification continues (Pelejero et al. (2010); Pandolfi et al. (2011)). As well as acidification, ocean ecosystems are facing the impacts of ocean warming, which has the potential to worsen the impact on species and ecosystems. For example, the combination of ocean warming and acidification is predicted to reduce the habitable area for tropical and subtropical corals around Japan by half by 2020-2030 (Yara et al. (2012)). The impact of the two stressors together is highly species specific and can also vary with developmental stage, with studies showing that the impacts of the two stressors combined is sometimes synergistic, sometimes antagonistic (Talmage and Gobler (2011); Duarte et al. (2014); Ong et al. (2017)).

Also, it is possible to create an acidification target that is relevant to ocean ecosystems. Elevated CO_2 in seawater will increase acidification (via chemical reactions that result in larger concentration of H^+ ions) and reduce aragonitic calcium carbonate ($CaCO_3$) saturation – so ocean pH can be linked to aragonite saturation (Ridgwell and Zeebe (2005); Cao and Caldeira (2008)). The saturation state with respect to aragonite is an important modulator of coral growth (Martindale et al. (2012); Guan et al. (2015)), the general consensus being that modern shallow water corals require a consistent aragonite saturation state Ω_{arag}>3.4 to be able to grow (e.g. Kleypas et al. (1999)). Cao and Caldeira (2008) found that stabilising atmospheric CO_2 at 450ppm will mean only 8% of existing coral reefs will inhabit waters that satisfy these conditions. The link between increased atmospheric CO_2, ocean acidification and aragonite saturation makes it possible to decide on a communicable acidification target that prevents damage to ocean ecosystems that are in danger from acidification. The well-constrained relationship between cumulative emissions and ocean acidification (Steinacher and Joos (2016)) will aid in reducing uncertainty in the RCB that is caused by the uncertain relationship between carbon emissions and warming.

Although discussion concerning the impacts of ocean acidification is wide-ranging, there has been little successful effort to address ocean acidification in climate policy (Harrould-Kolieb and Herr (2012); Galdies et al. (2020)). In the existing legal framework under the UNFCCC there is no explicit mention of ocean acidification. The Paris agreement, which is arguably the most prominent aspect of climate policy in global discourse, focuses solely on limiting global warming (Oral (2018)). There have been multiple proposed ways to ensure that ocean acidification is properly addressed by the UNFCCC mandate (Lamirande (2011); Harrould-Kolieb and Herr (2012); Kim

(2012)), including the possibility of framing ocean acidification as an effect of warming-related climate change, rather than a concurrent problem (Harrould-Kolieb and Herr (2012)). Putting ocean acidification under the umbrella of warming does mean increased discourse around ocean acidification as an issue and goes some way towards encouraging policy that effectively addresses acidification. However, it is possible to address warming without addressing acidification - for example through geoengineering such as solar radiation management (Zhang et al. (2015)), so the approach is not watertight. An RCB based on an ocean acidification target and a warming target provides a basis to incorporate marine issues into global policy, which have so far been underrepresented in global efforts to mitigate dangerous climate change (Harrould-Kolieb and Herr (2012); Oral (2018); Galdies et al. (2020)).

The aim for this study is to quantify carbon emission pathways that are consistent with both warming and ocean acidification targets, and then use these pathways to explore the impact of multiple climate targets on the RCB. To examine this, we propose a pair of mean ocean pH targets that are analogous with the Paris Agreement range of acceptable global mean warming (as close as possible to 1.5 and well below 2°C warming). The scientific questions for the study follow these aims, and can be summarised as:

1. What are two pH targets that are analogous to 1.5 and 2°C warming targets in terms of feasibility and impacts avoided?
2. How does including these acidification targets change the remaining carbon budget?

2.3 Methods

This study uses an 'Adjusting Mitigation Pathway' algorithm (AMP) to create carbon emissions pathways that restrict global mean warming to a single policy-driven target (Goodwin et al. (2018a)). Originally, the algorithm creates emissions pathways towards a a single warming target. Here, it is extended to include the option of restricting surface ocean acidification to an additional pre-set target of similar stringency to the warming thresholds mentioned in the Paris Agreement, to be used either instead of, or in conjunction with, a warming target. Every 10 years until 2150, the algorithm chooses an emissions rate to stabilise towards the more stringent target (here termed a strict scenario), the less stringent target (lenient), or to take the mean of the emissions rate towards each target (a weighted scenario). It is worth noting that this method will produce different results to the method of Steinacher et al. (2013), because the algorithm effectively addresses one target at a time, with the option to change targets every 10 years at the check point. This means that interdependence

between the target variables does not impact the resulting RCB. After 2150, the algorithm removes carbon if it is above the given target and allows carbon emissions if not, but the scale of carbon emissions or drawdown is no longer calculated using the relationship between warming/acidification and cumulative emissions. The rate of carbon drawdown is greater for a greater overshoot. For more details on the algorithm structure, see Section 2.3.1.

2.3.1 The WASP Model and AMP Algorithm

The Warming, Acidification and Sea-level Projector (WASP) is an 8-box model of the heat and carbon flux between atmosphere (1 box), land (2 boxes) and ocean (5 boxes). 19 parameters describing the climate response to radiative forcing from CO_2, other greenhouse gases and aerosols, and the exchange of carbon and heat between the 8 boxes, are varied randomly within a prescribed range according to Goodwin et al. (2018a). Variation of these parameters causes variation between ensemble members. A visual representation of heat and carbon exchange between these boxes is available in Figure 2.2.

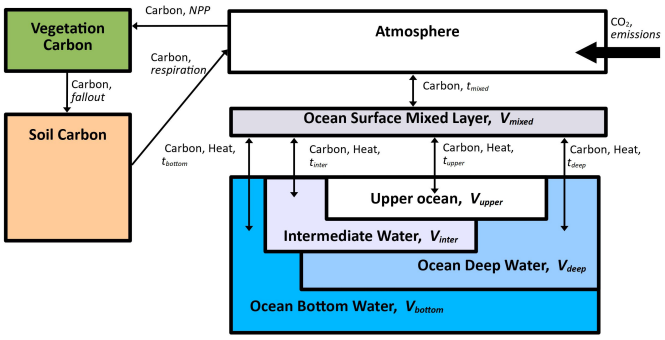

FIGURE 2.2: Schematic of WASP model, adapted from Goodwin (2016).

The model generates a prior Monte Carlo ensemble of 2.5×10^6 simulations with Earth system parameters varied independently according to the current understanding of the climate system (parameters are varied after Goodwin et al. (2018a). Of this initial ensemble, only the model runs that are consistent with historical observations of climate characteristics such as surface warming, ocean heat uptake and ocean carbon uptake are used in projections into the future. See Table 2.1 for a complete list of the observational checks used. Although ocean acidification is not explicitly constrained here, ocean carbon uptake is constrained and the two are linked - constraining both using different datasets may lead to overfitting. Atmospheric CO_2 is also not constrained, because atmospheric CO_2 is the prescribed forcing of the model rather than one of the observational constraints. It is worth noting that the algorithm begins in the year 2020, and the data used for history matching only reaches a maximum of

2016. This means that four years of rapid climate change are omitted, and including these may impact the observationally consistent range of Earth system parameters that result from the history matching. More recent datasets may also be more spatially explicit, leading to a better representation of climate change on the globe and potentially leading to a global mean value with better confidence, narrowing the range of observationally consistent parameters. However, Goodwin (2021) found little change in the WASP model outputs after updating the observational constraints by a few years.

Once the history matching has been completed, the model produces a posterior ensemble of around 10^3 members out of the original 2.5x10^6. Simulations are allowed into the posterior ensemble if they lie within the 90% range of at least 8 out of 9 of the historical observation checks (see Goodwin (2016) for more detailed explanation). Uncertainty in processes impacting warming is represented in the model via variations in, e.g., climate sensitivity and ocean heat uptake, and uncertainty in processes impacting acidification are represented via variations the timescale of equilibration between atmosphere and surface ocean, and timescales of ventilation between ocean layers. These parameters are kept constant throughout a simulation but are varied across the ensemble members.

One of the functions of the WASP model is to create adjusting mitigation pathways towards a given climate target. In its original form, the Adjusting Mitigation Pathways (AMP) algorithm (Goodwin et al. (2018a)) creates pathways towards just a warming target. Here, we expand the AMP algorithm to aim for a warming target and an acidification target. In this section we outline how the AMP algorithm creates pathways towards a target. The key principle of the AMP algorithm is to calculate a carbon budget ($I_{remaining}$) based off a pre-set climate target, then set the emissions rate (C_{rate}) at time t such that carbon budget described by $I_{remaining}$ is linearly reduced to zero:

$$C_{rate}(t) = C_{rate}(t_n)\Big(1 - \frac{t - t_n}{t_{C=0}}\Big) \tag{2.1}$$

Until $t - t_n = t_{(C=0)}$, where $t_{(C=0)}$ is the time at which the carbon emissions rate is reduced to zero (i.e., the carbon budget is used up). This process is repeated every 10 years, to allow for adjustments in the emissions rate that may become necessary in the event of over- or under-estimation of $I_{remaining}$.

$I_{remaining}$ for a given target quantity, X, is defined as

$$I_{remaining}(t_n) = \Big[\Delta X_{target} - \Delta X_{obs}(t_n)\Big] / \Big[\frac{\Delta X}{\Delta I}\Big] \Big|_{obs} \tag{2.2}$$

Where $\frac{\Delta X}{\Delta I}$, the response of quantity X to emissions, is assumed constant over the 10-year assessment period. For warming, this is the transient climate response to

TABLE 2.1: Observational data used for history matching

Climate System Proprty	Reference Period	Period	Observation Consistent Range	Source
Global mean temperature anomaly	1850 to 1900	1986 to 2005	0.55 to 0.67 °C	IPCC (2013)
		2007 to 2016	0.56 to 0.69 °C	Morice et al. (2012), GISS Surface Temperature Analysis (2018)
	1951 to 1960	2007 to 2016	0.54 to 0.78 °C	Hansen et al. (2010), Smith et al. (2008), Vose et al. (2012)
OHC anomaly (upper 700m)	1971	2010	98 to 170 ZJ	Levitus et al. (2012), Giese and Ray (2011), Balmaseda et al. (2013), Good et al. (2013), Smith et al. (2015), Cheng et al. (2017)
OHC anomaly (whole ocean)			117 to 332 ZJ	
SST anomaly	1850 to 1900	2003-2012	0.56 to 0.68 °C	Huang et al. (2015), Kennedy et al. (2011)
Terrestrial carbon uptake	preindustrial	2011	70-250 PgC	IPCC (2013)
Rate of terr. carbon uptake	-	2000 to 2009	1.4-3.8 PgC/year	
Ocean carbon uptake	preindustrial	2011	128-185 PgC	

emissions. For acidification, further explanation is given in Section 2.3.2. An example pathway resulting from this algorithm is shown in Figure 2.3. After 2150 (marked with a vertical line) the algorithm changes so that a linear rate of negative emissions is prescribed if the target has been overshot. Note that there is a difference in the reference period in the algorithm, which is taken as zero radiative forcing. This means that warming is represented as negative for the preindustrial era, and warming seemingly stabilises too low. Because the algorithm is in 'strict' mode, the acidification also stabilises within the target range. For a complete description of how the AMP algorithm works to stabilise at acidification target, see Appendix B. Figure 2.4 shows the algorithm in a simplified flowchart.

2.3.2 Relating Ocean pH to Atmospheric CO_2

Surface ocean pH is closely tied to atmospheric CO_2, since there is an approximately annual timescale for CO_2 exchange between the atmosphere and ocean mixed layer, and seawater pH reduces with ocean CO_2 uptake (Zeebe and Wolf-Gladrow (2001)). Thus, any given minimum surface ocean pH target can be accurately expressed as the

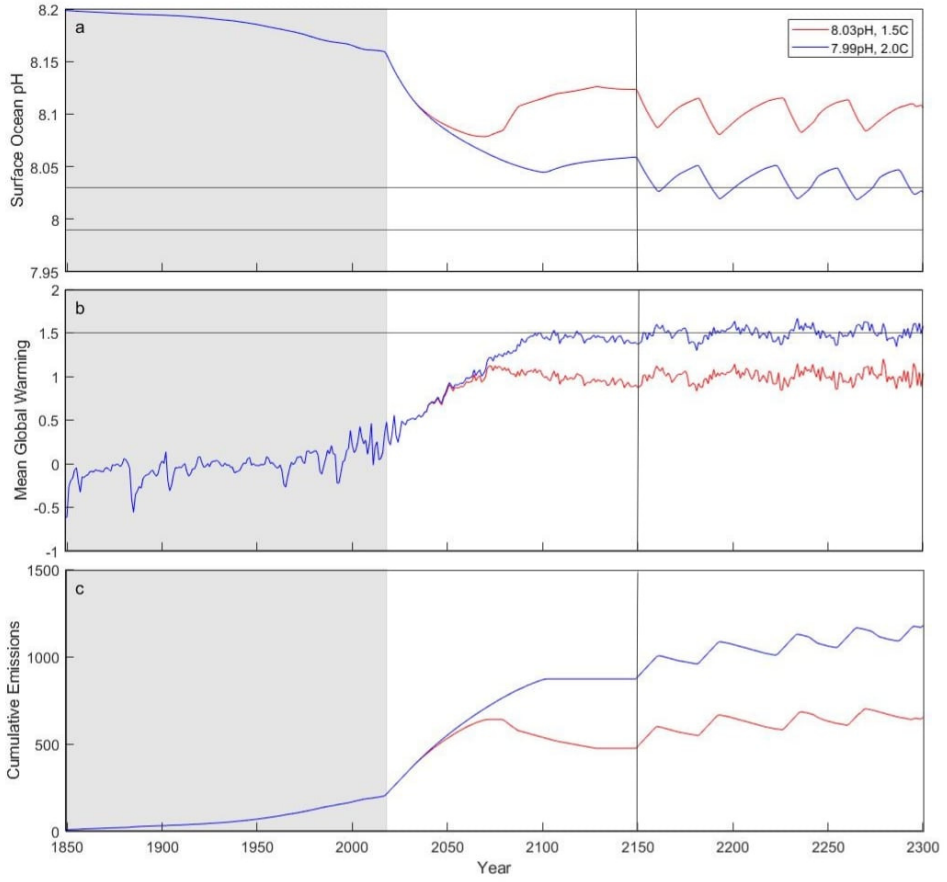

FIGURE 2.3: Example acidification, warming and cumulative emissions pathways following the strict scenario in the AMP algorithm (i.e. the most stringent carbon emissions rate is chosen at each 10-year checkpoint). The red line stabilises towards a warming target of 1.5 (since preindustrial), and a pH target of 8.03. The blue line stabilises towards a warming target of 2.0 (since preindustrial), and a pH target of 7.99. The grey box covers the historical period, where the AMP algorithm is not applied. The vertical line at year 2150 shows where the algorithm changes from an emissions rate calculated using the response of warming or acidification to emissions, from prescribing a rate of emissions based on whether (and by how much) the target is being overshot. Note that the warming appears lower than the target because the algorithm outputs warming relative to zero radiative forcing, rather than relative to the 1850-1900 baseline.

maximum atmospheric CO_2 that corresponds to that surface ocean pH. However, because of the lag of around a year between a change in atmospheric CO_2 and the corresponding change in surface ocean pH, tuning CO_2 emissions directly to a surface acidification target could lead to acidification stabilising just above the set target. To avoid this issue, we express the ocean acidification (minimum surface pH) target in the algorithm as a maximum atmospheric CO_2, corresponding to that ocean surface pH value once the atmosphere and surface ocean have reached chemical equilibrium. The corresponding atmospheric CO_2 is calculated online using the pre-existing

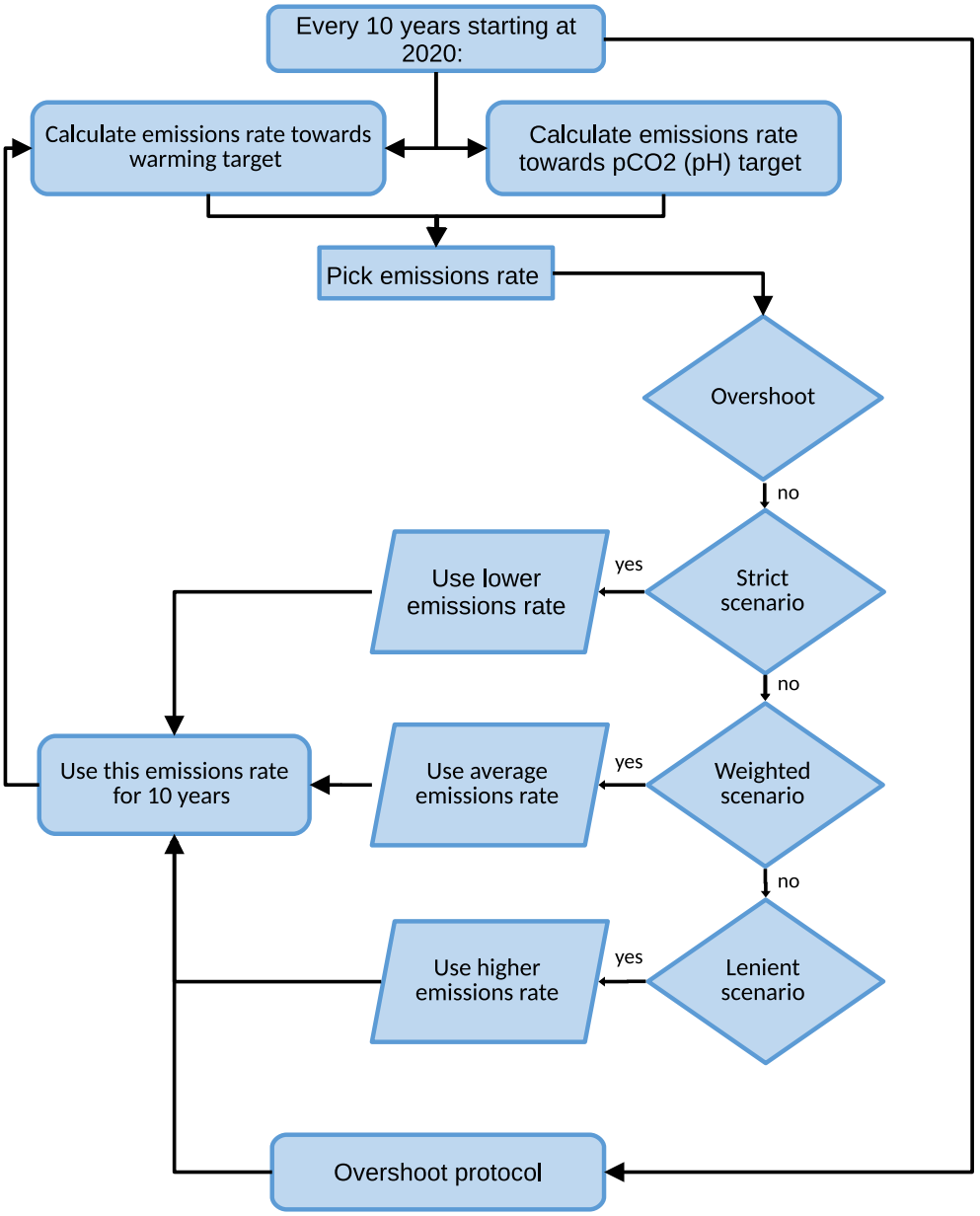

FIGURE 2.4: A flowchart showing how the algorithm works to keep emissions either to a strict, lenient or weighted combination of targets. The acidification-only and pH-only options are omitted for simplicity.

equation within the WASP model relating surface ocean pH to atmospheric carbon:

$$\Delta ln(CO_2(limit) = \frac{\Delta pH(target) - C_{pH1}(-\Delta C_{sat})}{C_{pH1}} \tag{2.3}$$

Where $\Delta C_{sat}$is the difference between the current dissolved inorganic carbon concentration, and the dissolved inorganic carbon that brings the surface ocean into equilibrium with atmospheric CO_2, and C_{pH1} and C_{pH2} are coefficients calculated using a perturbation experiment in an explicit numerical carbonate chemistry solver (Follows et al. (2006)).

This CO_2 target is then used in the AMP algorithm as a proxy for the surface pH target, with the assumption that the atmospheric fraction of emitted CO_2 (the amount of total emissions that remain in the atmosphere, $\Delta CO_{2.atmos} / I_{em}$), remains roughly constant over the duration of each 10-year assessment period (Friedlingstein et al. (2006)), such that the allowable remaining emissions at the beginning of each assessment period is given according to Equation 2.2.

2.3.3 Developing Acidification Targets Analogous to 1.5 and 2°C

We begin by considering changes to regional aragonite saturation that would be considered dangerous to local ecosystems - in the tropics, this would most likely be $\Omega_{arag} < 3.4$ as this is the point where coral growth is compromised (Kleypas et al., 1999). It is worth noting that in higher latitudes, $\Omega_{arag} < 1$ is a more pressing threshold, as this is the point at which other calcifying organisms struggle to build their shells (Kleypas et al. (1999)). For this exercise we focus on the $\Omega_{arag} < 3.4$ threshold at the tropics, which here we define as the band between 30 degrees North and South of the equator. To create a pair of acidification targets, we use the climate projections of the Hadley Centre UKESM1.0-LL (Good et al. (2019)) to find the global mean pH when the area of the tropics that is habitable to corals (where aragonite saturation is above 3.4) reduces to 75% and 50% of the habitable area in 2020. We use projections following SSP245, because the amount of warming in this scenario is great enough to have a favourable signal to noise ratio, and still comfortably within the range of forcing the WASP emulator can simulate (Goodwin (2016)).

We use projections of dissolved inorganic carbon, pH, total alkalinity, ocean surface temperature and salinity from UKESM1.0-LL in an offline carbonate chemistry solver (Follows et al. 2006) to calculate aragonite saturation for every grid point between 30 degrees north and south of the equator. This calculation is initially done for the years 2015, 2050 and 2100. From just these three time points a significant area of ocean with $\Omega_{arag} > 3.4$ is lost by 2050 following SSP245. The global mean pH values that we wish not to exceed therefore lie somewhere in this range. To find them, we count the number of grid squares where $\Omega_{arag} > 3.4$ for several years from 2015 to 2050. Plotting these values against the global mean pH for that year (averaging all grid squares from UKESM1.0-LL), we find that the number of grid squares with $\Omega_{arag} > 3.4$ decreases to 75% of its initial value when global mean pH is 8.03, and to 50% of its 2020 value when global mean pH is 7.99 (Figure 2.5). This yields acidification targets of -0.17 (75%

area remaining) and -0.21 (50% area remaining) for initial ocean pH of 8.2. It is important to note that this relationship is subject to some uncertainty (shown in the shaded areas of the graph in Figure 2.5) so the derived targets are also subject to a small amount of uncertainty. Because the uncertainty is small, we continue the study with just one set of targets rather than examining the impact of uncertainty here.

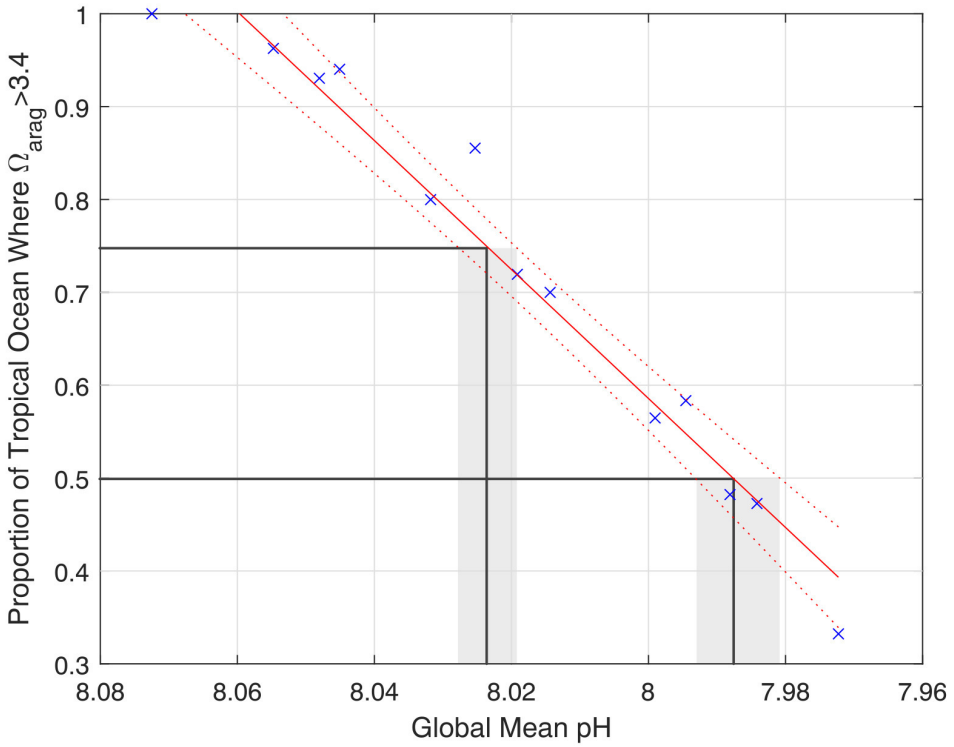

FIGURE 2.5: The global average ocean acidity vs proportion of tropical ocean area where aragonite saturation is sufficient for tropical corals to survive. Red dotted lines indicate confidence intervals, which introduce minimal uncertainty to the resulting acidification targets.

2.3.4 Evaluating the Achieved vs Actual Acidification and Warming for Each Combination Scenario

We run the AMP algorithm for warming targets around the Paris Agreement range, and the acidification targets proposed in Section 2.3.3. For warming, this range is 1.5-2.1°C; for acidification this is -0.225 to -0.1 units. To simplify analysis in later sections, we will assess the performance of each combination scenario in terms of whether the four climate targets of interest are met and discard scenarios that do not consistently meet enough of the targets considered.

Figure 2.6 shows the resultant median warming and acidification for the strict, lenient and weighted scenarios. Figure 2.7 shows the difference between the target and resultant warming and acidification for the same scenarios. Here it is clear that in the

lenient scenario, the warming targets are not reliably met for any combination of targets, and only the less stringent acidification targets are met. The stipulation for the lenient scenario is that the carbon trajectory for the next 10 years should be consistent with at least one target, but it is possible for both targets to be missed by 2100. This outcome can occur if the algorithm overestimates the allowable carbon budget by underestimating the climate sensitivity to emissions, or by underestimating the zero emissions commitment of warming. While this can happen regardless of strict or lenient scenario, overshoot in a lenient scenario is likely to result in both targets being missed, because the algorithm is already choosing to aim towards the climate target that will likely result in the other climate target being missed. The purpose of the multiple targets framework is to prevent additional damage to the climate system, so it is not useful in this case to consider lenient combinations of targets going forward because this does not represent an improvement to current climate discourse.

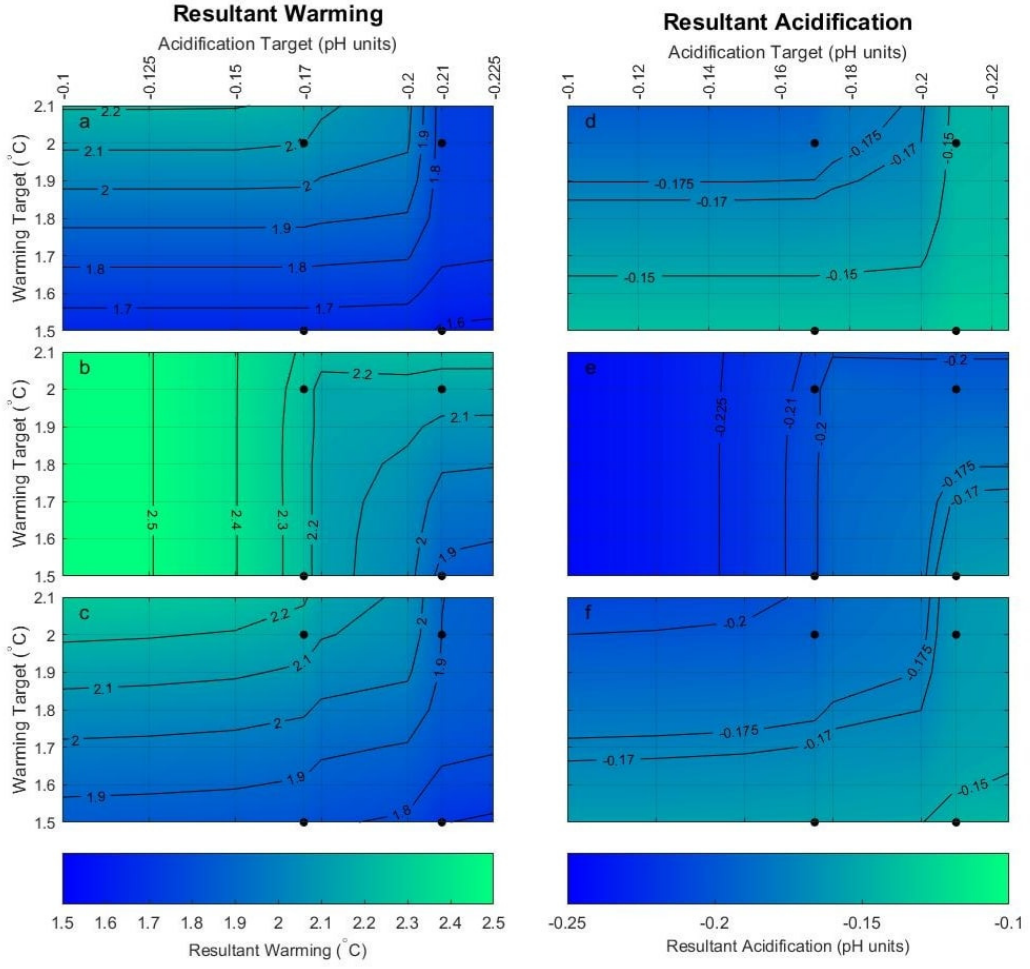

FIGURE 2.6: The resultant warming (right column) and acidification (left column) from strict (top row), lenient (middle row) and weighted (bottom row) combinations of warming and acidification targets.

Figure 2.1b shows the resultant warming from following carbon trajectories towards

just acidification targets, with the black horizontal lines showing warming targets of 1.5 and 2°C. For acidification targets that allow 0.2 units or more of acidification, the median resultant warming exceeds 2°C. We conclude that, although acidification is important, it must be considered in combination with warming targets otherwise it is possible for the warming targets to be exceeded. It is therefore also not worth considering emissions pathways that stabilise at just acidification targets, as this does not constitute an improvement to current political efforts. We will therefore mainly present RCBs for the strict and weighted target combinations in the results section.

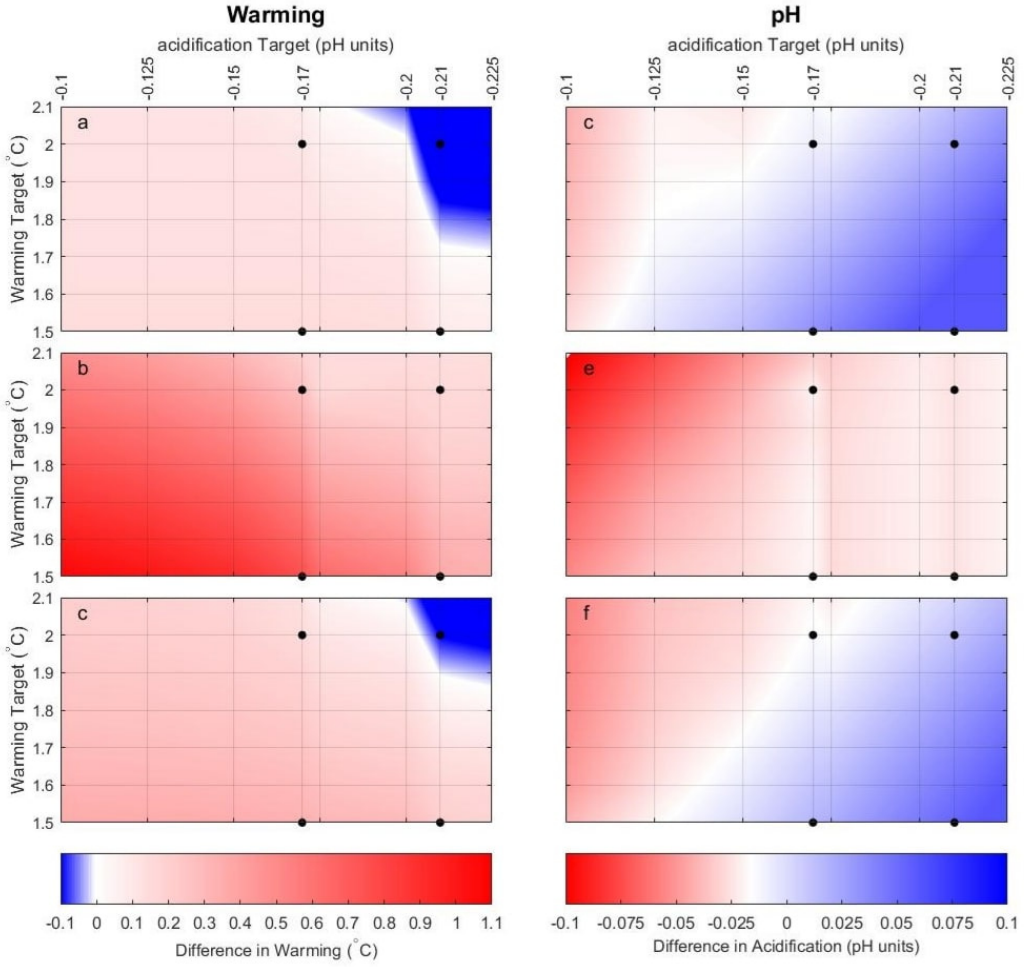

FIGURE 2.7: The difference between resultant and target warming (right column) and acidification (left column) from strict (top row), lenient (middle row) and weighted (bottom row) combinations of warming and acidification targets. Red indicates target has not been met. Based on this, we discard lenient combinations of targets for analysis as they consistently fail to meet warming targets.

2.3.5 Remaining Carbon Budget (RCB)

The nature of the AMP algorithm (creating a cumulative emissions pathway that stabilises to be in line with a given climate target) means it is straightforward to

calculate a carbon budget for the future. This can be done by subtracting the cumulative emissions (CE) for the start year (2020) from the cumulative emissions at a policy relevant and/or time-stable point (t) in the model:

$$RCB = CE_t - CE_{2020} \tag{2.4}$$

Here, the RCB will be evaluated using $t = 2100$, a policy-relevant point as most policy focuses on changes in the nearest century. Many studies now calculate the RCB using the time of peak warming (an avoidance budget rather than an exceedance budget Rogelj et al. (2016)). However the point here is to assess two different sets of targets, so calculating the RCB using the time of peak warming (or acidification) negates the aim of considering the two things together. The year 2100 is chosen because by 2150, the nature of the algorithm changes.

2.4 Results

2.4.1 Remaining Carbon Budgets Towards Two Climatic Targets

Figure 2.8 shows the RCB for a strict combination of warming and acidification targets. To examine uncertainty in projections, we present the 5th, 50th and 95th percentiles. Here, horizontal contours indicate that the choice of pH target has no impact on the RCB (i.e., the algorithm favours the warming target-consistent emission rate at each ten-year interval), and vertical contours the opposite. From these contours we can find the median, 95th and 5th percentiles of the carbon budget consistent with a strict combination of the warming targets and the pH targets chosen in this study. For a combination of 8.03pH and 1.5°C warming (the two more stringent targets) the median (5th-95th percentile) RCB is 24 (-73.8 to 129.8) PgC. For the two less stringent targets of 7.99pH and 2°C warming, the RCB is 315.2 (114.4 to 502.4) PgC.

Figure 2.9 shows cumulative emissions of carbon over time since 2018 for a select combination of pH and temperature targets. In these panels, stable cumulative emissions indicate that yearly emissions have been reduced to 0. A 'combined target' trajectory corresponding with a 'single target' trajectory indicates that the model is favouring the emissions rate consistent with the same target at every 10-year interval. The shaded area shows the 5-95th percentile range: a narrower plume indicates more certainty in the cumulative emissions consistent with the set target(s). Note that the uncertainty is noticeably narrower for the trajectories towards combined targets (strict and weighted), than when towards just a warming target. In all panels, we see a peak-and-decline pattern in cumulative emissions to stay on track towards the given combination of targets. This prompts us to consider the benefit of considering the

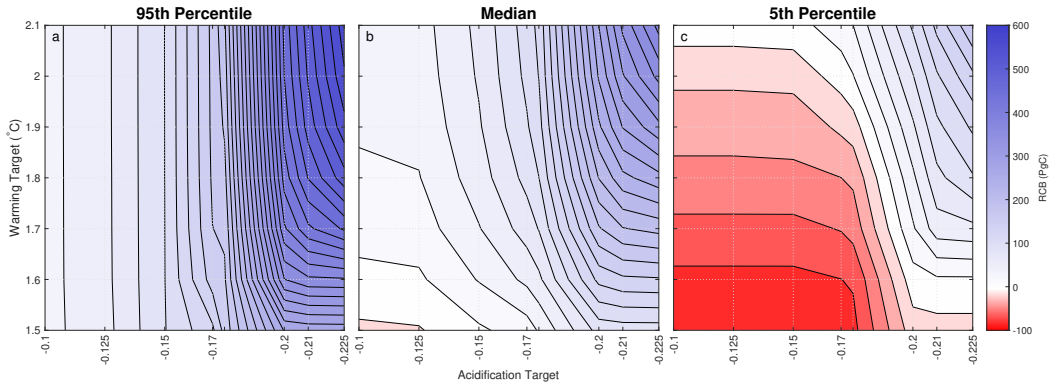

FIGURE 2.8: Contours of the 95th, 50th and 5th percentile RCB (panels a, b, c respectively) for a strict combination of all warming and pH targets considered in the study.

extra target of acidification in terms of the difference in emissions reductions necessary to stay on target between the peak in cumulative emissions and 2150, when the 10-year checks for re-assessing carbon emissions rate cease. For the more stringent acidification target (-0.17) and less stringent warming target, the necessary emissions reduction reduces from 145PgC for just a warming target to 10PgC for both: a 93% change (top right panel). Although this change is smaller in other panels (and non-existent in 8d, where the warming target is more stringent than the acidification target), there is still a change of 58% and 32% in Figure 2.9b and c respectively.

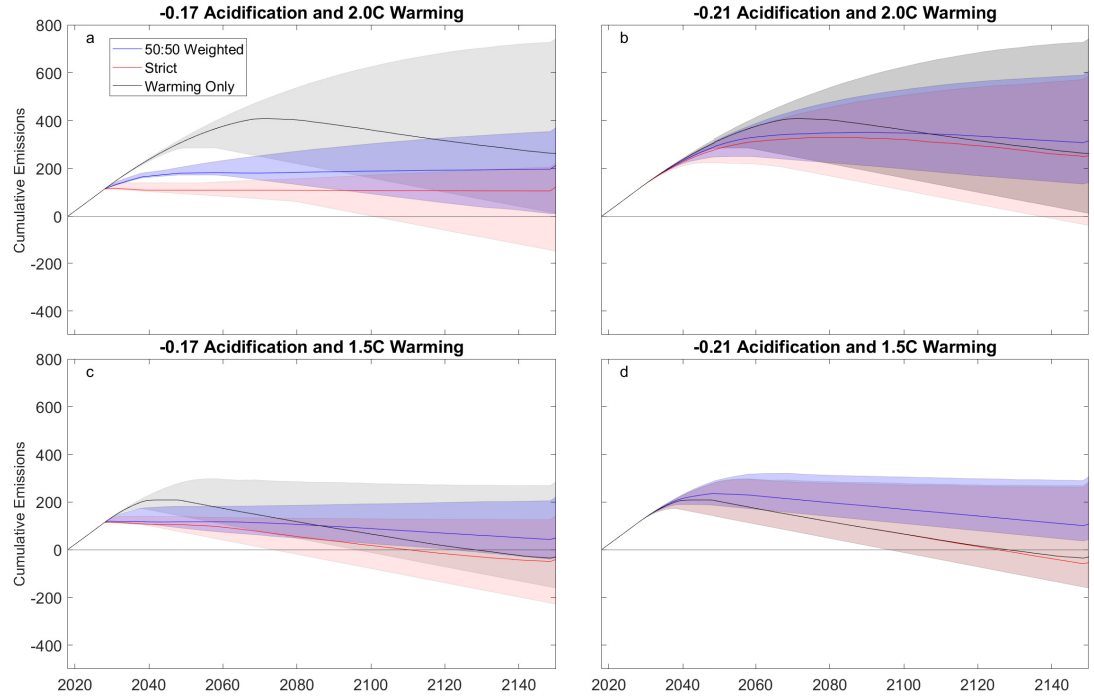

FIGURE 2.9: Plumes of cumulative emissions since 2010 for warming and pH targets of 1.5/2°C and 7.99/8.03pH respectively. Here we present strict, warming only and 50:50 weighted, as these are the more likely to hit both targets. Solid line = median, shading = 5-95 percentile.

In Figure 2.10, we see the impact on the parameter space of taking a 50:50 weighting of the two potential emission rates. Note that this is not necessarily a weighting of the strict and lenient scenarios, but a weighting of the temperature-only and the pH-only scenarios.

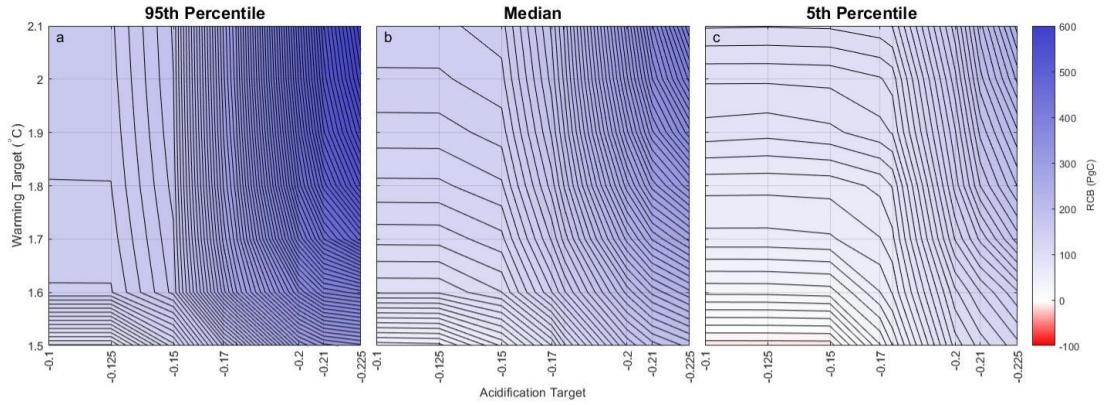

FIGURE 2.10: Contours of the 95th, 50th and 5th percentile RCB (panels a, b, c respectively) for a weighted combination of all warming and pH targets considered in the study.

The RCB for the pH targets is generally larger than the RCB for warming targets (Figure 2.6 and Figure 2.7, respectively). For the pH targets of 8.03 and 7.99pH, the median (5-95th percentile) RCB is 140.2 (59.2 to 192.1) PgC and 377.9 (218.3 to 519.2) PgC, respectively. For the warming targets of 1.5 and 2°C, the RCBs are 92.4 (-7 to 297.2) PgC and 378.2 (165.7 to 618.7) PgC, respectively.

Figure 2.11 shows the probability distribution of RCB for the warming and pH targets generated in this study. This indicates when the range of acceptable future emissions is reduced by introducing another climatic target. For combinations of targets where one target is obviously more stringent than the other (panel d), the RCB consistent with a strict combination of the two targets matches the more stringent target (consistent with the nature of the algorithm) and therefore there is no reduction. In cases where the targets are of a comparable stringency (panels b, c), the lines do not intersect because the algorithm is less likely to favour just one target, and may switch targets at the next check point. In these cases, the strict RCB has a narrower range than the RCB towards just a warming target. The probability distribution of an RCB following an acidification target is considerably narrower than that for a warming target due to the higher certainty in the relationship between atmosperic carbon and surface ocean acidification in the WASP model. Also note the double peak in the strict scenario in 10c (the two more stringent targets in combination). This likely arises from the way the AMP algorithm handles overshooting each target – if the warming target is overshot, the algorithm prescribes negative carbon emissions at a rate that is scaled to the level of overshoot. If the acidification target is overshot, the same rate of carbon removal is prescribed regardless of how much the target is overshot. The double peak

will only exist for target combinations where overshoot of both targets is feasible, otherwise the algorithm would deal with the overshoot more consistently.

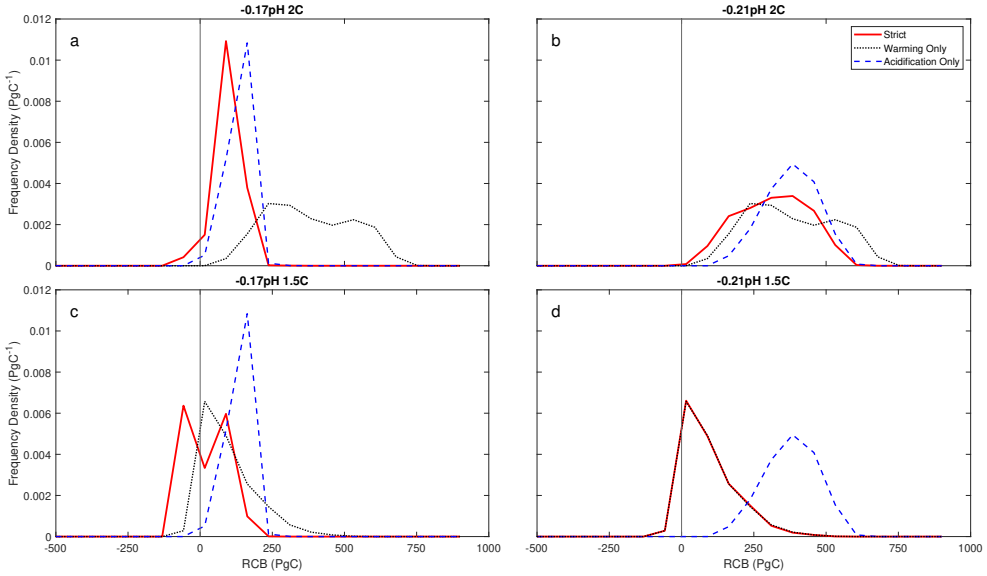

FIGURE 2.11: probability density functions of the RCB for 2100 for warming and pH targets of 1.5/2°C and 7.99/8.03pH respectively.

2.5 Discussion and Conclusions

A central goal in climate science is to create communicable carbon emissions trajectories and budgets that are consistent with a politically chosen climate goal. Conventionally, this is a single target of global mean surface warming, but emissions trajectories consistent with the political warming targets of 1.5 and 2°C are not sufficient to prevent dangerous change in other aspects of the Earth system. The purpose of this study is to explore whether considering a second carbon-related target alongside warming makes a difference to the remaining carbon budget, and therefore to provide some impression of how comprehensive a single warming target is as a unifying goal in climate mitigation policy. To do this, we quantify the difference between carbon budgets consistent with one climate target and two climate targets. We examined the RCB for a range of temperature and pH targets between 1.5 and 2.1°C and 8.1 and 7.9pH, respectively. Based on a strict combination of these targets (i.e., where emissions reductions take the pathway to the most stringent target as analysed every ten years), the median RCB for 2100 ranges from 500PgC for the least amount of mitigation (2.1°C warming, -0.3 acidification) to -100PgC for the most amount of mitigation (1.5°C warming, -0.1 acidification). The median RCB and the year at which the budget will be spent (assuming a constant emission rate of 10.9PgC/year, equal to that in 2021 according to the IEA) is given in Table 2.2.

	Remaining Carbon Budget (PgC)				Year of Expiry			
	1.5°C		2.0°C		1.5°C		2.0°C	
	strict	weighted	strict	weighted	strict	weighted	strict	weighted
-0.17	24.6	98.3	104.1	194.0	2023	2029	2030	2038
-0.21	91.5	182.7	315.2	354.4	2029	2037	2050	2053

TABLE 2.2: The remaining carbon budget and year of expiry for strict and weighted combinations of the main targets considered in this study

A key result from the study is the impact on the RCB of including a second target for ocean acidification. To illustrate, we consider the impact when running the AMP algorithm on a strict setting – i.e., both targets must be met. If the acidification target is considerably more relaxed than the warming target (see Figure 2.11d), the AMP algorithm consistently favours the warming target, so there is no impact. However, in cases where the acidification and warming targets are of a similar stringency (Figure 2.11b,c), uncertainty is reduced – and this reduction comes from cutting off the high-end estimate of the RCB derived from just aiming for the warming target. If the acidification target is considerably more stringent (Figure 2.11a), the difference in the median and spread of the RCB is more marked. Uncertainty in the combined RCB is lower than the carbon budget based on a single warming target, but the RCB with the highest certainty is framed using a single acidification target. This is due to the high level of certainty in the relationship between atmospheric carbon dioxide and ocean pH, caused by the short timescale of CO_2 exchange between atmosphere and ocean. We also find that the emissions trajectories towards combined targets are 'smoother', with less of a peak-and-decline shape – where declining cumulative emissions means that carbon is being removed from the atmosphere. This means a more urgent need to reduce emissions in the short term, with the benefit of needing less carbon dioxide removal (CDR) in the future. Given that CDR technology is still nascent, and its impacts on aspects of the climate system beyond warming are still uncertain, a scenario that commits us to less need for CDR is beneficial.

The motivation for considering more than one climate target when calculating a remaining carbon budget is that the uncertainty in the relationship between warming and cumulative carbon emissions means that there is a range of potential allowable emissions that is consistent with one warming target. This means that there is a range of potential damage to the climate system that may be sustained, even if warming stays consistent with the Paris Agreement (for example). We therefore wish to consider whether a second climate target will avoid additional damage to other aspects of the Earth System. We find that the adoption of the additional aim to limit ocean acidification reduces uncertainty in the remaining carbon budget by lowering the upper limit of the probability distribution. This decrease in allowable emissions (if honoured in global climate change mitigation policy) will increase the likelihood that

the most dangerous effects of climate change can be avoided across multiple facets of the climate system.

2.6 Extra Published Material

The following materical accompanies the above peer-reviewed paper.

2.6.1 Plain Language Summary

The relationship between atmospheric CO_2 and warming is uncertain, which means that we do not know precisely how much carbon we have left to emit until we reach the acceptable range of warming outlined in the Paris Agreement (keeping warming well below 2°C and as close as possible to 1.5°C). However, the relationship between atmospheric CO_2 and ocean acidification is better understood, so by considering targets for acidification rather than warming alone, we can narrow down our estimate of how much emitted carbon is acceptable. Including acidification targets as well as warming targets means that we can directly address the issue of ocean acidification, which poses a threat to corals and the ecosystems reliant on them. By considering acidification and warming targets together, we can lower uncertainty in acceptable carbon emissions by 29%.

Key Words: Remaining Carbon Budget

Acidification

Warming

Earth Systems Model

2.6.2 Supplementary Materials

The supplementary materials that were published with this chapter are available in Appendix B.

Chapter 3

Nonlinear Ice Interactions in a Simple Earth Systems Model and their Implications for Future sea-level rise

3.1 Abstract

sea-level rise (SLR) is a major result of climate change that threatens coastal communities and has the potential to affect the lives and livelihoods of hundreds of millions of people and incur significant economic damage. Projecting SLR as temperatures increase is therefore crucial for climate mitigation policy and adaptation decisions. One key issue when projecting SLR is uncertainty in the land ice response to warming. Although nonlinearities exist within processes affecting this response, most existing semi-empirical models treat the relationship between warming and ice-melt as linear. This study will examine the effect on semi-empirical projections of SLR of observed nonlinearities in the relationship between historical warming and sea-level rise from ice, by adding a nonlinear term to the relationship between warming and the rate of SLR within a large ensemble of historically constrained efficient earth systems model simulations. The results show that that nonlinearities have a bigger impact on the uncertainty range of sea-level rise projections than on the best estimate, so the nonlinear setup increases the upper end of projections more than the median. This effect is exaggerated in higher warming scenarios, with the 97.5th percentile for SSP585 increasing by 1.6m by 2300, and the rate of sea-level rise increasing to up to 6 times the current rate for 4 times the amount of warming (97.5^{th} percentile). This has important implications for practitioners who are interested in high-impact, low-probability futures.

3.2 Introduction

sea-level rise (SLR) caused by global warming is a significant threat to human existence and coastal ecosystem health, and its impacts are expected to worsen as warming continues. From 1901-2018, sea levels rose by 20.2 cm (with a likely range of 15.0 to 25.3), meaning a median rate of 1.73mm/year. This is accelerating, with the median rate of SLR from 2006-2018 reaching 3.69mm/year. As well as the SLR that is already occurring, there is a certain amount of committed SLR due to the time lag in the sea level response to warming. With the long-term sea level sensitivity to warming at around 2.3 m/°C (Levermann et al. (2013)), at current warming levels we are already committed to a SLR of around 2.7m over 2000 years. Mengel et al. (2018) calculated that if greenhouse gas emissions peak in 2020 and then are reduced to net zero at a rate of 0.3GtC/year, the resulting global mean SLR would still be around 1m by 2300. If warming is avoided through reducing CO_2 emissions alone (rather than reducing all greenhouse gases), the resultant SLR by 2300 is around 40 cm higher. Nauels et al. (2019) estimated that warming up to 2016 has led to a likely range of committed SLR of 0.7-1.1m by 2300, and the latest NDC commitments increase this to 0.8-1.4m by 2300. The addition of a warming target of 1.5°C in the Paris Agreement marks a political effort to limit warming to a level consistent with manageable SLR; the main proponents of the extra warming target were representatives from small island nations who are most at risk from SLR (Ourbak and Magnan (2018)). In order for the goals of the Paris Agreement to be met, emissions must be net-zero by 2100. The ratification of the Paris Agreement into law in the signatory nations therefore means that SLR by 2300 can be related to 2050 emissions levels (Mengel et al. (2018)). The difference in median sea-level by 2030 in scenarios that reach net-zero CO_2 by 2050 is caused by just the difference in emissions rates before 2050, implying that near-term emissions reductions can be used as a predictor for long-term SLR in a scenario where the Paris Agreements are to be met.

A significant, and growing, contributor to SLR is melting ice from ice sheets, ice caps and glaciers (Fox-Kemper et al. (2021)). This study will focus on the ice melt contribution, examining how the relationship between ice melt and warming can be expressed in a climate emulator and how the observed relationship progresses into the future.

Uncertainties in ice melt and its contribution to SLR is a consistent issue in SLR projections; especially the contribution from the Antarctic Ice Sheet, which is characterised by 'deep uncertainty' in the latest IPCC report (Fox-Kemper et al. (2021)). This can be related to uncertainty in three things: (1) external forcing, (2) the ocean response to external forcing, and (3) the ice sheet response to oceanic forcing (Levermann et al. (2014)). In exploring these, Levermann et al. (2014) found that the greatest source of uncertainty is in external forcing (i.e. scenario uncertainty – melt in

Antarctica is highly dependent on how much warming is experienced there). Li et al. (2023) explored the uncertain sensitivity of the Antarctic ice sheet to external forcing. They found that differences in the atmosphere-ocean models used to force ice sheet models can lead to wide variation in the projected equilibrium states of the Antarctic Ice Sheet, and different outlooks on whether self-sustaining retreat mechanisms like marine ice sheet instability (MISI) and Marine Ice Cliff Instability (MICI, as described by DeConto and Pollard (2016) and DeConto et al. (2021). MISI describes a viscous positive feedback mechanism where the grounding line retreats inwards along a retrograde slope. Parts of the Amundsen Sea Embayment are exhibiting accelerating retreat that could be MISI, but it is difficult to quantify whether this is retreat following a MISI-like tipping point (Rosier et al. (2021)). MICI describes a brittle positive feedback mechanism, where an ice cliff collapses under its own height once an ice shelf has disappeared. This is so far unobserved, and support for MICI having occurred in previous periods of ice cliff retreat mainly derives from a lack of ice cliffs above a critical height of 90m (Bassis and Walker (2012)).

Edwards et al. (2021) assessed uncertainty in the Antarctic ice sheet response to forcing by considering two sets of projections, one 'standard' and one 'risk-averse' which contained a more pessimistic set of assumptions about the sensitivity of Antarctic melt. They found that for a middle of the road SSP scenario, (SSP 245), the range of land-ice contribution to sea-level was significantly different depending on the assumptions made about ice melt in Antarctica. Their projections ranged by around 25cm in the standard projections by 2100, and by up to 40cm in a risk-averse model configuration. The difference caused by making the standard versus risk-averse assumptions is impactful enough that the low-end scenario (SSP119) projections in the risk-averse configuration overlap with the high-end scenario (SSP585) in the standard configuration. The change in the range of SLR for the risk-averse configuration reflects the specific uncertainty of the reaction of Antarctic ice to a warming world, due to the competing feedbacks of increased snow versus increased ocean temperature that are caused by global warming. They also found some nonlinearity in the relationship between warming and ice melt from glacier regions in Central Europe and the Caucasus, as well as ice melt in the Antarctic and Subantarctic periphery.

The two methods most widely used to project future changes in sea level are process-based modelling and semi-empirical modelling. Process-based models rely on combining outputs from coupled atmosphere-ocean models for each component of SLR, such as those that were used for the IPCC Sixth Assessment Report (Fox-Kemper et al. (2021)). Semi-empirical models calculate sea level as an integrated response to either warming (e.g. Kopp et al. (2014)) or radiative forcing (e.g. Jevrejeva et al. (2010)) using simple physically motivated relationships with parameters that are derived from past observations. Historically, there is little agreement in sea-level projections between these two methods, with semi-empirical projections exceeding

processed-based projections by 2-3 times (Orlić and Pasarić (2013)). Indeed, some of the semi-empirical models used in IPCC AR5 projected median and 95th percentile SLR up to twice as high as the process-based models (Church et al. (2013)).

Studies since AR5 have narrowed the gap between semi-empirical and process-based projections (e.g. Mengel et al. (2016); Bittermann et al. (2017); Kopp et al. (2017)), notably by separating contributions to SLR, to avoid problematically combining processes that act on different time scales (e.g. Mengel et al. (2016); Goodwin et al. (2017)). By the time the IPCC SCROCC was published, the gap between semi-empirical models and process-based models had narrowed considerably (Oppenheimer et al. (2019)). It was noted that progress in understanding ice dynamics and the sea level budget had reduced the need for semi-empirical models as a process-blind point of comparison, and semi-empirical models were not used for this purpose in AR6 (Fox-Kemper et al. (2021)). The SROCC also noted that the semi-empirical method for calculating sea-level rise often poorly represented the contribution from ice. Jackson et al. (2018) compared 21st century SLR in line with the Paris Agreement targets from process-based and semi-empirical models, and found that the mean and variance of sea level in 2100 are both larger in semi-empirical models. They found that the difference in the median and spread in projections is mainly due to the difference in estimates of ice melt contributions.

The use of semi-empirical models as a basis for comparison becomes helpful due to the number of processes that are too complex to be resolved in process-based models. Because semi-empirical models are computationally cheap, they can be used to create larger ensembles than process-based models, and are therefore an effective way to explore uncertainty in SLR projections. However, although semi-empirical models are not limited by difficulty in resolving small-scale processes, there are issues associated with the methods used to represent the relationship between ice melt and warming. This relationship is generally represented as linear in semi-empirical projections of SLR (Meehl et al. (2012); Levermann et al. (2020)), but nonlinearities do exist (e.g. Pollard and Deconto (2005); Tigchelaar et al. (2019); Grinsted and Hesselbjerg Christensen (2021)). One notable example of this is the inclusion of MICI in ice-melt simulations. There is low confidence in the timing and magnitude of the impact of MICI on SLR, but IPCC AR6 (Fox-Kemper et al. (2021)) included projections of SLR in AR6 that allow MICI. This increased the likely range of SLR to 1.1 to 2.1m by 2100, compared to the low-confidence projections with no MICI that had a likely range of 0.6 to 1m (following SSP585). DeConto et al. (2021) found that in scenarios where warming reached 3.0°C, the rate of Antarctic ice loss in a model that allows MISI and MICI-like retreat suddenly increases around 2060, and reaches around 0.5cm of sea-level rise by 2100.

Grinsted and Hesselbjerg Christensen (2021) defined a transient sea level sensitivity (TSLS) as the ratio of the rate of SLR at the end of a century to the average warming of

the preceding century. This was assumed to stay constant over short timescales (century-scale) and was therefore recommended as a sense check for model representations of SLR through comparison with the TSLS calculated from observations. When comparing the TSLS projections from IPCC AR5 (Church et al. (2013)) to that from observations, they find the TSLS is lower in the AR5 projections – implying either that the projections are biased low, or that nonlinearities are impacting the consistency of the transient sensitivity. Given that these nonlinearities would have to be sublinear for the projected TSLS to be lower, which is inconsistent with understanding of how sea level contributors behave with warming, it can be assumed that the issue is low bias in IPCC projections. This fits with other studies that have concluded that underestimation of SLR has been common for IPCC reports (see Garner et al. (2018)). The study by Grinsted and Hesselbjerg Christensen (2021) may omit nonlinearities that are small at low levels of warming (and therefore less visible in the observational record), but that begin to take place at higher levels of warming. Further, any such nonlinearities that are omitted in the IPCC AR5 projections (Church et al. (2013)) would cause a low bias when comparing the TSLS.

Grinsted et al. (2022) took the concept of TSLS further and considered the TSLS of observations, CMIP6/ISMIP projections and the structured expert judgement of Bamber et al. (2019). Differences in the TSLS between models and structured expert judgement studies can be interpreted as reflecting a mismatch between expert understanding and modelling capabilities. There are instances (relating to the Greenland and Antarctic ice sheets especially) where the DOI: 10.1111/gcb.14431 estimate of TSLS is higher than that calculated from ISMIP studies (Bamber et al. (2019); Payne et al. (2021)), and (crucially) higher than that calculated from observations. This implies knowledge of potential superlinear relationships between warming and ice melt that is not yet represented in the model projections examined in the study, but that can cause the TSLS to increase with warming. One concrete example they cite is the linear parameterisation for dynamic ice melt in Greenland, which leads to a weaker dynamic response to warming. There is also a large difference between model and Structured Expert Judgement-based TSLS for Antarctic ice melt, with model results implying a sensitivity about a third of that of the sensitivity based on Structured Expert Judgement. Nonlinear interactions and their potential to impact the future SLR contribution from melting ice sheets should not be ignored, because these nonlinear processes have the potential to contribute to a significant amount of SLR in scenarios with a larger amount of warming (Pattyn et al. (2018)).

This study will assess SLR projections following SSPs 126, 245 and 585 scenarios, using the WASP climate emulator with a semi-empirical method for calculating SLR (Goodwin et al. (2017)).The method used in the WASP model for calculating SLR is configured here, for the first time, with a nonlinear component in the ice-melt contribution to SLR. This study represents a new insight into the impact on SLR

projections of allowing the contribution from ice melt to vary nonlinearly with warming. Using a climate emulator for this allows an in-depth exploration into the nature of this nonlinearity, because it is computationally cheap so allows for efficient examination of a wide parameter space. The SLR projections also extend up to 2300 (consistent with AR6, Fox-Kemper et al. (2021)), which provides insight into the timing and magnitude of changes in sea level for the next couple of centuries. Section 3.3.1 outlines how SLR is calculated in the climate emulator, and how it is calibrated using observational data. Section 3.4 describes the resulting sea level projections and explore the nature of the observation-consistent nonlinearities, and Section 3.5 discusses these results.

3.3 Methods

3.3.1 Climate Emulator Equations

This study uses the Warming, Acidification and Sea Level Projector (WASP) climate emulator developed by Goodwin et al. (2017). This model has already been used to estimate sea-level change (Goodwin et al. (2017); Brown et al. (2018)). Goodwin et al. (2017) projected SLR following RCPs 4.5, 6.0 and 8.5, and assessed the flood risk at 20 tide gauges around the world in 2100. They also compared the difference in projections and model behaviour when calibrating the model using CMIP5 outputs and observations, and found a higher sensitivity to ice melt when calibrating using observations. Brown et al. (2018), used the updated WASP SLR projections of Goodwin et al. (2018a), to assess the land and population impacted by SLR consistent with 1.5 and 2.0°C of warming, by quantifying the land and people exposed in the 1 in 100 year flood plain. In both of these papers, the ice melt contribution to SLR is linearly related to warming and calibrated using observations, and steric rise has been linearly related to ocean heat content. For more details on each component of global mean sea-level rise, see Appendix C. This method is an expansion of the method of Rahmstorf (2007), where SLR from all sources is linearly related to warming via a single constant. This linear relationship between warming and SLR from ice melt may hold for analysis of the next century – however to assess longer term changes, it becomes necessary to consider ice melt in response to warming in more depth. The method for this study is an extension of a previous method of Goodwin et al. (2017), where $\frac{d}{dt}GMSL_{ice} \propto \Delta T$, to allow the sea level contribution of ice melt to vary nonlinearly with warming, such that:

$$\frac{d}{dt}GMSL_{ice} = (a\Delta T + b\Delta T^2)\left(\frac{c\Delta T - \Delta GMSLR_{ice}}{c\Delta T}\right) \tag{3.1}$$

where $\frac{d}{dt}GMSL_{ice}$ is the rate of global mean SLR from ice melt in m yr^{-}1; ΔT is global mean temperature rise in K; $\Delta GMSL_{ice}$ is the global mean sea-level rise from ice in m; a is the linear sensitivity of SLR from ice melt to global mean surface temperature in m yr^{-1} K^{-1}; b is the second order sensitivity of SLR from ice melt to surface warming in m yr^{-1} K^{-2}; and c broadly represents the equilibrium SLR sensitivity to warming from ice melt in m K^{-1}.

For this study, the extra term ('b' in Equation 3.1) has been added to the ice melt contribution to allow for a nonlinear relationship between warming and ice melt to continue. The equation also includes a term to stabilise SLR from ice melt towards an equilibrium, with a third parameter 'c' broadly representing the equilibrium sensitivity of SLR from ice melt to global temperature change – for more details on how this is defined, see Appendix C. This final term accounts for the lowering contribution of ice to SLR as global ice volume declines. This value of equilibrium SLR is obtained from palaeo records of the Last Interglacial by Kopp et al. (2009), which serves as an analogue of a 2°C warmer world.

It is important to account for ice sheet hysteresis: the fact that it requires substantially more cooling to refreeze the same volume of ice as a given amount of warming will melt - see e.g. Pollard and Deconto (2005). This is done by making the ice melt contribution zero if the change in temperature is negative (i.e., atmospheric cooling). This method assumes that ice melt due to ocean heat content is also reduced to zero in the event of atmospheric cooling. Although some surplus heat will remain in the ocean, ice melt is predominantly influenced by surface ocean temperature. Surface ocean heat content is more strongly linked to atmospheric warming than ocean heat content throughout the water column, so the assumption is acceptable – and preferable to allowing ice to regrow at the same rate that it melts.

3.3.2 Large Ensembles and Bayesian History Matching

The WASP model generates a large initial (prior) ensemble of simulations with randomly varied Earth system parameters. The simulations that can accurately recreate observations of climate characteristics outlined in Table 3.1 are then kept for the posterior ensemble. For this study, the prior ensemble has 16x10^{8} members, and the posterior ensemble (upon which the analysis is conducted) has a simulation number in the order of 10^{4}. The results cover sea-level rise projections for SSPs 126, 245 and 585, to cover a range of potential futures. While SSP585 is an extreme future and is generally not considered feasible, it is used here for comparison with projections from IPCC AR6 (Fox-Kemper et al. (2021)).

For SLR from ice melt, there are two observational consistency checks. The model is tested to see if it can recreate the gradient of SLR from ice from 1901-1990, and

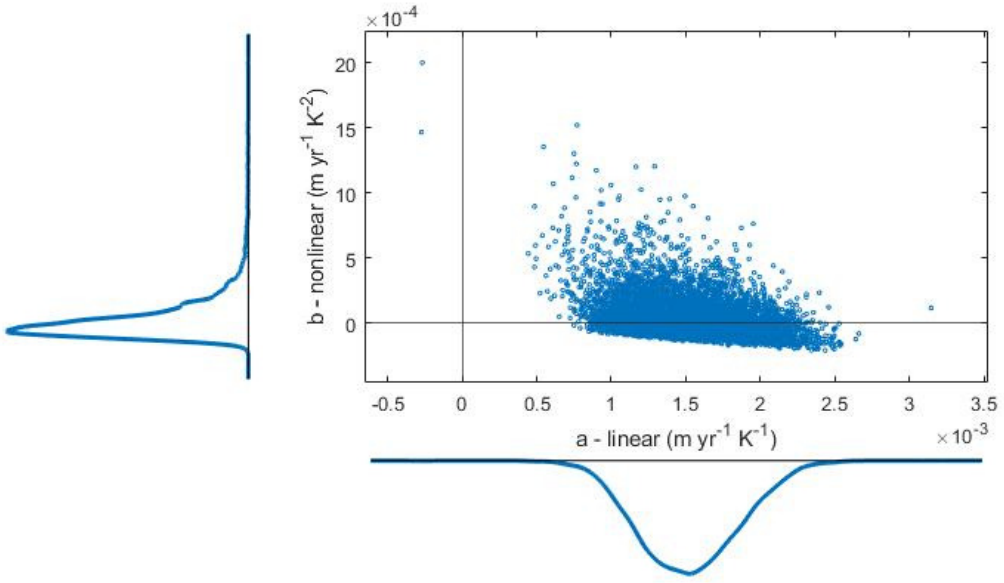

FIGURE 3.1: The values of linear coefficient a and nonlinear coefficient b according to Equation 3.1

1993-2018. The data used for these checks are obtained from IPCC AR6 (Fox-Kemper et al. (2021)). sea-level rise from ice is constrained alone because the thermosteric contribution is already constrained by the observation consistency checks for ocean heat content. The simulations that pass the checks are then weighted according to how well they fit observations, and run to 2300 to provide projections of SLR. The resultant projections are therefore an extrapolation of observed Earth system dynamics, and do not contain any representation of thresholds or tipping points that were not passed during the historical period. This means that this study essentially provides a baseline assessment of how nonlinearities in the relationship between warming and ice-melt can impact SLR, with the potential for these effects to be increased in the future as further thresholds may be crossed.

Figure 3.1 shows the values of the linear versus nonlinear coefficients in the SLR equation (a and b respectively). Due to the history matching method used by WASP, there is a largely compensatory pattern between the two coefficients, with a larger value for the linear coefficient corresponding to a lower value for the nonlinear coefficient. While the nonlinear coefficient centres on 0, positive values are of a larger magnitude than negative values. This makes sense in the context of the equation: b is multiplied by dT squared, so has to be much bigger for a slightly smaller value of a when warming is small (as it is over the observational period).

For each quadrant of this graph (representing different combinations of positive and negative linear and nonlinear interactions), different processes may be dominating. Here, it is important to remember that negative values for the nonlinear coefficient mean processes that contribute to a sublinear relationship with warming, but not

TABLE 3.1: The observational data used for Bayesian history matching.

Climate System Property	Reference Period	Period	Mean	Standard Deviation	Source
Surface Warming Anomaly	2000 to 2018	1850 to 1899	-0.973°C	0.074°C	HadCRUT5 ensemble, Morice et al. (2021)
		1900 to 1919	-1.042°C	0.067°C	
		1920 to 1939	-0.820°C	0.061°C	
		1940 to 1959	0.666°C	0.064°C	
		1960 to 1979	-0.706°C	0.027°C	
		1980 to 1999	-0.374°C	0.023°C	
OHC anomaly (700m)	1960 to 1969	2006 to 2015	177.8 zJ	13.8 zJ	Cheng et al. (2017)
OHC anomaly (700-2000m)			75.6 zJ	12.3 zJ	
OHC anomaly (whole ocean)			360.0 zJ	35.0 zJ	
SST anomaly	1961 to 1990	1850 to 1899	-0.281°C	0.105°C	HadSST4, Kennedy et al. (2019)
Rate of SLR from ice melt	-	1970 to 2018	1.03 mm/yr	0.18 mm/yr	IPCC AR6, Fox-Kemper et al. (2021
		1993 to 2018	1.25 mm/yr	0.11 mm/yr	

necessarily a negative relationship with warming. Negative values for the linear coefficient do imply a negative first-order relationship with warming but may be compensated by strong positive non-linear contributions. Also note, the coefficients are based on historic ice-melt contribution to SLR, which is dominated by glacial melt with contributions from Greenland and Antarctica.

The quadrant that is found to be feasible in the fewest simulations shows a negative linear relationship, with strong positive nonlinearities to compensate. In a warming world, decelerating glaciers and advancing grounding lines are unlikely enough that these mechanisms can be discounted. One process that could lead to a negative linear relationship with warming is a positive surface mass balance (i.e. a negative contribution to SLR) in Antarctica, due to increased precipitation with atmospheric warming. This must be compensated by strongly positive nonlinear dynamic change – possibly meaning an onset of MISI during the observational period – or a stronger nonlinear negative surface mass balance in Greenland and over mountain glaciers. Grinsted and Hesselbjerg Christensen (2021) found a positive linear relationship between surface mass balance and warming in Greenland, so assuming this is true, the nonlinearities here would be attributed to glacial thinning and retreating grounding lines. The opposite quadrant (positive linear relationship with negative nonlinearities) also could imply positive surface mass balance; in this case in such a way that it contributes to a positive, but sublinear, relationship with warming. However, it could also imply negative surface mass balance that is compensated for

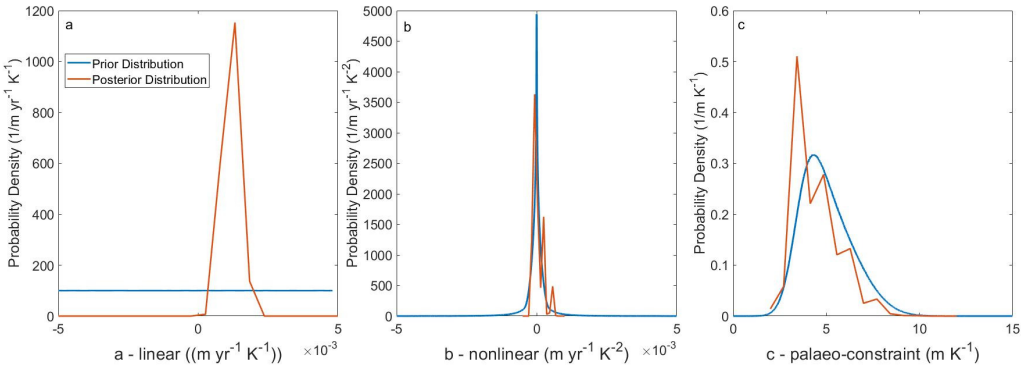

FIGURE 3.2: Prior (blue) and posterior (orange) distributions of parameters *a*, *b*, and *c* (panels a, b and c respectively). For details on how the prior distributions are defined, see Supplementary Materials 2

by dynamic change. The quadrant where linear and nonlinear interactions are both positive is relatively easily explained; surface mass balance and dynamic change both, on average, contribute positively to SLR. Given that sea level has been rising over the observational period, there is clearly no world in which both coefficients can be negative – so the bottom left quadrant is empty.

Figure 3.1 shows the distribution of the linear and nonlinear coefficients in the equation used to calculate SLR, but gives no indication about how strongly each ensemble member is weighted. Figure 3.2 shows a probability distribution of the coefficients a, b and c taking into account the weighting of the simulation they are pulled from. The peak value for *b* is still 0 (implying that the most effective way to simulate the observational period is by keeping ice melt linearly related to warming) and coefficient *a* is always positive.

3.4 Results

This section outlines the SLR projections obtained using a linear and nonlinear model setup and the differences between the two. It then examines how historically precedented nonlinearities in the relationship between warming and ice melt impact the rate of sea-level rise at different levels of warming, and the relative importance of these nonlinearities in low and high emissions scenarios.

The first step is to run WASP with no nonlinear component to the SLR equation (a linear setup). From this, the median SLR from ice melt in this setup reaches 0.7 and 1.9m by 2300 following SSPs 126 and 585 (respectively), with 97.5^{th} percentiles of 1.1 and 3.5m (Figure 3.3, panels c and k). When the nonlinear component to the equation is included, median SLR from ice melt reaches 0.7m and 2.7m by 2300 following SSPs 126 and 585, respectively, and the 97.5^{th} percentiles reach 1.1 and 5.1m (Figure 3.4, panels c and k). When including nonlinear interactions, the most notable difference is

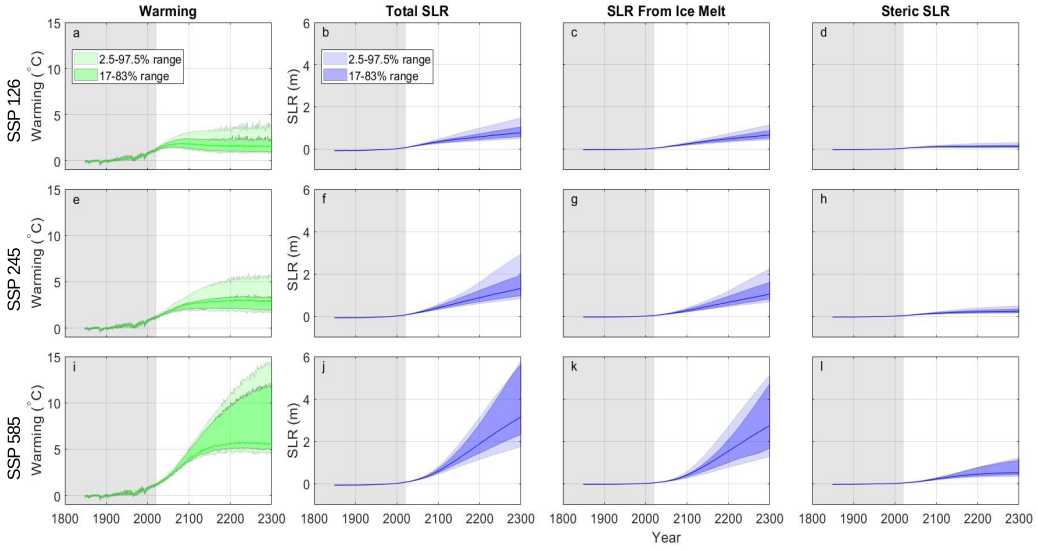

FIGURE 3.3: The projections of warming (first column), total SLR (second column), SLR from ice-melt (third column) and thermosteric SLR (fourth column) for SSPs 126 (top row), SSP245 (middle row) and 585 (bottom row), until 2300, using the version of WASP with a linear equation for SLR.

in the high end (97.5^{th} percentile), which is considerably higher, especially in the higher emissions scenario of SSP585 (see Figure 3.3 and Figure 3.4, panel k). There is little change in the low emissions scenario, and in the higher emissions scenario the largest change is in the 97.5^th percentile (1.6m by 2300).

Figure 3.7 shows the projections from this study using a nonlinear setup compared to sea-level rise projections from other studies. The projections from this study are are within range but lower than in IPCC AR6 (Fox-Kemper et al. (2021)) and other recent studies (see Figure 3.7. One reason for this is that the method for these projections means that they are purely an extrapolation of historical dynamics, meaning that any processes or feedbacks that start once warming gets higher than historical are not represented. However, allowing a nonlinear relationship between warming and ice melt has pushed projections of sea-level rise upwards, bringing them closer to other projections in the literature than the projections made using a linear equation.

As well as impacting absolute SLR, nonlinearities impact the rate of SLR. Figure 3.5 shows the ratio of the rate of SLR at a given level of warming to the current rate of SLR. The red line follows a 1:1 relationship, which implies a linear relationship between warming and the rate of SLR (for example, that 2 degrees of warming leads to 2x the rate of SLR). The median behaviour of the model is to follow the 1:1 line, which implies linearity and matches the previous results in Figure 3.2. It is also consistent with the thinking of Grinsted and Hesselbjerg Christensen (2021). There is also a potential for the rate of SLR to increase faster than the rate of warming, leading to a 6x increase in the rate of SLR for 4 degrees of warming. This result implies positive nonlinearity, and is consistent with the skew towards more positive values for 'b'.

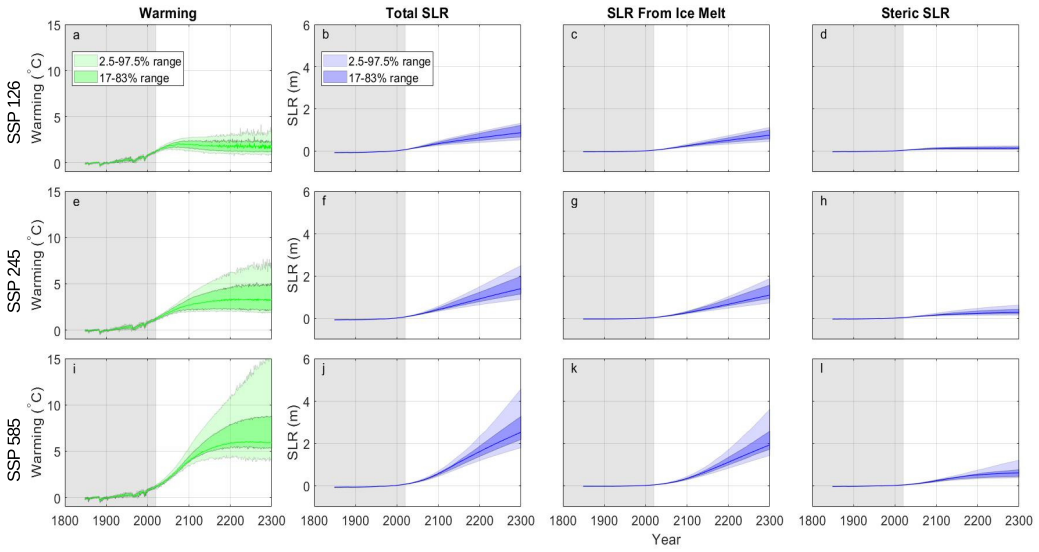

FIGURE 3.4: The projections of warming (first column), total SLR (second column), SLR from ice-melt (third column) and thermosteric SLR (fourth column) for SSPs 126 (top row), SSP245 (middle row) and 585 (bottom row), until 2300, using the version of WASP including a nonlinear component in the SLR equation.

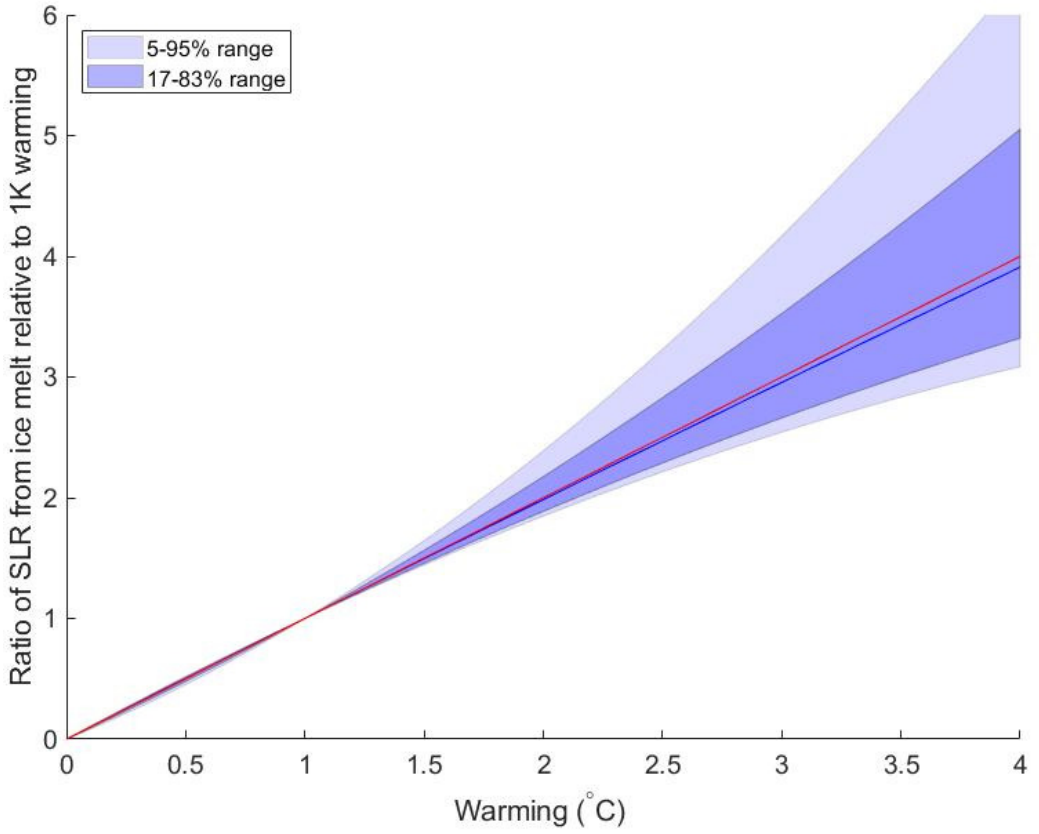

FIGURE 3.5: The rate of SLR at any given amount of warming compared to the rate of SLR at 1 degree of warming – red line follows linear behaviour (i.e. $SLR_{NdT} = N * SLR_{1dT}$, where dT is the amount of warming experienced to date).

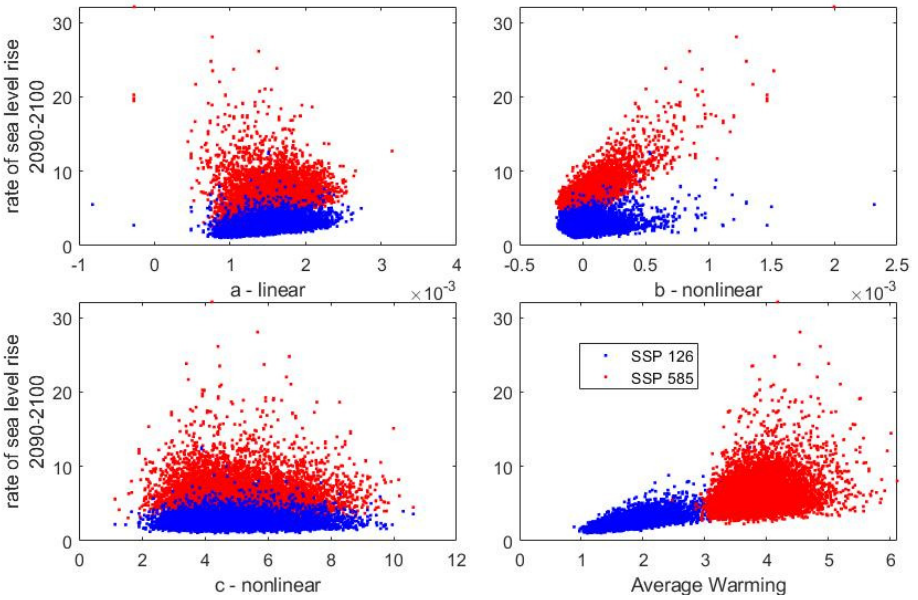

FIGURE 3.6: The rate of SLR between 2090 and 2100 versus a- linear coefficient a, b- nonlinear coefficient b, c- palaeo constraint c and d- average warming over the decade.

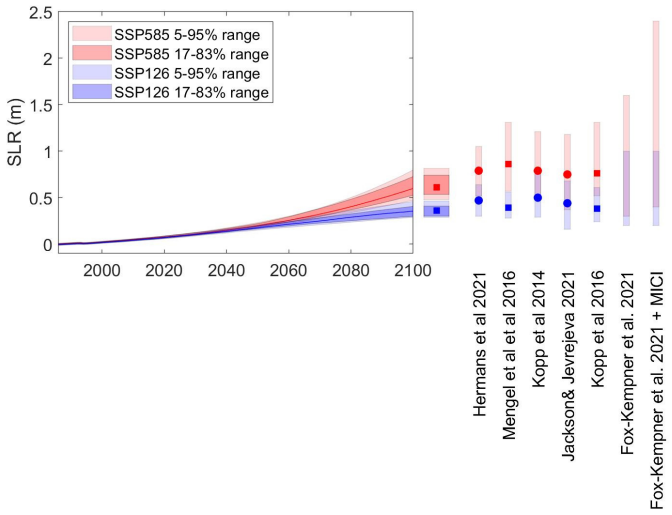

FIGURE 3.7: The projections of sea-level rise from a nonlinear equation in WASP up to 2100, compared to sea-level rise projections from Hermans et al. (2021), Mengel et al. (2016), Kopp et al. (2014), Jackson and Jevrejeva (2016), Kopp et al. (2016) and Fox-Kemper et al. (2021) (with and without MICI included - note that projections including MICI are low confidence, whereas without MICI the projections are medium confidence.)

On short (end-of-century) timescales, the palaeo constraint on equilibrium SLR ('*c*' in Equation 3.1) has little impact on the rate of SLR – all of the uncertainty is dominated by the first half of Equation 3.1) (lower two panels of Figure 3.6). In lower emission scenarios (i.e. less warming), uncertainty is largely controlled by linear interactions (*a*). However as warming increases, uncertainty becomes more dominated by nonlinear interactions (*b*) (see the upper panels of Figure 3.6 for visual representation and Table 3.2 for R^2 values).

TABLE 3.2: R^2 for the rate of SLR over different periods versus the linear (*a*) and nonlinear (*b*) components of the SLR equation, as well as warming over that period

	R squared		
time period, scenario	a (linear)	b (nonlinear)	warming
2010-2020	0.22	0.02	0.18
2090-2100 SSP126	0.14	0.09	0.5
2090-2100 SSP245	0.09	0.3	0.27
S090-2100 SSP585	0.01	0.64	0.07

3.5 Discussion and Conclusion

Nonlinearities in the relationship between warming and ice-melt are a source of significant uncertainty in projections of SLR, but are generally neglected in projections derived using semi-empirical approaches (Meehl et al. (2012); Levermann et al. (2020)). This study adapts a (previously linear) semi-empirical method of projecting SLR due to ice-melt, to include nonlinear interactions. These projections are extended to 2300, consistent with AR6 and providing a longer overview of the magnitude and timing of change than studies that project to 2100. With the new method allowing a nonlinear relationship between observed warming and ice melt, projected sea-level rise reaches 0.7m, 1.3m and 3.1m by 2300 following SSPs 126, 245 and 585, respectively.

The magnitude of the nonlinear contribution to SLR centres on 0 (i.e., the best way to simulate the rate of historical SLR in the climate emulator was to keep ice-melt linearly related to warming). However, once included in SLR projections in a climate emulator, these nonlinearities begin to dominate uncertainty in high emissions scenarios – i.e., historically-precedented nonlinearities that have little impact in the observational record, begin to have more impact as warming increases. For example, these nonlinearities have little impact on the rate of SLR when warming is low, but can lead to a 6-fold increase in the rate of SLR for a 4-fold increase in the amount of warming. They also drive the 97.5^{th} percentile of sea-level rise projections in this

study up by around 2.5m by 2300 in SSP585 (a high emissions scenario) whereas the difference they make in a low emissions scenario (SSP126) is negligible.

Some specific processes are not resolved in the model. A notable example in this study is the lack of explicit representation of ice melt caused by increasing ocean heat content, as ice melt is only related to atmospheric warming in Equation 3.1. This is particularly relevant for the future contribution of melting ice from the Antarctic, which is already a source of large uncertainty in SLR projections. The influence of increasing surface ocean heat content is not entirely omitted because atmospheric warming and ocean heat content are linked. However, not representing this relationship explicitly may further obscure an already uncertain contribution to SLR. Further, the emulator used for this study is constrained using observations, and therefore does not capture any shift in climate state that may occur in high emissions scenarios. This means there is no representation of processes that are expected to take effect in the future at higher levels of warming (for example MICI). These are likely to drive SLR higher than predicted in this study. Although the impact of MICI (and other processes that are not expected to take effect until warming increases), the results from this study are still relevant as a way of exploring how past nonlinearities will manifest in the future. Even if no new nonlinear processes begin, it is still beneficial to understand how existing nonlinearities will impact sea-level rise as warming continues.

The results presented in this study represent the plausible impact that historically-precedented nonlinearities in ice melt will have on sea level as warming continues, and show that the importance of these nonlinearities grows at higher amounts of warming. This finding, in combination with the increasing likelihood of historically unprecedented nonlinearities in the relationship between warming and ice melt in higher warming scenarios, provides further incentive to limit emissions sooner rather than later. Even nonlinearities that have remained relatively small in the observational record have the capacity to increase sea level by up to 2.5m in 2300 under SSP585, and nonlinearities associated with high-warming thresholds may increase sea level even further.

During the historical period, and in low-emissions futures, historically-precedented nonlinearities in the relationship between warming and ice melt are small, and their effect on SLR is minimal. However, for higher emissions scenarios (and therefore high warming futures), SLR projections increase when accounting for these nonlinearities. These nonlinearities also cause the rate of sea-level rise to accelerate faster as warming increases, which provides further incentive to limit future warming and keep the impact of these nonlinearities minimal. It also demonstrates how projections of sea-level rise must be able to account for nonlinear ice-melt interactions so that practitioners have a full understanding of how sea level will change as warming continues. This is especially relevant because of the apparent interest on the side of

practitioners in the very likely (5-95%) range of projections (e.g. Hinkel et al. (2019)). The tail-end (97.5%) of the probability distribution is impacted more than the median estimate of sea-level rise by including nonlinear interactions in our calculations, which is an important results for practitioners interested in low-probability, high-impact scenarios.

This chapter considered how sea-level rise projections and uncertainty are impact if the ice melt contribution to sea-level rise is allowed to vary nonlinearly with warming. The next chapter remains on the sea-level rise theme, using the sea-level rise formulation from this chapter and the AMP concept from the previous chapter to explore how sea-level rise can be used as a climate target.

Chapter 4

The Carbon Removal Needed for Stabilisation of the Sea Level Commitment to Near Zero

4.1 Abstract

sea-level rise is a major impact of climate change, and its impacts are compounded by the fact that populations are densest in the coastal areas of countries. Further, because of the long response times of processes like thermosteric expansion of the ocean and melting of the ice sheets, sea-level rise is a committed change even if warming is halted immediately. There has been a distinct lack of consideration of how much cooling (and therefore carbon removal) it would take to significantly reduce this commitment. The effort it would take to undo committed change is a relevant question in the context of recent discussion around reparations for loss and damage, as well as the conversation around devoting increasing effort towards carbon dioxide removal (CDR). This study addresses this gap by employing a semi-empirical sea-level rise model to assess the amount and rate of carbon removal needed to stabilise future sea-level rise. A large observation-constrained ensemble of model runs is used to create pathways consistent with a given warming target, defined as the temperature needed to stabilise sea-level rise at the committed level by 2040. With the assumption that warming in the historical period of the model is heading towards a level consistent with the Nationally Determined Contributions defined in COP27, and the subsequent goal of stabilising sea-level rise at the level consistent with the 2040 commitment, we must limit our cumulative emissions between -200 to 500 PgC since 1850. In the median case, this means returning to the cumulative emissions reached in around 1914 (around 167PgC). Assuming a constant rate of removal of 8PgC/year, this takes until the middle of the 22nd century. Given that 10.9PgC were emitted from

fossil fuels in 2021, this pathway would require the development of a significant industrial sector dedicated to the removal of the carbon already emitted, on top of the technology required to keep future emissions to zero.

4.2 Introduction

Global mean sea-level rise (SLR) is a major impact of climate change, with important consequences compounded by the fact that populations are concentrated in the coastal areas. Alongside local and regional process, global mean SLR leads to relative mean sea level change that puts coastal areas at higher risk of hazards such as incremental submersion and more frequent and extreme coastal flooding, erosion, ecosystem loss and saltwater intrusion. This poses risk to coastal communities, infrastructure and the environment. Glavovic et al. (2022) collate results from multiple studies and found that without adaptation, SLR will contribute to the 1-in-100-year extreme sea level impacting 158 to 510 million people and 7,919 to 12,739 billion USD by 2100 following RCP4.5. These numbers increase to 176 to 880 million people and 8,813 to 14,178 billion USD in assets following RCP8.5. Compared to this, they found plausible adaptation for SLR before 2050 would cost $223 to 768 billion USD – significantly lower than the longer-term loss if no adaptation measures are followed. It is worth noting on top of this, that although ecosystem services may end up being included in the broad term 'assets', loss of habitat and damage to ecosystems is not explicitly included here.

Because of the long response times of processes like thermosteric expansion of the ocean and melting of the ice sheets, sea-level rise is a committed change even if warming is halted immediately. Given continuing carbon emissions, it is widely accepted that we are committed to sea-level rise beyond this minimum commitment, and beyond a level that is easy to adapt to. Levermann et al. (2013) used a combination of palaeo-evidence and physical climate models to constrain a committed sea-level rise of 2.3m/°C over 2000 years, which implies a total multi-millennial commitment of around 2.5m from anthropogenic warming to date. This total is dominated by the land-ice response, with 1.6m from Antarctica, 0.3m from Greenland, 0.2m from glaciers and ice caps (adding to 2.1m) and 0.4m from thermal expansion. The current largest contributor is thermal expansion, but the slow response of ice sheets and the presence of tipping points in their response to warming means that they will continue to contribute to sea level rise after thermal expansion has reached equilibrium (10,000 years versus 2000 years), and their contribution will grow in a nonlinear manner (Fox-Kemper et al. (2021), Levermann et al. (2013), DeConto et al. (2021)). Given the lack of plans to decarbonise, warming will continue past current levels, so the equilibrium estimate of Levermann et al. (2013) can be considered the minimum amount of sea level rise. Mengel et al. (2018) considered the impact of

delayed mitigation on sea-level rise by 2300, finding that each 5-year delay in peaking emissions before declining emissions added 20cm to the median sea-level rise by 2300. Nauels et al. (2019) calculated a median GMSLR commitment from historical emissions and the Nationally Determined Contributions (NDCs) until 2030 of signatories of the Paris Agreement of 1m by 2300.

As warming continues, carbon dioxide removal (CDR) is becoming more of a focus in the mitigation discourse to keep warming to 1.5°C, following the Paris Agreement. It is widely appreciated that reducing the greenhouse gas emission rate to zero will reduce the commitment to future surface warming, and CDR can 'undo' some of the warming to date. However, there is little consideration of how much cooling (and therefore carbon removal) is required to undo any commitment to future sea-level rise. Given the scale of the long-term sea level commitment, large-scale political and technological change is needed for this to be practically addressed. On top of this, because of the long timescales of rising seas, the benefits of acting to mitigate sea-level rise will not be fully evident in the near future; until 2050, there is little difference in the resultant sea-level rise between more and less strongly mitigated scenarios (Fox-Kemper et al. (2021)). The focus in policy therefore lies on mitigating warming (a more short-term process), which in turn mitigates sea-level rise. As such, many studies that consider mitigation of sea-level rise do so by considering the damage avoided by faster or more stringent mitigation of warming, and compare this to the damage inflicted by failing to mitigate warming sufficiently (e.g., Brown et al. (2018); Nicholls et al. (2018) Mengel et al. (2016)). Li et al. (2020) examined how carbon pathways towards sea-level rise targets differ from pathways towards a warming target. They found that steering emissions directly towards a sea-level rise target consistent with a given warming target, rather than a warming target consistent with the same amount of sea-level rise, allows for more carbon emissions (meaning the potential for more flexibility in short-term climate policy) yet limits sea-level rise more effectively in the long term.

Previous studies have examined both the impact on sea-level rise of limiting warming, and the impact on carbon pathways of limiting sea-level rise rather than warming. However, the effort needed to reduce the gap between current and committed sea-level rise (which would involve significant carbon removal) is relatively unexplored. Grinsted et al. (2022) defined the amount of cooling necessary to reduce the sea level commitment to zero (the 'balance temperature') and found this to be around 1.1°C, which is roughly the amount of global mean warming that we have experienced since the preindustrial era (Gulev et al. (2021). Foster and Rohling (2013) came to a similar conclusion by examining the relationship on equilibrium timescales between atmospheric CO_2 and sea level, stating that to avoid significant sea-level rise in the long term, atmospheric CO_2 should be returned to preindustrial levels or similar.

Bouttes et al. (2013) examined the relationship between radiative forcing and sea-level rise from thermal expansion and found that thermal expansion is in principle reversible if radiative forcing is sufficiently reduced, although the resulting fall in thermosteric sea level is still slow. Theoretically this implies that committed thermosteric sea-level rise is not physically inevitable (albeit leading to a different spatial pattern of sea level once mean sea level is restored), although in practical terms reducing this commitment to zero is unlikely. Ehlert and Zickfeld (2018) found that thermosteric sea-level rise persists even after CO_2 concentrations are restored to preindustrial concentrations after being ramped up to 4x preindustrial concentrations. However, both of these studies only considers the commitment from thermosteric rise, wheras sea-level rise from ice melt is subject to different processes. Martin et al. (2022) find that resulting changes in sea-level rise from modelled freshwater release from the Greenland ice sheet is a lasting impact on the timescales considered in their study (100 years of freshwater input followed by 100 years of stabilisation). However this study only considers the impact of freshwater influx in an idealised preindustrial setting, rather than considering pathways of warming (or radiative forcing). There is also no reversal of the freshwater forcing, only stabilisation.

With the majority of the impacts of climate change being experienced by countries and people less responsible for historic emissions, the concept of climate justice has become a cornerstone of the climate change discourse. This is especially the case for Small Island Developing States (SIDS) who were the driving force behind the Paris Agreement due to the fact that they are more at risk from sea-level rise. Recently Loss and Damages have been highlighted at the previous two Conference of the Parties (COP) meetings (COP26 in Glasgow and COP27 in Sharm El-Sheikh). The broadness of the term 'Loss and Damage' means that there has always been some debate over how it can be quantified, and how to make sure that it is correctly attributed to climate change. Quantifying historical responsibility for future global mean sea-level rise is one way of addressing this issue, because global mean sea-level rise is readily attributed to global mean warming and carbon emissions.

The overall aim of this paper is to quantify how much CDR is necessary to stabilise the sea level commitment to 0 (or as close as possible), and to create a carbon pathway to achieve this. This result can also be presented as returning to the cumulative emissions level of a certain historical year, which will serve to quantify how many years of emissions have yet to be fully realised in terms of sea level change. This holds some relevance in the loss and damage conversation as it will highlight the historical timescales over which human activities have been responsible for future sea-level rise. It will also serve to illustrate the extent to which CDR can be viewed as a tool to mitigate future sea-level rise. This study uses the Adjusting Mitigations Pathway algorithm of Goodwin et al. (2018a) within an efficient climate emulator to generate

mitigation pathways towards a warming target that is defined as the temperature needed to stabilise sea-level rise at the committed level by 2040.

4.3 Methods

4.3.1 The WASP Model

This study uses the Warming, Acidification and Sea Level Projector model (WASP; Goodwin et al. (2018a)). This is an 8-box model of the atmosphere-ocean-terrestrial system (1 atmosphere box, 2 land boxes and 5 ocean boxes), where the climate response to radiative forcing, and transfer of carbon and heat between each box, is described using 19 parameters which are varied at random between physically feasible limits (outlined in Appendix A). The model generates a prior ensemble of 16×10^8 simulations, where variation of these 19 parameters generates variation between ensemble members, and uses a Bayesian history matching protocol to narrow this prior ensemble down to an observationally consistent posterior ensemble of order 10^4. Each member of the posterior ensemble is weighted according to how well it matches observational data of climate that are outlined in Table 3.1. Historical sea level is also used as an observational constraint, using estimates of sea-level rise from land ice from (Fox-Kemper et al. (2021)) over two periods: 1901-1990 and 1993-2018.

sea-level rise from ice in the model is calculating using the following equation (see Chapter 3):

$$\frac{d}{dt}GMSL_{ice} = (a\Delta T + b\Delta T^2)\Big(\frac{c\Delta T - \Delta GMSLR_{ice}}{c\Delta T}\Big) \tag{4.1}$$

The first term of this equation is a Taylor expansion of the semi-empirical method originally proposed by Rahmstorf (2007), allowing sea-level rise from ice to vary nonlinearly with warming. a and b are parameters that remain constant. The second term stabilises SLR from ice melt towards an equilibrium, with the third parameter c describing the equilibrium relationship between temperature rise and SLR, which is defined using data from the Last Interglacial (LIG):

$$c = \frac{\Delta GMSL}{\Delta T}\Big|_{LIG} \tag{4.2}$$

$\Delta GMSL$ is defined using results from Kopp et al. (2009), who found a peak value of sea level during the last interglacial of 7.2+/-1.3m (67% confidence interval). ΔT is defined assuming a mean global temperature difference between 1 and 2°C, as described by Wilcox et al. (2020).

4.3.2 Application

The adjusting mitigation pathway (AMP) algorithm is designed to create carbon emissions pathways that are consistent with a preset warming target. Every 10 years, the remaining carbon budget is calculated using the Transient Climate Response to Emissions (TCRE) to linearly relate the warming target to the associated remaining emissions. The emissions rate for the next 10 years is then assigned as the rate that would, if held constant, reduce the allowable emissions to 0 by the end of the model timeframe. The reassessment of the carbon budget every 10 years allows for adjustment if the TCRE is over- or under-estimated. The algorithm starts in 2020, using the warming commitment due to the current Nationally Determined Contributions (NDCs) as the initial warming target, which is taken to be 2.5°C (United Nations (2022)). At year 2039, this target is changed to a second target, defined as:

$$dT_2^{target} = \frac{dZ_{ice}}{c} \tag{4.3}$$

Given the definition of 'c' in Equation 4.2, this is equivalent to the temperature from the last interglacial scaled by the ratio of current sea-level rise from ice to total sea-level rise during the LIG:

$$dT_2^{target} = dT_{LIG}\frac{dZ_{ice}}{dZ_{LIG}} \tag{4.4}$$

Note that the change in sea level over the LIG considers ice melt and sea level contributions from other sources, but it can be assumed that ice melt is the dominant cause of global mean sea level change on equilibrium timescales, following Levermann et al. (2020). The reason only ice melt is chosen for stabilisation in this method is that this is ultimately a method to constrain atmospheric warming. Using this to stabilise thermosteric rise would mean reducing atmospheric temperatures enough to reduce ocean warming at depth, which would be more removal of CO_2 than can feasibly be represented in the model.

The target is set in 2039 so that it takes effect in the algorithm at the 2040 checkpoint. This gives some time for political and technological advancement in the area of CDR before the target is established.

4.4 Results

Using Equation 4.3, the secondary warming target peaks at around 0.01 ($\pm$0.08)°C (Figure 4.1a) – close to no warming since the preindustrial era. This corresponds to

cumulative emissions of around 167 (±151)PgC (Figure 4.1b), which implies the same level of cumulative emissions as in 1914 (±26 years) (Figure 4.1c). This means that 109 years of emissions will need to be 'undone' (assuming that sea level rise begins to move towards stabilising in 2039, when the secondary target is adopted) with the aim of stabilising sea level. The return to preindustrial conditions is clearly visible in Figure 4.2 a and b, with cumulative emissions and warming dropping sharply after the secondary warming target is introduced. The median rate of change of sea-level rise declines to around 0.5mm/year over the ∼60 years after the secondary target is introduced, and the near-stabilisation of sea level begins to take effect around 2100. This is a decline in emissions at almost the same rate that carbon is currently being emitted, meaning that to put this scenario into practice would mean ceasing all current emissions and employing carbon dioxide removal methods (CDR) at almost the same scale that emissions are currently taking place. This drop in emissions, and the resulting drop in warming and near-stabilisation of sea level rise, is therefore more speculative than feasible.

There is a drift in the model that causes sea-level rise from ice to continue at a slow rate whenever the AMP algorithm allows a small amount of warming. This is because the method for calculating sea level rise from ice does not allow ice sheet regrowth in the event of cooling (to account for hysteresis), but allows melt in response to small amounts of warming. The result is that while the AMP algorithm allows warming to fluctuate around the target, this leads to incremental increases in ice melt during years of warming that are not compensated for during years of cooling. In order to represent regrowth of ice sheets the model would need historical data to constrain the rate of regrowth per unit cooling. While this means that there is not complete stabilisation of global mean sea-level rise from ice, a rate of 0.5mm/year (or 5 cm/century) is manageable. It is worth noting that this does not show any change in committed rise from thermosteric expansion, but given that thermal effects can be expected to slow under cooling and the majority of equilibrium rise is from ice melt, nearly stabilising the land ice commitment is a significant contribution to keeping the sea-level rise commitment to near zero.

Figure 4.3 allows comparison between the cumulative emissions, warming and sea-level rise in the AMP scenario towards minimising SLR commitment (adjusted AMP), an AMP scenario towards a 2°C warming target and SSP245. The latter two scenarios have been chosen for comparison because they both represent feasible middle-of-the-road scenarios: one where emissions are prescribed in the model and warming is calculated (SSP245) and one where warming is prescribed and emissions are calculated (AMP2.0). Note that due to uncertainty in the transient climate response to emissions, there is uncertainty in the emissions pathway where warming is prescribed, and where emissions are prescribed, the uncertainty is in the resultant warming. The difference in median emissions between SSP245 and the adjusted AMP

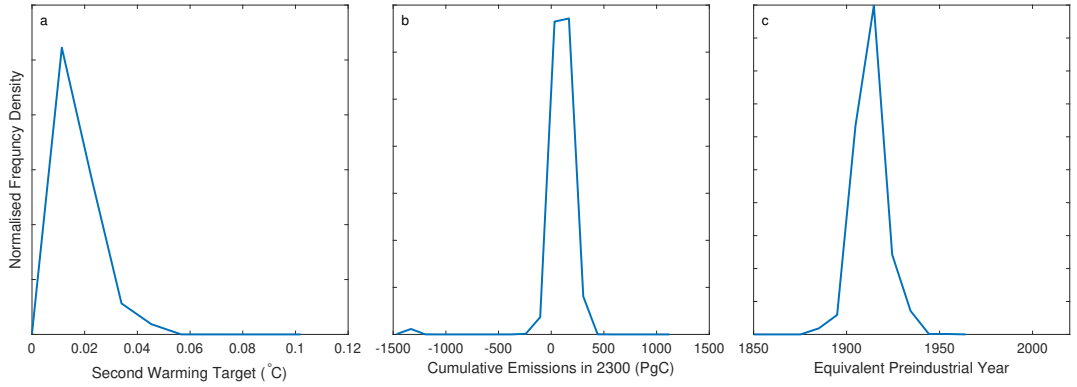

FIGURE 4.1: Probability distributions weighted according to simulation weighting, showing a- the secondary warming target adopted by the adjusted AMP algorithm in year 2039 (calculated using Equation 4.3), the cumulative emissions in 2300 once the AMP algorithm has run, and the last year before 2300 when cumulative emissions were at the same level as they are in 2300.

TABLE 4.1: Cumulative emissions, warming and sea-level rise from land ice in 2100 and 2300 following SSP245, and AMP algorithm stabilising warming at $2°C$, and an adjusted AMP algorithm where the sea-level rise commitment is minimised.

	Cumulative Emissions (PgC)		Warming (°C)		SLR from ice (m)	
	2100	2300	2100	2300	2100	2300
SSP245	1727	2357	2.47	2.49	0.26	0.99
AMP 2.0	1339	2017	1.9	2.2	0.22	0.8
AMP SLR=0	206	175	0.4	0.22	0.15	0.2

is roughly 2500PgC, and roughly 2000PgC for AMP2.0. In all scenarios warming eventually stabilises, but only with significant near-term negative emissions can the committed SLR be minimised (but not zeroed, due to the drift in the model). This is shown again in Table 4.1, with AMP SLR=0 being the only scenario where cumulative emissions and warming in 2300 is lower than in 2100. Despite this, sea-level rise in 2300 is still marginally higher – although the difference in the adjusted AMP is minimal: 0.05m in 200 years, compared to 0.73m and 0.58m in SSP245 and AMP2.0, respectively.

4.4.1 Discussion and Conclusion

Due to the long response time of ice and ocean processes that contribute to global mean sea-level rise, it is well established that there is sea-level rise commitment even if warming were to immediately stop. Undoing this commitment would take CDR efforts far beyond a scale that is currently feasible or where the impacts on other aspects on the Earth system are well understood, which may be why little effort has been put into quantifying what it would take to undo this commitment. The recent

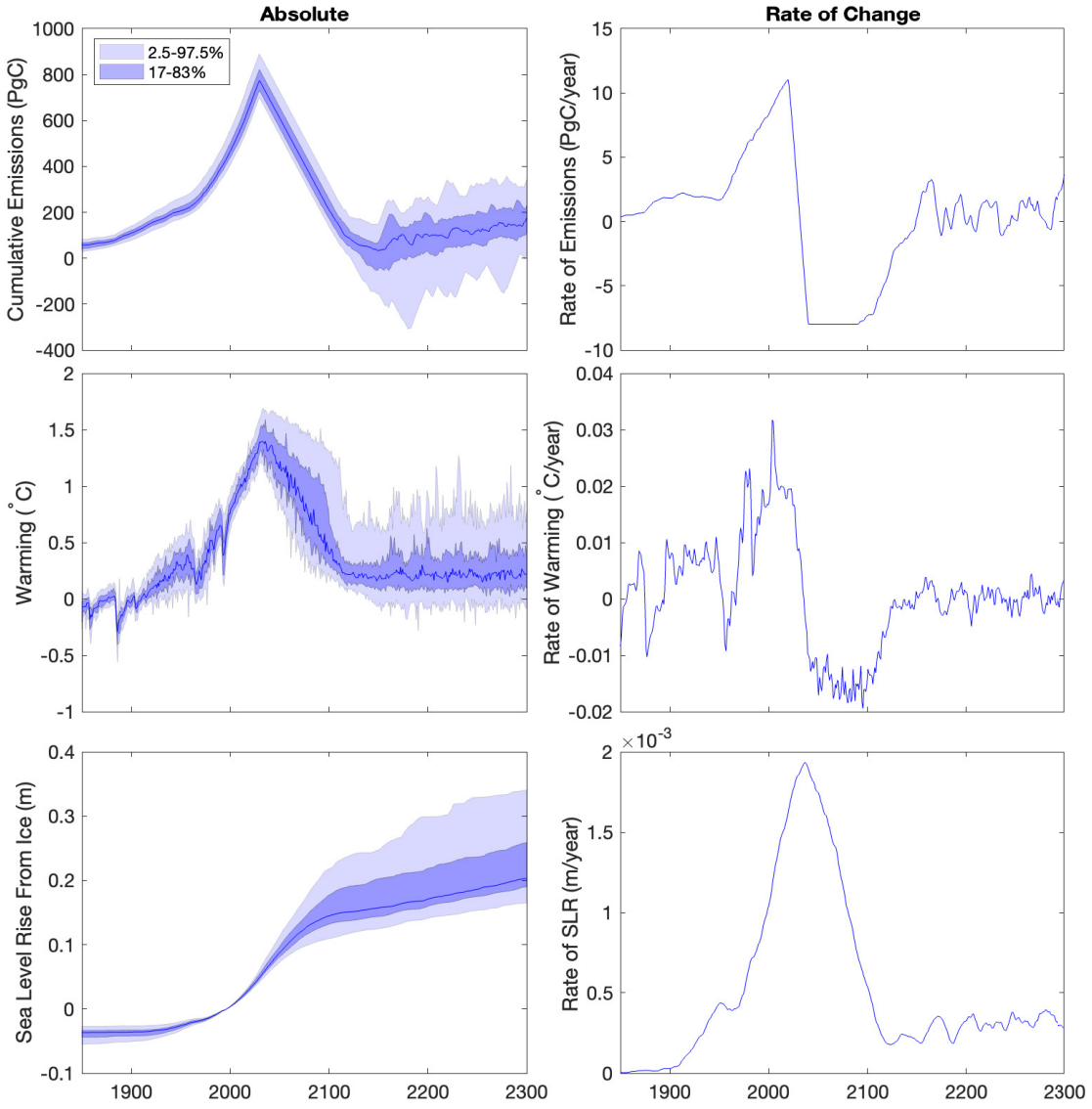

FIGURE 4.2: Cumulative emissions, warming and sea-level rise from ice (and their median rates of change) following the adjusted AMP scenario towards a warming target that will near-stabilise the sea level commitment from ice melt.

focus on loss and damage funds in global climate change political discourse may prompt us to wonder how much of the emissions generated so far are actively contributing towards the committed loss of land. The increased focus on CDR as it becomes clear that the 1.5°C warming target is likely to be overshot also prompts consideration of whether CDR can be used to 'undo' sea-level rise in the same way that it can 'undo' warming. The aim of this study was to establish what it would take (in terms of CDR) to minimise committed global mean SLR. This is done by creating adjusting mitigation pathways according to the method of Goodwin et al. (2018a) towards a warming target consistent with minimising the committed SLR. This warming target is calculated by exploiting the relationship between equilibrium

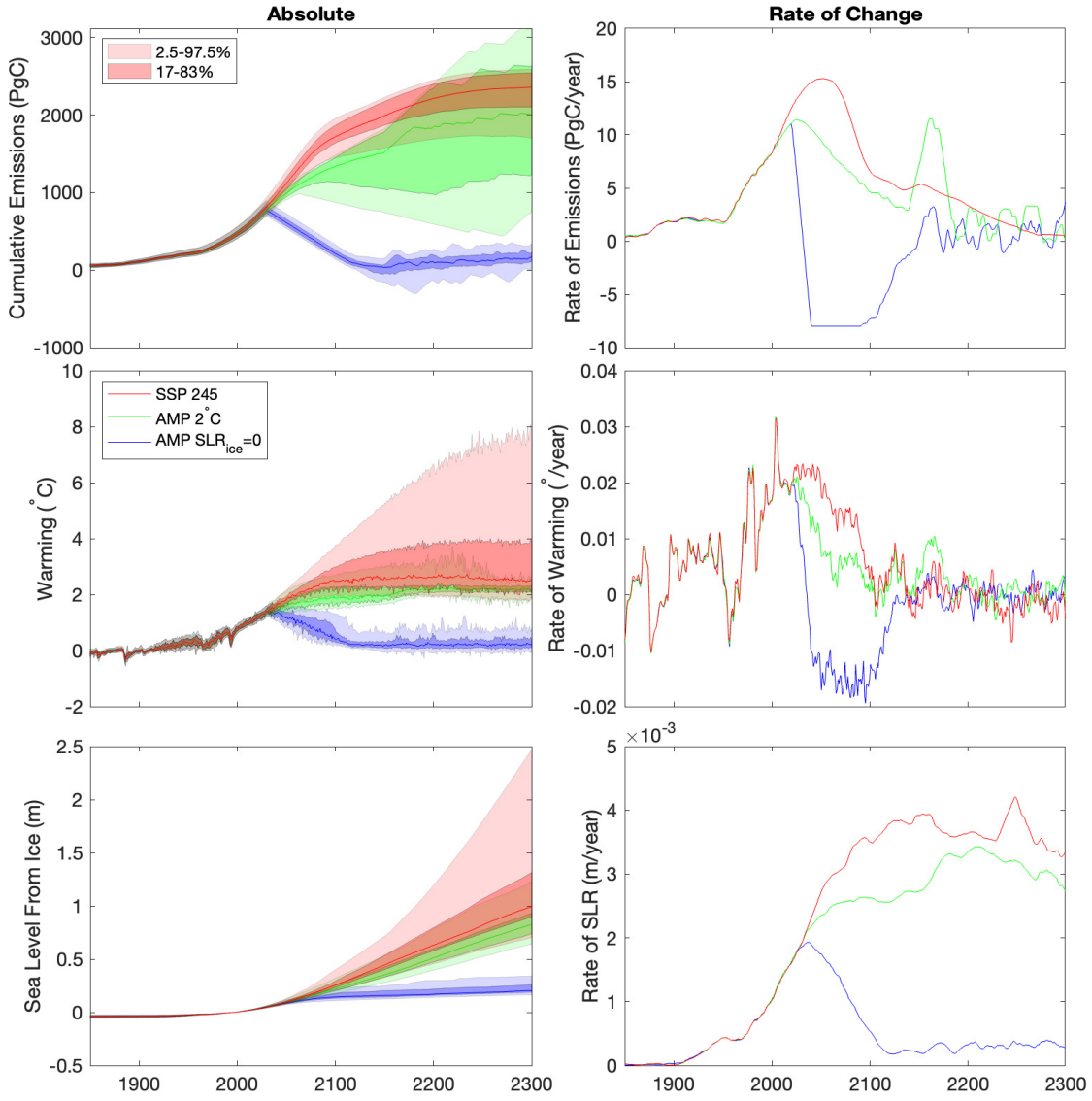

FIGURE 4.3: Cumulative emissions, warming and sea-level rise from ice (and their median rates of change) following the adjusted AMP algorithm, SSP245 and an AMP algorithm stabilising at just a warming target of 2.0°C.

sea-level rise and warming over the last interglacial, which is commonly used as an analogue for a 2°C warmer world. This relationship is defined in the WASP model using sea level change estimates from Kopp et al. (2009) and warming from Wilcox et al. (2020). The secondary warming target is implemented at year 2040, before which the emissions trajectory is set towards 2.5°C (consistent with the most recent NDCs) to allow some time to implement CDR policy and technology.

The secondary warming target defined to minimise committed SLR has a relatively narrow distribution and peaks at around 0.01°C (±0.008°C), consistent with removing all cumulative emissions since 1914 (±26 years). This is consistent with a cumulative emissions level of 167 (±151)PgC. Note that this uncertainty is much less than the

uncertainty in the remaining carbon budget for 1.5°C of warming, which is around 850PgC according to the most recent estimate of the TCRE from Forster et al. (2021). With a constant rate of CDR of 8PgC/year, it takes until 2150 to remove this carbon from the atmosphere, at which point cumulative emissions fluctuate around 0 PgC. In both other scenarios cumulative emissions and warming both continue, leading to a difference in median emissions of at least 2000PgC, and a difference in warming of around 2°C. The adjusted AMP algorithm emissions pathway succeeds in limiting the rate of SLR from ice melt to 0.05m in 200 years (0.2mm/yr by 2300), which is a rate of SLR that can certainly be managed and planned for, compared to 0.58m in 200 years (2.9mm/yr) for AMP2.0, and 0.73m in 200 years (3.2mm/yr) for SSP245. Note that there is still some commitment to thermosteric expansion in the event of CDR (e.g. Ehlert and Zickfeld (2018)), but the majority of equilibrium sea-level rise on millennial timescales comes from ice melt, so nearly stabilising this is significant.

One motivation for this study was the recent focus on loss and damage in the climate discourse. By calculating what year's value of cumulative emissions we should return to if we wish to stabilise sea level in 2040, this study quantifies the length of time over which emissions have been contributing to sea-level rise that is yet to be felt (i.e., human activities have been responsible for sea-level rise post-2040, since 1914 ($\pm$ 26 years)). A benefit of this study is that it focuses on a root cause of global mean sea-level rise (ice melt) which is already attributed to warming, and therefore circumvents any discussion about attribution that can sometimes be a limiting factor in assessing loss and damage. This study can fit into the general discussion about loss and damage by providing a framework to assess what proportion of anthropogenic emissions are actively contributing towards the ice melt/SLR commitment, or how much of these emissions would have to be removed from the atmosphere to keep future SLR at a manageable level by 2300.

Another motivation for this study was to assess the role of CDR in mitigating sea-level rise, compared to mitigating warming. Although CDR is a necessary part of most emissions trajectories that keep warming in line with the Paris Agreement targets, this study shows that CDR cannot be used to undo sea-level rise in the same way that it can undo warming. Even to nearly stabilise the committed sea level rise from ice, all emissions since 1914 ($\pm$ 26 years) must be removed from the atmosphere, and there are some outside cases (see Figure 4.2) where this means cumulative emissions briefly becoming negative (i.e. atmospheric carbon dipping below preindustrial values), which has dangerous implications for ecosystem health. Undoing sea-level rise that has already occurred would necessitate even more CDR, increasing the likelihood of having to decrease atmospheric carbon concentrations until they are lower than preindustrial.

In conclusion, to stop sea-level rise from ice melt would require returning cumulative carbon emissions to nearly 0. Given a constant rate of removal of 8PgC/year, this

takes from 2040 to around 2150, in the median case. The median level of cumulative emissions this brings the atmosphere back to is the same as it was in 1914 ($\pm$ 26 years), although there are some outside cases where atmospheric CO_2 concentrations get lower than preindustrial values. This result can be interpreted to mean that we have yet to experience the full effects (in terms of sea-level rise) of the past 109 years of emissions.

Chapter 5

Synthesis

This chapter will bring together results from the previous three chapters, and consider how they all fit into the narrative of the thesis. Section 5.1 will outline the results of each chapter and discuss their implications in a wider context, Section 5.2 will consider how each chapter can be extended to tell a more complete story, and Section 5.3 will consider each chapter in the context of the broader purpose of the thesis.

5.1 Discussion and Implications

The study in Chapter 2 was motivated by two things: first, by the fact that ocean acidification is related to carbon emissions, but not to warming. Second, that the relationship between carbon emissions and warming is not well constrained (Forster et al. (2021)), leading to a range of potential carbon budgets. Both of these together combine to mean that it is possible to limit warming to a desirable level, without explicitly preventing undesirable amounts of ocean acidification. The aim of this chapter was to explore a method to limit ocean acidification alongside warming, using two sets of targets for warming and surface ocean acidification. To do this, the Adjusting Mitigation Pathways (AMP) algorithm in the WASP climate emulator was adapted so that it would create carbon dioxide emissions pathways that were consistent with some combination of a warming target and an acidification target. The first step was to create two acidification targets, by considering the proportion of tropical ocean (between 30° North and South of the equator) where the saturation state of aragonite (Ω_{arag}) is above 3.4 (i.e. habitable for corals, according to Kleypas et al. (1999)). Outputs of dissolved inorganic carbon, pH, total alkalinity, ocean surface temperature and salinity from the Hadley Centre UKESM1.0-LL (Good et al. (2019)) were used in an offline carbonate chemistry solver (Follows et al. (2006)) to calculate global mean pH when the habitable area for tropical corals reaches 75% and 50% of its 2020 value. The two values of global mean pH using this method were 8.03

(acidification of -0.17 since preindustrial), and 7.99 (acidification of 0.21 since preindustrial), respectively.

Limiting acidification as well as warming lessens uncertainty in the carbon budget by removing the upper end of the distribution, such that the range of the remaining carbon budget is narrower, and the median is lower. For example when the algorithm creates an emissions trajectory consistent with limiting warming to 1.5°C and surface ocean acidification to -0.17 (the two most stringent targets in the study), the remaining carbon budget ranges from -74.0 to 129.8PgC. This reduces uncertainty in the carbon budget by 29% (from 286.2PgC to 203.8PgC). Assuming an emissions rate held constant since 2021 (which is a conservative assumption), this budget will be spent between 2023 and 2029. It is also notable that emissions trajectories towards combined targets have a less notable peak and decline shape, implying a need for less carbon dioxide removal in order to reach both targets. For example, for the more stringent acidification target (-0.17) and more stringent warming target, the necessary emissions reduction reduces from 145PgC for just a warming target to 10PgC for both, which is a 93% difference.

This chapter provides some framework to address issues caused by ocean acidification that are otherwise not explicitly considered in global climate mitigation policy. Because the main results are communicated in a way that is already well-established in climate science/policy (i.e., a remaining carbon budget towards a climate target), implementing this framework should not change the direction of climate change mitigation discourse, as the collective aim will still be to keep carbon emissions in line with a remaining carbon budget. Keeping in line with an acidification target as well as a warming target will (in the case of these targets) be a surer way of keeping the tropical oceans in a habitable state for corals that require an aragonite saturation state $\Omega_{arag} > 3.4$, and the narrowed range of the carbon budget also reduces the likelihood that a given warming target will be overshot. There is also a benefit to following an emissions trajectory with a less dramatic peak-and-decline shape, as this will require less urgent deployment of carbon dioxide removal technology, which is still nascent.

In Chapter 3, the aim was to find some way to capture nonlinearities in the relationship between warming and ice melt. This relationship is often treated as a linear one, but nonlinearities do exist (e.g. Edwards et al. (2019); Tigchelaar et al. (2019); Pollard and Deconto (2005)). A comparison of the transient sea level sensitivity (TSLS) of model studies and structured expert judgment by Grinsted and Hesselbjerg Christensen (2021) also implied that there are processes and nonlinearities that experts know of that are not represented well in models, as the TSLS is larger for the structured expert judgment projections. The work for this chapter is done using a low-complexity Earth systems model with a semi-empirical method for calculating sea-level rise. The method of calculating sea-level rise is extended to represent a nonlinear relationship between warming and ice melt. The results from this setup are

compared to a version of the same model that keeps the relationship between warming and ice melt linear. Using a low-complexity model to experiment with nonlinearising this relationship makes it possible to conduct an in-depth exploration of how changing the relationship between warming and ice melt can impact uncertainty in sea level projections, because the model is computationally cheap so a large (10^4 simulations) ensemble can be created. The model is calibrated using observational data from (Fox-Kemper et al. (2021)), which means that the nonlinearities that are captured in this setup are nonlinearities that have already impacted observed sea-level rise.

The difference between the linear and nonlinear model setup is bigger in the upper uncertainty range (97.5%), and in higher emissions scenarios (i.e., higher warming). For example, the percentage change from the linear to nonlinear projections of median sea level is -11%, 3% and 42% in SPPs 126, 245 and 585 (respectively), and the percentage change for the 97.5th percentile is 3%, 16% and 46% (respectively). This impacts the rate of sea-level rise as well, with the instantaneous rate of rise following a 4-fold increase in current warming being up to 6x the current rate of sea-level rise (in the 97.5th percentile). However for low levels of warming (up to around 1°C) and in the median case, nonlinearities are small enough that the relationship between warming and the rate of rise is roughly linear; that is, $SLR_{n \cdot dT} = n \cdot SLR_{dT}$ (see Figure 3.5). Note that these are results from a model calibrated using observations, so they are best interpreted as an exploration of how historically-precedented dynamics can impact future sea levels. Nonlinearities that begin to impact ice melt at higher levels of warming are not represented here, and can be expected to drive projections of sea-level rise up further.

It is important for uncertainty to be well understood and clearly communicated so that practitioners can plan effectively. The exploration of uncertainty in this study therefore has important implications for practitioners who are interested in knowing a large (5-95%) range of potential sea level outcomes (Hinkel et al. (2019)). The upper end of projections (in our case the 97.5th percentile) is impacted by allowing sea-level rise from ice to vary nonlinearly with ice melt, further increasing the impact of low-probability, high-impact futures. Although the study is focused on global mean sea-level rise, there is still importance for local regions where extreme sea level events are made worse by background mean sea-level rise (e.g. Hermans et al. (2023); Tebaldi et al. (2021)). The results of this study also highlight the importance of limiting global mean warming as much as possible, because historically-precedented nonlinearities are small when warming is low, but begin to make a difference of over a meter (1.6m) in higher emissions scenarios.

The motivation for Chapter 4 is related to the sea-level rise commitment that arises from the longer timescale of ice melt. There is a distinct lack of studies in the literature that seek to quantify how much carbon dioxide removal it would take to undo the

commitment to future sea-level rise. The aim of the study in this chapter is to fill this gap by adapting the AMP algorithm again, this time to create emissions pathways where emissions stabilise at a warming target that is consistent with keeping the sea level commitment to zero. To begin with the AMP algorithm is set with a warming target of 2.5°to reflect the warming that current NDCs are consistent with. In 2039, the target is changed to one that will limit the total amount of sea-level rise after 2040 to the committed rise consistent with the warming up until 2039 (effectively reducing the commitment after 2039 to zero). This warming target is calculated by exploiting the equilibrium relationship between sea-level rise and warming, constrained using Palaeo data from Kopp et al. (2009). The target is implemented in 2039 to allow 15 years of preparation for the high level of carbon dioxide removal that will be needed to reduce warming.

Preventing further sea-level rise in 2040 requires a secondary warming target of 0.01°C ($\pm$0.008°C), which is consistent with removing all cumulative emissions emitted since 1914 ($\pm$26 years). While this does not fully stabilise the sea level commitment at zero, after 2100 the total amount of sea-level rise is 5cm in 200 years, which is manageable from a practitioner standpoint. When comparing this to emissions pathways that are broadly consistent with 2°C warming (SSP 245 and an AMP-generated trajectory towards 2°C), the difference in median cumulative emissions in 2300 is 2500PgC and 2000PgC, and a difference in sea-level rise of around 0.7m and 0.6m. With a constant rate of carbon dioxide removal of 8PgC/year, this carbon is removed by around 2150.

It is important to note that the equation that defines the secondary warming target using sea-level rise from ice, so our secondary warming target is one that stabilises the committed sea-level rise just from ice melt, rather than from all sources of global mean sea-level rise. However melting ice sheets dominate the millennial commitment to sea-level rise, stabilising the committed rise from ice sheets at near-0 is still a significant result. Note also that there are some outside cases where cumulative emissions briefly become negative to keep to the warming target. This means that atmospheric carbon would temporarily be lower than it was in the preindustrial era, which has dangerous implications for ecosystem health (carbon dioxide is necessary for photosynthesis). It would be sensible to set a limit on CDR that atmospheric carbon must not get any lower than preindustrial concentrations, and in this case that would mean there are outside cases where the temperature goal necessary to keep the sea level commitment to zero after 2040 is not possible to meet as quickly as the simulations suggest.

This study is relevant in the context of the increasing focus on carbon dioxide removal (CDR) as part of the solution for climate change. It has been shown that the linear relationship between cumulative emissions holds even if net CO_2 emissions are negative (although the constant of proportionality is different – Zickfeld et al. (2016)), and removing carbon dioxide from the atmosphere is an important part of most

emissions trajectories that keep warming in line with the Paris Agreement targets. However, this study shows that in the context of sea-level rise, CDR cannot be used to 'turn back the clock' in the same way. By undoing warming it is possible to reduce the commitment to sea-level rise, but reducing the commitment to zero requires a prohibitively large scale of CDR, and undoing sea-level rise that has already occurred would mean removing CO_2 to the point that atmospheric concentrations of CO_2 would have to go below preindustrial values.

Understanding the scale of CDR it would take to reduce the sea level commitment to zero has relevance in the discussion around loss and damage that began to take centre stage at COP26 in Glasgow. The result that undoing the sea-level rise commitment would mean undoing all emissions since 1914 ($\pm$26 years) can be interpreted as quantifying that we have yet to experience the full effect of any emissions since 1914 ($\pm$26 years). Similarly, it can be assumed that emissions before 1914 ($\pm$26 years) but since the preindustrial period have already had their impact on sea-level rise, and it may take even more sustained negative cumulative emissions to reverse that rise, reducing atmospheric carbon concentrations even further below preindustrial values. This can be tied to the conversation around loss and damages because it quantifies the length of time over which emissions have been contributing to sea-level rise that is yet to be felt: i.e., that human activities have been responsible for sea-level rise post-2040, since 1914 (in the median case). One benefit of addressing a root cause of sea-level rise (in this case, ice melt) for this purpose is that it diminishes any issues with attribution, because ice melt is known to be a direct result of global mean warming and therefore carbon emissions. Attributing specific instances of loss and damage to climate change has been a limiting factor in determining how loss and damage funds can be allocated, and framing this study using a process that is linked to global carbon emissions, and presenting the results in the form of global carbon dioxide removal, circumnavigates this. However, this broad outlook means that the study does not by itself help in addressing loss and damage from sea-level rise in specific regions.

5.2 Future Work

There are various ways that the study in Chapter 2 can be extended. First of all, the set of acidification targets considered in this chapter is framed using coral habitability in the tropics, informed by the aragonite saturation state. These targets could just as easily have been informed by the saturation state in the high latitudes (especially the Arctic ocean) where the ocean is expected to become undersaturated with respect to aragonite sooner than other regions (Steinacher et al. (2009)). Framing the acidification targets using this threshold, either instead of or as well as tropical coral habitability, provides a new perspective on this study that takes high-latitude change into account, as well as just focusing on tropical corals. There is an interesting comparison to be

made between a carbon budget informed by tropical species, and a carbon budget informed by Arctic species. Secondly, tropical corals are not just impacted by acidification/aragonite saturation. Many studies have found that the impacts of ocean warming and acidification act together to create change (e.g. Yara et al. (2012); Talmage and Gobler (2011)). This is particularly true in the case of corals, where bleaching events are caused by warming surface oceans; although the impacts of warming and acidification are difficult to separate (Hoegh-Guldberg et al. (2018)). Future work could further adapt the AMP algorithm so that it stabilises carbon emissions in line with an acidification target and an ocean heat target that are both informed by regional projections for the tropics, framed using habitable levels of acidification (aragonite saturation) and ocean heat.

Both of these ideas would benefit from assessing not just global mean quantities, but having a more regional outlook. One way to do this that still saves computational expense is by having a latitudinally resolved model (one that outputs latitudinal means across lines of longitude). This would provide some idea of the different changes occurring at tropical and polar latitudes, which is sufficient to aid in differentiation for the two proposed continuations of the work done in Chapter 2. A more spatially resolved model also goes some way towards making this study more representative of spatial variation in surface ocean acidification. Many of the issues with having global mean warming as a target are related to the lack of certainty around how a certain amount of global mean warming will impact different areas of the globe, and the same is true of having a target for global mean acidification. Showing changing ocean acidification from the poles to the equator goes some way towards remedying this.

One important caveat of the work done in Chapter 3 is the fact that the model is calibrated using observational data. The WASP model has not previously been used as an emulator (calibrated using outputs from one or more outputs from a complex model) but rather a reduced complexity/semi-empirical model (calibrated using observations). Calibrating WASP using consistency checks that involve projections and hindcasts from a complex model (or suite of models) and comparing results from the same experimental setup to the results from this chapter would provide some insight into the impacts of historically unprecedented nonlinearities (such as MISI). If this is done, the contribution of Antarctica will no longer be as small as it has been over the observational period, particularly in high warming scenarios, and this can be captured in the consistency checks. This means that it may be worth exploring whether relating ice melt from Antarctica to ocean heat content (which is the dominant driver of Antarctic ice melt rather than atmospheric warming) makes a difference to projections. As with the proposed future work for Chapter 2, this work would benefit from having a latitudinally-resolved model so that ocean heat and

atmospheric warming in the regions where they are most relevant can be used as the predictor for the ice melt they are most responsible for.

One way that the study in Chapter 4 could be extended is to consider a method to include stabilising the commitment from thermosteric rise in the AMP algorithm explicitly; currently the study only focuses on ice melt. This would likely mean an even more dramatic reduction of atmospheric CO_2, as Ehlert and Zickfeld (2018) found that in a scenario where emissions were ramped up to $4\times$ their preindustrial concentration, then reversed to preindustrial, thermosteric sea-level rise continued for several decades after preindustrial carbon concentration is restored, and the commitment is not undone for over 1000 more years. There is also more to be done on the exploration of what it would take to reverse sea-level rise completely. This would take significant global cooling and therefore sustained negative cumulative emissions. Currently, the sea-level rise calculations in the WASP model deal with ice sheet hysteresis by assuming no change in ice sheets in the event of cooling. To explore ice sheet regrowth, there would have to be a more sophisticated way of navigating this, and the timescales of the WASP model would have to be extended far beyond 2300. The impacts of large scale CDR are still relatively unexplored, so this study would pair well with an exploration of what the ecological impacts would be of the CDR necessary to undo committed sea-level rise. As well as this, the study in Chapter 4 would benefit from a more rigourous way of choosing the rate of carbon removal, for example through an understanding of how much CDR (and what type of CDR) may be feasible to deploy by 2040. Assessing the impact on environmental or other Earth system factors (for example productivity and acidification) of these pathways depends on making an assumption about how this carbon is removed from the atmosphere, because different methods of CDR act in different ways and are effective on different timescales.

5.3 Conclusions

The motivation for this thesis was to explore the gaps in future climate change that are left by addressing only a global mean warming target. In each chapter, a reduced-complexity Earth systems model was used to consider either ocean acidification or sea-level rise in the context of anthropogenic carbon emissions, and how these can be used to inform carbon pathways and remaining carbon budgets that are more representative of these issues. The main way of doing this was to adapt the Adjusting Mitigation Pathways (AMP) algorithm in the Warming, Acidification and Sea level Projector of Goodwin et al. (2018a). Table 5.1 shows a collection of all the remaining carbon budgets calculated in this thesis, as well as a brief outline of how they were calculated and why they were used as targets.

TABLE 5.1: A collection of all remaining carbon budgets (RCBs) from Chapters 2 and 4.

	Warming (IPCC AR6)	**Warming (this study)**	**Acidification**
Nature of target	Remaining Carbon budget in PgC	Remaining Carbon budget in PgC	Remaining Carbon budget in PgC
Rationale	Linear relationship between warming and cumulative emissions allows for calculation of RCB for warming targets	Linear relationship between warming and cumulative emissions allows for calculation of RCB for warming targets	Using just warming as a target does not allow for explicit consideration of issues caused by carbon but not warming (i.e. acidification)
Method of calculation	According to SR15 report	AMP algorithm towards a warming target, then calculating difference in cumulative emissions at 2100 and beginning of algorithm	AMP algorithm towards an acidification target, then calculating difference in cumulative emissions at 2100 and beginning of algorithm
Result (median)	1.5C: 140; 2.0C: 370	1.5C: 70.2; 2.0C: 365.4	8.03pH: 143.0; 7.99pH: 381.3
Notes		Calculated as an 'exceedance budget' using a time horizon to avoid choosing a peak in either warming or acidification, to aid consistency between targets	

	Warming and Acidification (STRICT)	**sea-level rise**
Nature of Target	Remaining Carbon budget in PgC	year to return to
Rationale	Both targets together provide a more complete image of how to avoid dangerous change to terrestrial and marine systems.	sea-level rise is pathway dependent, but warming is not, so warming-based RCBs neglect this
Method of Calculation	AMP algorithm calculates emissions rate towards both targets and picks (in this case) most stringent emissions rate. Then RCB calculated as for single target.	Find the last time cumulative emissions were at the level they reach in AMP algorithm once SLR is (nearly) stable
Result (median)	8.03pH/1.5C: 24.6; 7.99pH/2.0C: 315.2	1914
Notes		Presented as a year to demonstrate how many years of warming have not yet been fully realised as sea-level rise

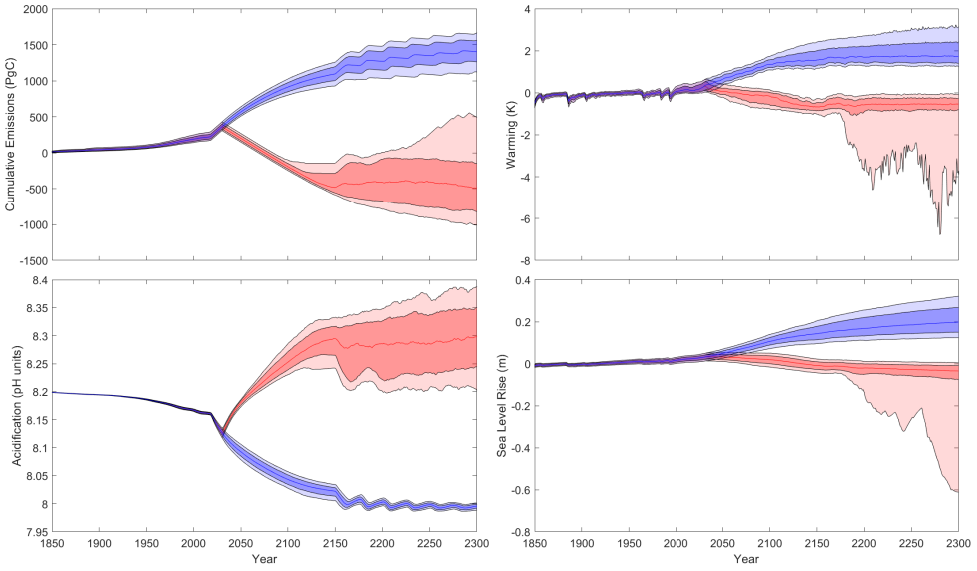

FIGURE 5.1: The strict and lenient carbon trajectories following and integrated AMP setup where the initial warming and acidification targets are 2.0C and -0.21C respectively, and the warming target switches in 2039 to be consistent with stabilising the SLR commitment to 0 (or as close as possible).

For the purposes of this synthesis, both AMP formats devised in this thesis have been integrated into one, where the algorithm has the option to pick an acidity-based or a warming-based emissions rate, and in 2039 the warming target switches to one consistent with stabilising the SLR commitment at 0. The vast difference in stringency between the acidification targets from Chapter 2 and the sea level target in Chapter 3 means that once the sea level target is implemented in 2039, there is little competition between the two targets. Figure 5.1 shows the strict and lenient trajectories with the acidification target at -0.21, and an initial warming target of 2.0 (which is changed in 2039). Once the 'sea level' target is introduced, the lenient scenario follows the acidification target, and the strict scenario follows the warming/sea level target. The scale of CO_2 removal needed to reach the warming/sea level target means that there are outside cases where the WASP model reacts unphysically to the negative emissions, leading to the fringes in the distribution of warming and total sea level rise (which is due to the reaction of steric sea level to warming), and the considerably wider distribution of ocean acidification than in the lenient scenario.

A recurring theme throughout the thesis has been the importance of reduced-complexity Earth systems modelling as a tool for exploring uncertainty in climate science. Each of the chapters in this thesis make use of this. In Chapter 2, uncertainty in the remaining carbon budget is explored, and is found to be narrowed by considering multiple climate targets (in this case, warming and acidification together). In Chapter 3, a key result of the study pertains to the impact on uncertainty in sea-level rise projections of allowing ice melt to vary nonlinearly with warming. In Chapter 4, it is noteworthy that the uncertainty in the amount of cumulative emissions

consistent with the secondary warming target is considerably lower than uncertainty associated with the remaining carbon budget according to the most recent estimate of the TCRE (Forster et al. (2021)). This is the case despite the fact that all calculations are done with a sea-level rise equation that increases uncertainty in the sea-level rise projections (see Chapter 3). The reduction in uncertainty here could be because there is inherently less uncertainty associated with framing a carbon budget by returning to a previous state, rather than projecting to a future one. It is important to note that the form of uncertainty explored here is parametric uncertainty (uncertainty relating to how model parameters are defined) rather than process uncertainty (uncertainty related to physical process that impact climate change and its effects).

Each chapter has a focus on different aspects of ocean change: Chapter 2 on limiting ocean acidification alongside warming, Chapter 3 on how nonlinearities in ice melt behave as warming increases, and Chapter 3 on stabilising the sea-level rise commitment to as close to zero as possible. However there is a unifying message between all of these chapters, and is not new. The sooner carbon emissions are limited, the fewer issues from ocean change we can expect to experience, and the less work has to be done in later years to mitigate damage. In Chapter 2, this is shown in the smaller peak-and-decline pattern in carbon trajectories that include an acidification target (either wholly or partly). In Chapter 3, it is visible in the increased impact of nonlinear ice melt at higher global mean warming. In Chapter 4, it is shown in the CDR needed to undo over 100 years of emissions since 1914, of which we have yet to experience the full impact in terms of global mean sea-level rise.

The purpose of this thesis was to examine climate change beyond global mean warming, and pathways towards climate targets that represented ocean-based issues. Although acidification and sea-level rise are separate processes (one chemical one physical), the root cause of both of these hazards is carbon emissions. The chapters in this thesis examine how carbon emissions can be altered so that they do not just limit global mean warming, but also prevent dangerous changes in ocean properties like surface acidity or sea level. The targets chosen in each study are illustrative (limiting acidification to -0.17 and 0.21, or limiting the sea-level rise commitment to 0), but a similar method can be applied to any differently framed target. There are two prevailing messages through all of these chapters. Firstly that uncertainty is an unavoidable aspect of projecting climate change, but parametric uncertainty can be explored and understood using tools like reduced-complexity models, and used for communication with practitioners. Secondly, that whatever aspect of the Earth system is addressed and used to frame the remaining carbon budget, there is everything to be gained by limiting carbon emissions earlier rather than later.

Appendix A

Table of Parameters in the Version of WASP used in Chapters 2, 3 and 4

TABLE A.1: Earth system parameters in the version of WASP used in Chapter 2

Earth system parameter	Description	Distribution Shape	Range	Mean, S.D
a_CO2	Radiative forcing coefficient for a log change in CO_2	normal		5.35±0.27
dNPP/dT	Sensitivity of global Net Primary Production to temperature anomaly	uniform	-5.0 to 1.0 yr °C^{-1}	
Γ_K	CO_2 fertilisation coefficient for NPP	uniform	0 to 1.0	
r_1	Ratio of warming between global surface air temperatures and global sea surface temperatures at equilibrium	uniform	0.30 to 1.45	
r_2	Ratio of warming between global whole-ocean warming and global sea surface warming at equilibrium	uniform	0.01 to 0.75	
$d\tau/dT$	Sensitivity of global soil carbon residence time to global temperature anomaly	normal		-1.36 ± 0.45 W/m^2
λ_{Planck}	Planck climate feedback	normal		3.15±0.04 W/^{2}
λ_{WVLR}	Combined water vapour/lapse rate equilibrium feedback	normal		-1.15±0.09 W/^{2}
λ_{fast}^{cloud}	Equilibrium feedback from clouds with original SST patterns	normal		-0.43±0.33 W/^{2}
λ_{SST}^{cloud}	Change in equilibrium feedback from clouds with final SST patterns	normal		-0.47±0.3 W/^{2}
λ_{albedo}	Surface albedo feedback	normal		0.37±0.10 W/^{2}
λ_{1000yr}	Equilibrium climate feedback from slow processes, such as large ice sheets	normal		0
$f\_heat - ocean$	Fraction of total Earth system heat uptake that enters the ocean	uniform	0.9 to 0.96 yr	

TABLE A.2: Earth system parameters in the version of WASP used in Chapter 2, continued

Earth system parameter	Description	Distribution Shape	Range	Mean, S.D
τ^{C}_{mixed}	e-folding timescale of carbon exchange between atmosphere and surface ocean mixed layer	uniform	0.5 to 1.0 yr	
τ^{C}_{upper}	e-folding timescale of carbon exchange between surface ocean mixed layer and upper thermocline	uniform	5.0 to 40.0 yr	
τ^{C}_{inter}	e-folding timescale of carbon exchange between surface ocean mixed layer and intermediate water	uniform	15.0 to 60.0 yr	
τ^{C}_{deep}	e-folding timescale of carbon exchange between surface ocean mixed layer and deep water	uniform	75.0 to 500.0 yr	
τ^{C}_{bottom}	e-folding timescale of carbon exchange between surface ocean mixed layer and bottom water	uniform	250.0 to 1500.0 yr	
I_b	buffered carbon inventory	uniform	3100 to 3900 PgC	
tau_{WVLR}	e-folding timescale of cloud/lapse rate processes with original SST patterns	normal		0.024383562±0.00109589
tau^{cloud}_{fast}	e-folding timescale of fast cloud processes (set here equal to the WVLR timescale)	$tau^{cloud}_{fast} = tau_{WVLR}$	-	-
tau_{albedo}	e-folding timescale of surface albedo feedback processes	uniform	0.5 to 5.0 yr	
$R^{uncert}_{aerosol}$	uncertainty in radiative forcing from aerosols	normal		-0.057±0.4298
t$R^{uncert}_{WMGHG-nonCO2}$	Uncertainty in radiative forcing from well mixed, non-CO_2 greenhouse gases	normal		0.0±0.06079
$R^{coeff}_{volcanic}$	radiative forcing from volcanoes			

TABLE A.3: Earth system parameters in the version of WASP used in Chapter 3 and 4

Earth System Parameter	Description	Distribution	Range	Mean, S.D.
λ_{Planck}	Planck climate feedback	log-normal		3.3±0.1W$/^2$
λ_{fast}^{equil}	equilibrium climate feedback from fast processes	log-normal		$-\lambda_{Planck}, \lambda_{Planck}$
τ_{fast}	e-folding timescale of fast climate feedback processes	normal		8.9±0.4 days
$\lambda_{multidecadal}^{equil}$	equilibrium climate feedback from slow processes	uniform	-3.0 to 3.0 W$/^2$	
$\tau_{multidecadal}$	e-folding timescale of slow climate feedback processes	uniform	20 to 45 years	
a_{CO2}	radiative forcing coefficient for a log change in CO_2	normal		5.35±0.27 W$/^2$
	uncertainty in N_2O radiative forcing (dimensionless)	normal		1.0±0.05
	uncertainty in CH_4 radiative forcing (dimensionless)	normal		1.0±0.07
	uncertainty in CH_4 radiative forcing (dimensionless)	normal		-19.0±0.5 W$/^2$
$\gamma_{SOx}E_{SOx}$	Radiative forcing from SO_x aerosols in 2010	normal		-0.31±0.11 W$/^2$
$\gamma_{BC}E_{BC}$	Radiative forcing from black carbon aerosols in 2010	normal		-0.18±0.07 W$/^2$
$\gamma_{NOx}E_{NOx}$	Radiative forcing from nitrous oxide aerosols in 2010	normal		-0.08±0.04 W$/^2$
$\gamma_{SOA}E_{NMVOC}$	Radiative forcing from volatile organic compounds in 2010	normal		-0.06±0.09 W$/^2$
$\gamma_{OC}E_{OC}$	Radiative forcing from organic compounds in 2010	normal		-0.03±0.01 W$/^2$
$\gamma_{NH3}E_{NH3}$	Radiative forcing from NH_3 aerosols in 2010	normal		-0.08±0.04 W$/^2$

TABLE A.4: Earth system parameters in the version of WASP used in Chapter 3 and 4, continued

Earth System Parameter	Description	Distribution	Range	Mean, S.D.
$R_{aci:2011}$	Radiative forcing from indirect aerosol effects in 2011	skew-normal		-0.55±0.37 $W/^2$, skew = -2.0
	e-folding timescale of carbon exchange between atmosphere and surface ocean mixed layer	uniform	0.5 to 1.0 years	
	e-folding timescale of tracer exhange between surface ocean mixed layer and upper thermocline	uniform	5 to 40 years	
	e-folding timescale of tracer exchange between surface ocean mixed layer and intermediate water	uniform	15 to 60 years	
	e-folding timescale of tracer exchange between surface ocean mixed layer and deep water	uniform	100 to 500 years	
	e-folding timescale of tracer exchange between surface ocean mixed layer and bottom water	uniform	400 to 1500 years	
	Atmosphere-ocean buffered carbon inventory	uniform	3100 to 3900 PgC	
r_1	Ratio of near-surface global warming to global sea surface warming at equilibrium	uniform	0.20 to 1.5	
r_2	Ratio of whole-ocean global warming to global sea surface warming at equilibrium	uniform	0.1 to 1.0	
a	SLR from ice per degree warming per year	uniform	-0.005 to 0.005 m/year/K	
	Ratio of SLR from ice at 1 degree warming to 10 degrees warming	log-normal		log(1.0), log(2.0)
dT_{LIG}	Difference in warming during LIG	uniform	1.0 to 2.0 K	
dZ_{LIG}	Difference in sea level during LIG	normal		7.2±1.3 m

TABLE A.5: The resultant equilibrium climate sensitivity (ECS) over various timescales from the WASP model as calculated in Goodwin (2018). The short timescale values (1-year) are consistent with estimates from Earth's current energy balance. The longer timescale values are consistent with previous estimates on the century-scale. This indicates that a WASP ensemble is consistent with the range of ECS estimates in the literature.

	climate sensitivity (degrees C)		
response timescale	median	66% range	95% range
0.1years	1.9	1.7 to 2.2	1.5 to 2.6
1 year	2.1	1.8 to 2.4	1.6 to 2.8
10 years	2.4	2.1 to 2.9	1.8 to 3.4
100 years	2.9	2.3 to 3.5	1.9 to 4.6

Appendix B

Adjusting Mitigation Pathways Algorithm for an Acidification Target

This is an in-depth description of the rationale and equations used in the Adjusting Mitigations Pathways (AMP) algorithm to achieve carbon pathways towards a specified acidification target.

Surface ocean pH is closely tied to atmospheric CO_2 levels, since there is an approximate annual timescale for CO_2 exchanges between the atmosphere and surface ocean mixed layer and seawater pH reduces with ocean CO_2 uptake due to carbonate chemistry equations (Zeebe and Wolf-Gladrow (2001)). Thus, any given minimum surface ocean pH target can be accurately expressed as the maximum atmospheric CO_2 level that corresponds to that surface ocean pH level. To account for lag between atmoshperic CO_2 emissions and surface ocean acidification, the ocean acidification (minimum pH) target in the scenario algorithm is expressed as the maximum atmospheric CO_2 that corresponds to that ocean surface pH value. To do this, we assume that the atmospheric fraction of emitted CO_2 (the amount of total emissions that remain in the atmosphere, $\Delta CO_{2.atmos} / \Delta I_{em}$), remains roughly constant over the assessment period (10 years) (Friedlingstein et al. (2006)).

We begin by deriving the historic atmospheric fraction of CO_2 from observations of the last three years compared to the 2009 to 2012 reference period:

$$\left(\frac{\Delta CO_{2.atmos}}{\Delta I_{em}}\right)_{obs}(t_n) = \frac{CO_2(t_n - 3 \rightarrow t_n - 1) - CO_2(2009 \rightarrow 2012)}{I_{em}(t_n - 2) - I_{em}(2010)} \tag{B.1}$$

Note that this takes the observation period to end one year before the time when the emissions rate is altered, to allow some time for policy discussion and implementation

(Goodwin et al. (2018a)). The remaining allowable carbon emissions, $I_{remaining}$, is then given by

$$I_{remaining} = \frac{CO_{2.atmos}(target) - CO_{2.atmos}(t)}{\Delta I_{em}} - \Delta CO_{2.atmos} \tag{B.2}$$

where $\Delta CO_{2.atmos}(target)$ is the change in CO_2 associated with the target ΔpH, and is calculated using the relationship between atmospheric CO_2 and surface ocean pH:

$$\Delta pH = c_{pH1}\Delta lnCO_2(t) + c_{pH2}(-C_{sat}) \tag{B.3}$$

where ΔC_{sat} is the difference between the current dissolved inorganic carbon concentration, and the dissolved inorganic carbon that brings the surface ocean into equilibrium with atmospheric CO_2, and C_{pH1} and C_{pH2} are coefficients calculated using a perturbation experiment in an explicit numerical carbonate chemistry solver (Follows et al. (2006)). This equation is rearranged so that

$$CO_{2.atmos}(target) = exp\Big(\frac{8.2 - pH_{target}}{0.387}\Big) \tag{B.4}$$

This can be substituted into Equation B.2 to find the remaining emissions budget at the beginning of each time step.

This protocol is followed every 10 years until 2150, whereupon the algorithm changes to remove carbon at a constant and discrete rate (dependent on the size of the overshoot) if the target has been exceeded, and allow carbon emissions at a constant rate if the target has not yet been met.

When the AMP algorithm is applied, it runs once for the temperature target as per the algorithm developed by Goodwin et al. (2018a) and once for the acidification target as described above, generating two potential emission rates for the next ten years. Depending on what combination of targets we wish to look at, the algorithm can be set to take the most strict (i.e. lowest) emissions rate, the most lenient (highest) emissions rate, or a weighted combination of the two emission rates generated by following the temperature and pH targets. For the purposes of this study, the weighting is assigned as 50:50, but this can be adapted to prioritise acidification or warming as necessary.

Following the AMP algorithm of Goodwin et al. (2018a), the annual global net carbon emission rate is then linearly reduced to zero so that total future cumulative emission after time t_n is $I_{remaining}(t_n)$ using

$$C_{rate}(t) = C_{rate}(t_n)\Big(1 - \frac{t - t_n}{t_{C=0}}\Big) \tag{B.5}$$

Appendix C

Sea Level Rise Formulation in WASP

The WASP model calculates SLR as the combination of change due to land-ice melting (including glaciers, excluding land-water storage) and thermosteric changes due to changes in ocean heat content:

$$\frac{d}{dt}GMSL(t) = \frac{d}{dt}GMSL_{ice} + \frac{d}{dt}GMSL_{thermosteric} \tag{C.1}$$

where the thermosteric component is process-based:

$$\frac{d}{dt}GMSL_{thermosteric} = c_{thermal}\Delta OHC \tag{C.2}$$

and the ice-melt contribution is semi-empirical:

$$\frac{d}{dt}GMSL_{ice} = (a\Delta T + b\Delta T^2)\Big(\frac{c\Delta T - \Delta GMSL_{ice}}{c\Delta T}\Big) \tag{C.3}$$

The first part of this is a Taylor expansion of the semi-empirical method used by Rahmstorf (2007), which originally had total SLR linearly linked to warming via a single constant. Here, the coefficients a and b are tuned by observations of SLR contributors during the historical period, given in Table 9.5 in the IPCC AR6 (Fox-Kemper et al. (2021)). The parameter a accounts for a linear component of ice contribution, and b accounts for the nonlinear component. The second term encourages SLR towards an equilibrium level based off palaeo constraints from the last interglacial, where c is the equilibrium relationship between temperature rise and SLR:

$$c = \frac{\Delta GMSL}{\Delta T}\Big|_{LIG} \tag{C.4}$$

The land ice contribution is assumed to be scenario independent, and is added offline. A final estimate of 2100 landwater-related SLR is randomly selected from the distribution of projected 2100 landwater storage change in IPCC AR6 (Fox-Kemper et al. (2021)), and a linear trajectory to that value is superimposed on the WASP-calculated SLR. After 2100, the landwater contribution is held constant, to avoid making any further assumptions about development etc.

Appendix D

Data Availability

D.1 Datasets for Observational Constraints

The datasets outlined in Tables 2.1 and 3.1 are publicly available and can be found at:

Paper associated with dataset	URL to dataset
Morice et al. (2012)	https://www.metoffice.gov.uk/hadobs/hadcrut4/data/current/download.html
GISS Surface Temperature Analysis	https://data.giss.nasa.gov/gistemp/
Hansen et al. (2012)	https://data.giss.nasa.gov/gistemp/
Smith et al. (2008)	https://www.ncei.noaa.gov/access/metadata/landing-page/bin/iso?id=gov.noaa.ncdc:C00759#:∼:text=The%20historical%20Merged%20Land%2DOcean,Network%20(GHCN)%20temperature%20database.
Vose et al. (2012)	https://www.ncei.noaa.gov/access/metadata/landing-page/bin/iso?id=gov.noaa.ncdc:C00759#:∼:text=The%20historical%20Merged%20Land%2DOcean,Network%20(GHCN)%20temperature%20database.
Levitus et al. (2012)	https://repository.library.noaa.gov/view/noaa/1195; https://www.ncei.noaa.gov/
Giese and Ray (2011)	http://apdrc.soest.hawaii.edu/datadoc/soda_2.2.4.php
Balmaseda et al. (2013)	https://www.cen.uni-hamburg.de/en/icdc/data/ocean/easy-init-ocean/ecmwf-ocean-reanalysis-system-4-oras4.html
Good et al. (2013)	https://www.metoffice.gov.uk/hadobs/en4/
Cheng et al. (2017)	http://159.226.119.60/cheng/images_files/IAP_OHC_estimate_update.txt
Huang et al. (2015)	https://psl.noaa.gov/data/gridded/data.noaa.ersst.v4.html
Kennedy et al. (2011)	https://icoads.noaa.gov/products.html
Morice et al. (2021)	https://www.metoffice.gov.uk/ hadobs/hadcrut5/data/current/download.html
Kennedy et al. (2019)	https://www. metoffice.gov.uk/hadobs/hadsst4/data/download.htm

D.2 The WASP Model

Versions of the WASP model used for Chapters 2 and 3 are available at https://zenodo.org/badge/latestdoi/554914531

D.3 IRIDIS

I acknowledge the use of the IRIDIS High Performance Computing Facility, and associated support services at the University of Southampton, in the completion of this work.

References

Myles R. Allen, David J. Frame, Chris Huntingford, Chris D. Jones, Jason A. Lowe, Malte Meinshausen, and Nicolai Meinshausen. Warming caused by cumulative carbon emissions towards the trillionth tonne. *Nature*, 458(7242):1163–1166, 2009. ISSN 00280836. . URL http://dx.doi.org/10.1038/nature08019.

V. K. Arora, A. Katavouta, R. G. Williams, C. D. Jones, V. Brovkin, P. Friedlingstein, J. Schwinger, L. Bopp, O. Boucher, P. Cadule, M. A. Chamberlain, J. R. Christian, C. Delire, R. A. Fisher, T. Hajima, T. Ilyina, E. Joetzjer, M. Kawamiya, C. D. Koven, J. P. Krasting, R. M. Law, D. M. Lawrence, A. Lenton, K. Lindsay, J. Pongratz, T. Raddatz, R. Séférian, K. Tachiiri, J. F. Tjiputra, A. Wiltshire, T. Wu, and T. Ziehn. Carbon–concentration and carbon–climate feedbacks in cmip6 models and their comparison to cmip5 models. *Biogeosciences*, 17(16):4173–4222, 2020. . URL https://bg.copernicus.org/articles/17/4173/2020/.

S. Avrutin, P. Goodwin, and T.H.G. Ezard. Assessing the remaining carbon budget through the lens of policy-driven acidification and temperature targets. *Climatic Change*, 2023, in press.

Magdalena Alonso Balmaseda, Kristian Mogensen, and Anthony T. Weaver. Evaluation of the ecmwf ocean reanalysis system oras4. *Quarterly Journal of the Royal Meteorological Society*, 139(674):1132–1161, 2013. . URL https://rmets.onlinelibrary.wiley.com/doi/abs/10.1002/qj.2063.

J. L. Bamber, M. Oppenheimer, R. E. Kopp, W. P. Aspinall, and Roger M. Cooke. Ice Sheet and Climate Processes Driving the Uncertainty in Projections of Future Sea Level Rise: Findings From a Structured Expert Judgement Approach. *Earth's Future*, 10(10):1–13, 2022. ISSN 23284277. .

Jonathan Bamber, Michael Oppenheimer, Robert E. Kopp, Willy P. Aspinall, and Roger M. Cooke. Ice sheet contributions to future sea-level rise from structured expert judgment. *Proceedings of the National Academy of Sciences of the United States of America*, 166(23):11195–11200, 2019. ISSN 10916490. .

J. N. Bassis and C. C. Walker. Upper and lower limits on the stability of calving glaciers from the yield strength envelope of ice. *Proceedings of the Royal Society A:*

Mathematical, Physical and Engineering Sciences, 468(2140):913–931, 2012. ISSN 14712946. .

Michael Bevis, Christopher Harig, Shfaqat A. Khan, Abel Brown, Frederik J. Simons, Michael Willis, Xavier Fettweis, Michiel R. Van Den Broeke, Finn Bo Madsen, Eric Kendrick, Dana J. Caccamise, Tonie Van Dam, Per Knudsen, and Thomas Nylen. Accelerating changes in ice mass within Greenland, and the ice sheet's sensitivity to atmospheric forcing. *Proceedings of the National Academy of Sciences of the United States of America*, 116(6):1934–1939, 2019. ISSN 10916490. .

Raphaël Billé, Ryan Kelly, Arne Biastoch, Ellycia Harrould-Kolieb, Dorothée Herr, Fortunat Joos, Kristy Kroeker, Dan Laffoley, Andreas Oschlies, and Jean Pierre Gattuso. Taking action against ocean acidification: A review of management and policy options. *Environmental Management*, 52(4):761–779, 2013. ISSN 0364152X. .

Klaus Bittermann, Stefan Rahmstorf, Robert E Kopp, and Andrew C Kemp. Global mean sea-level rise in a world agreed upon in paris. *Environmental Research Letters*, 12(12):124010, dec 2017. . URL https://dx.doi.org/10.1088/1748-9326/aa9def.

O Boucher, P R Halloran, E J Burke, M Doutriaux-Boucher, C D Jones, J Lowe, M A Ringer, E Robertson, and P Wu. Reversibility in an earth system model in response to co2 concentration changes. *Environmental Research Letters*, 7(2):024013, may 2012. . URL https://dx.doi.org/10.1088/1748-9326/7/2/024013.

Nathaelle Bouttes, Jonathan Gregory, and Jason Lowe. The reversibility of sea level rise. *Journal of Climate*, 04 2013. .

J. E. Box, X. Fettweis, J. C. Stroeve, M. Tedesco, D. K. Hall, and K. Steffen. Greenland ice sheet albedo feedback: thermodynamics and atmospheric drivers. *The Cryosphere*, 6(4):821–839, 2012. . URL https://tc.copernicus.org/articles/6/821/2012/.

Jason E. Box, Alun Hubbard, David B. Bahr, William T. Colgan, Xavier Fettweis, Kenneth D. Mankoff, Adrien Wehrlé, Brice Noël, Michiel R. van den Broeke, Bert Wouters, Anders A. Bjørk, and Robert S. Fausto. Greenland ice sheet climate disequilibrium and committed sea-level rise. *Nature Climate Change*, 12(September), 2022. ISSN 17586798. .

S. Brough, J. R. Carr, N. Ross, and J. M. Lea. Ocean-forcing and glacier-specific factors drive differing glacier response across the 69°n boundary, east greenland. *Journal of Geophysical Research: Earth Surface*, 128(4):e2022JF006857, 2023. . URL https://agupubs.onlinelibrary.wiley.com/doi/abs/10.1029/2022JF006857. e2022JF006857 2022JF006857.

S. Brown, R. J. Nicholls, Philip Goodwin, I. D. Haigh, D. Lincke, A. T. Vafeidis, and J. Hinkel. Quantifying Land and People Exposed to Sea-Level Rise with No

Mitigation and 1.5°C and 2.0°C Rise in Global Temperatures to Year 2300. *Earth's Future*, 6(3):583–600, 2018. ISSN 23284277. .

John F. Bruno and Elizabeth R. Selig. Regional decline of coral cover in the Indo-Pacific: Timing, extent, and subregional comparisons. *PLoS ONE*, 2(8), 2007. ISSN 19326203. .

Kevin Bulthuis, Maarten Arnst, Sainan Sun, and Frank Pattyn. Uncertainty quantification of the multi-centennial response of the antarctic ice sheet to climate change. *The Cryosphere*, 13(4):1349–1380, 2019. ISSN 19940424. .

Lauretta Burke, Katie Reytar, Mark Spalding, and Allison Perry. *Reefs at Risk Revisited*. World Resources Institute, 01 2011.

Wenju Cai, Fan Jia, Shujun Li, Ariaan Purich, Guojian Wang, Lixin Wu, Bolan Gan, Agus Santoso, Tao Geng, Benjamin Ng, Yun Yang, David Ferreira, Gerald A. Meehl, and Michael J. McPhaden. Antarctic shelf ocean warming and sea ice melt affected by projected El Niño changes. *Nature Climate Change*, 13(3):235–239, 2023. ISSN 17586798. .

J.G. Canadell, P.M.S. Monteiro, M.H. Costa, L. Cotrim da Cunha, P.M. Cox, A.V. Eliseev, S. Henson, M. Ishii, S. Jaccard, C. Koven, A. Lohila, P.K. Patra, S. Piao, J. Rogelj, S. Syampungani, S. Zaehle, and K. Zickfeld. *Global Carbon and other Biogeochemical Cycles and Feedbacks*, page 673–816. Cambridge University Press, Cambridge, United Kingdom and New York, NY, USA, 2021. .

Long Cao and Ken Caldeira. Atmospheric CO2 stabilization and ocean acidification. *Geophysical Research Letters*, 35(19):1–5, 2008. ISSN 00948276. .

Christopher Chambers, Ralf Greve, Takashi Obase, Fuyuki Saito, and Ayako Abe-Ouchi. Mass loss of the antarctic ice sheet until the year 3000 under a sustained late-21st-century climate. *Journal of Glaciology*, 68(269):605–617, 2022. .

Lijing Cheng, Kevin E. Trenberth, John Fasullo, Tim Boyer, John Abraham, and Jiang Zhu. Improved estimates of ocean heat content from 1960 to 2015. *Science Advances*, 3(3):e1601545, 2017. . URL https://www.science.org/doi/abs/10.1126/sciadv.1601545.

John A. Church, Jonathan M. Gregory, Anny Cazenave, Jonathan M. Gregory, Svetlana Jevrejeva, Anders Levermann, Mark A. Merrifield, Glenn A. Milne, R. Steven Nerem, Patrick D. Nunn, Antony J. Payne, W. Tad Pfeffer, Detlef Stammer, and Alakkat S. Unnikrishnan. Sea level change. In *Climate Change 2013: The Physical Science Basis. Contribution of Working Group I to the Fifth Assessment Report of the Intergovernmental Panel on Climate Change*, pages 493–499. Cambridge University Press, 2013. ISBN 9780128130810. .

Peter U Clark, Alan C Mix, Michael Eby, Anders Levermann, Joeri Rogelj, Alexander Nauels, and David J Wrathall. Sea-level commitment as a gauge for climate policy. *Nature Climate Change*, 8(August):653–655, 2018.

Fiona Clerc, Brent M. Minchew, and Mark D. Behn. Marine Ice Cliff Instability Mitigated by Slow Removal of Ice Shelves. *Geophysical Research Letters*, 46(21): 12108–12116, 2019. ISSN 19448007. .

Béatrice Cointe and Hélène Guillemot. A history of the 1.5°C target. *WIREs Climate Change*, 14(3):1–11, 2023. ISSN 1757-7780. .

Béatrice Cointe, Paul-alain Ravon Po, and Emmanuel Guérin. 2°C : the history of a policy-science nexus. *IDDRI Working Papers*, 19/11:1–28, 2011.

Sarah R. Cooley, Brittany Bello, Daniel Bodansky, Anthony Mansell, Andreas Merkl, Nigel Purvis, Susan Ruffo, Gwynne Taraska, Anna Zivian, and George H. Leonard. Overlooked ocean strategies to address climate change. *Global Environmental Change*, 59:101968, 2019. ISSN 0959-3780. . URL https://www.sciencedirect.com/science/article/pii/S0959378019301311.

Christopher E. Cornwall, Steeve Comeau, Niklas A. Kornder, Chris T. Perry, Ruben van Hooidonk, Thomas M. DeCarlo, Morgan S. Pratchett, Kristen D. Anderson, Nicola Browne, Robert Carpenter, Guillermo Diaz-Pulido, Juan P. D'Olivo, Steve S. Doo, Joana Figueiredo, Sofia A.V. Fortunato, Emma Kennedy, Coulson A. Lantz, Malcolm T. McCulloch, Manuel González-Rivero, Verena Schoepf, Scott G. Smithers, and Ryan J. Lowe. Global declines in coral reef calcium carbonate production under ocean acidification and warming. *Proceedings of the National Academy of Sciences of the United States of America*, 118(21), 2021. ISSN 10916490. .

R. M. DeConto and David Pollard. Contribution of Antarctica to past and future sea-level rise. *Nature*, 531(7596):591–597, 2016. ISSN 14764687. . URL http://dx.doi.org/10.1038/nature17145.

Robert M. DeConto, David Pollard, Richard B. Alley, Isabella Velicogna, Edward Gasson, Natalya Gomez, Shaina Sadai, Alan Condron, Daniel M. Gilford, Erica L. Ashe, Robert E. Kopp, Dawei Li, and Andrea Dutton. The paris climate agreement and future sea-level rise from antarctica. *Nature*, 593(7857):83–89, May 2021. ISSN 1476-4687. . URL https://doi.org/10.1038/s41586-021-03427-0.

A. Delhasse, X. Fettweis, C. Kittel, C. Amory, and C. Agosta. Brief communication: Impact of the recent atmospheric circulation change in summer on the future surface mass balance of the greenland ice sheet. *The Cryosphere*, 12(11):3409–3418, 2018. . URL https://tc.copernicus.org/articles/12/3409/2018/.

C. Duarte, J. M. Navarro, K. Acuña, R. Torres, P. H. Manríquez, M. A. Lardies, C. A. Vargas, N. A. Lagos, and V. Aguilera. Combined effects of temperature and ocean

acidification on the juvenile individuals of the mussel Mytilus chilensis. *Journal of Sea Research*, 85:308–314, 2014. ISSN 13851101. . URL http://dx.doi.org/10.1016/j.seares.2013.06.002.

M. Dumont, E. Brun, G. Picard, M. Michou, Q. Libois, J.-R. Petit, M. Geyer, S. Morin, and B. Josse. Contribution of light-absorbing impurities in snow to greenland's darkening since 2009. *Nature Geoscience*, 7(7):509–512, Jul 2014. ISSN 1752-0908. . URL https://doi.org/10.1038/ngeo2180.

Pierre Dutrieux, Jan De Rydt, Adrian Jenkins, Paul R. Holland, Ho Kyung Ha, Sang Hoon Lee, Eric J. Steig, Qinghua Ding, E. Povl Abrahamsen, and Michael Schröder. Strong sensitivity of pine Island ice-shelf melting to climatic variability. *Science*, 343(6167):174–178, 2014. ISSN 10959203. .

Tamsin L. Edwards, Mark A. Brandon, Gael Durand, Neil R. Edwards, Nicholas R. Golledge, Philip B. Holden, Isabel J. Nias, Antony J. Payne, Catherine Ritz, and Andreas Wernecke. Revisiting Antarctic ice loss due to marine ice-cliff instability. *Nature*, 566(7742):58–64, 2019. ISSN 14764687. . URL http://dx.doi.org/10.1038/s41586-019-0901-4.

Tamsin L. Edwards, Sophie Nowicki, Ben Marzeion, Regine Hock, Heiko Goelzer, Hélène Seroussi, Nicolas C. Jourdain, Donald A. Slater, Fiona E. Turner, Christopher J. Smith, Christine M. McKenna, Erika Simon, Ayako Abe-Ouchi, Jonathan M. Gregory, Eric Larour, William H. Lipscomb, Antony J. Payne, Andrew Shepherd, Cécile Agosta, Patrick Alexander, Torsten Albrecht, Brian Anderson, Xylar Asay-Davis, Andy Aschwanden, Alice Barthel, Andrew Bliss, Reinhard Calov, Christopher Chambers, Nicolas Champollion, Youngmin Choi, Richard Cullather, Joshua Cuzzone, Christophe Dumas, Denis Felikson, Xavier Fettweis, Koji Fujita, Benjamin K. Galton-Fenzi, Rupert Gladstone, Nicholas R. Golledge, Ralf Greve, Tore Hattermann, Matthew J. Hoffman, Angelika Humbert, Matthias Huss, Philippe Huybrechts, Walter Immerzeel, Thomas Kleiner, Philip Kraaijenbrink, Sébastien Le clec'h, Victoria Lee, Gunter R. Leguy, Christopher M. Little, Daniel P. Lowry, Jan Hendrik Malles, Daniel F. Martin, Fabien Maussion, Mathieu Morlighem, James F. O'Neill, Isabel Nias, Frank Pattyn, Tyler Pelle, Stephen F. Price, Aurélien Quiquet, Valentina Radić, Ronja Reese, David R. Rounce, Martin Rückamp, Akiko Sakai, Courtney Shafer, Nicole Jeanne Schlegel, Sarah Shannon, Robin S. Smith, Fiammetta Straneo, Sainan Sun, Lev Tarasov, Luke D. Trusel, Jonas Van Breedam, Roderik van de Wal, Michiel van den Broeke, Ricarda Winkelmann, Harry Zekollari, Chen Zhao, Tong Zhang, and Thomas Zwinger. Projected land ice contributions to twenty-first-century sea level rise. *Nature*, 593(7857):74–82, 2021. ISSN 14764687. .

Dana Ehlert and Kirsten Zickfeld. Irreversible ocean thermal expansion under carbon dioxide removal. *Earth System Dynamics*, 9:197–210, 2018.

Victoria J. Fabry, Brad A. Seibel, Richard A. Feely, and James C. Orr. Impacts of ocean acidification on marine fauna and ecosystem processes. *ICES Journal of Marine Science*, 65(3):414–432, 04 2008. ISSN 1054-3139. . URL https://doi.org/10.1093/icesjms/fsn048.

L. Favier, G. Durand, S. L. Cornford, G. H. Gudmundsson, O. Gagliardini, F. Gillet-Chaulet, T. Zwinger, A. J. Payne, and A. M. Le Brocq. Retreat of Pine Island Glacier controlled by marine ice-sheet instability. *Nature Climate Change*, 4(2): 117–121, 2014. ISSN 1758678X. .

X. Fettweis, B. Franco, M. Tedesco, J. H. Van Angelen, J. T.M. Lenaerts, M. R. Van Den Broeke, and H. Gallée. Estimating the Greenland ice sheet surface mass balance contribution to future sea level rise using the regional atmospheric climate model MAR. *Cryosphere*, 7(2):469–489, 2013. ISSN 19940424. .

Rebecca Fisher, Rebecca A. O'Leary, Samantha Low-Choy, Kerrie Mengersen, Nancy Knowlton, Russell E. Brainard, and M. Julian Caley. Species richness on coral reefs and the pursuit of convergent global estimates. *Current Biology*, 25(4):500–505, 2015. ISSN 18790445. . URL http://dx.doi.org/10.1016/j.cub.2014.12.022.

Michael J. Follows, Taka Ito, and Stephanie Dutkiewicz. On the solution of the carbonate chemistry system in ocean biogeochemistry models. *Ocean Modelling*, 12 (3-4):290–301, 2006. ISSN 14635003. .

P. Forster, T. Storelvmo, K. Armour, W. Collins, J.-L. Dufresne, D. Frame, D.J. Lunt, T. Mauritsen, M.D. Palmer, M. Watanabe, M. Wild, and H. Zhang. *The Earth's Energy Budget, Climate Feedbacks, and Climate Sensitivity*, page 923–1054. Cambridge University Press, Cambridge, United Kingdom and New York, NY, USA, 2021. .

Gavin L. Foster and Eelco J. Rohling. Relationship between sea level and climate forcing by CO2 on geological timescales. *Proceedings of the National Academy of Sciences of the United States of America*, 110(4):1209–1214, 2013. ISSN 10916490. .

B. Fox-Kemper, H.T. Hewitt, C. Xiao, G. Aðalgeirsdóttir, S.S. Drijfhout, T.L. Edwards, N.R. Golledge, M. Hemer, R.E. Kopp, G. Krinner, A. Mix, D. Notz, S. Nowicki, I.S. Nurhati, L. Ruiz, J.-B. Sallée, A.B.A. Slangen, and Y. Yu. *Ocean, Cryosphere and Sea Level Change*, page 1211–1362. Cambridge University Press, Cambridge, United Kingdom and New York, NY, USA, 2021. .

P Friedlingstein, R Betts, L Bopp, W Von Bloh, V Brovkin, S Doney, M Eby, I Fung, B Govindasamy, J John, C Jones, F Joos, T Kato, M Kawamiya, W Knorr, K Lindsay, H D Matthews, T Raddatz, P Rayner, C Reick, E Roeckner, K G Schnitzler, R Schnurr, K Strassmann, S Thompson, A J Weaver, C Yoshikawa, and N Zeng. Climate –carbon cycle feedback analysis, results from the C4MIP model intercomparison. *Journal of Climate*, 19:3337–3353, 2006. URL https://doi.org/10.1175/JCLI3800.1.

P. Friedlingstein, M. W. Jones, M. O'Sullivan, R. M. Andrew, J. Hauck, G. P. Peters, W. Peters, J. Pongratz, S. Sitch, C. Le Quéré, D. C. E. Bakker, J. G. Canadell, P. Ciais, R. B. Jackson, P. Anthoni, L. Barbero, A. Bastos, V. Bastrikov, M. Becker, L. Bopp, E. Buitenhuis, N. Chandra, F. Chevallier, L. P. Chini, K. I. Currie, R. A. Feely, M. Gehlen, D. Gilfillan, T. Gkritzalis, D. S. Goll, N. Gruber, S. Gutekunst, I. Harris, V. Haverd, R. A. Houghton, G. Hurtt, T. Ilyina, A. K. Jain, E. Joetzjer, J. O. Kaplan, E. Kato, K. Klein Goldewijk, J. I. Korsbakken, P. Landschützer, S. K. Lauvset, N. Lefèvre, A. Lenton, S. Lienert, D. Lombardozzi, G. Marland, P. C. McGuire, J. R. Melton, N. Metzl, D. R. Munro, J. E. M. S. Nabel, S.-I. Nakaoka, C. Neill, A. M. Omar, T. Ono, A. Peregon, D. Pierrot, B. Poulter, G. Rehder, L. Resplandy, E. Robertson, C. Rödenbeck, R. Séférian, J. Schwinger, N. Smith, P. P. Tans, H. Tian, B. Tilbrook, F. N. Tubiello, G. R. van der Werf, A. J. Wiltshire, and S. Zaehle. Global carbon budget 2019. *Earth System Science Data*, 11(4):1783–1838, 2019. . URL https://essd.copernicus.org/articles/11/1783/2019/.

P. Friedlingstein, M. O'Sullivan, M. W. Jones, R. M. Andrew, L. Gregor, J. Hauck, C. Le Quéré, I. T. Luijkx, A. Olsen, G. P. Peters, W. Peters, J. Pongratz, C. Schwingshackl, S. Sitch, J. G. Canadell, P. Ciais, R. B. Jackson, S. R. Alin, R. Alkama, A. Arneth, V. K. Arora, N. R. Bates, M. Becker, N. Bellouin, H. C. Bittig, L. Bopp, F. Chevallier, L. P. Chini, M. Cronin, W. Evans, S. Falk, R. A. Feely, T. Gasser, M. Gehlen, T. Gkritzalis, L. Gloege, G. Grassi, N. Gruber, Ö. Gürses, I. Harris, M. Hefner, R. A. Houghton, G. C. Hurtt, Y. Iida, T. Ilyina, A. K. Jain, A. Jersild, K. Kadono, E. Kato, D. Kennedy, K. Klein Goldewijk, J. Knauer, J. I. Korsbakken, P. Landschützer, N. Lefèvre, K. Lindsay, J. Liu, Z. Liu, G. Marland, N. Mayot, M. J. McGrath, N. Metzl, N. M. Monacci, D. R. Munro, S.-I. Nakaoka, Y. Niwa, K. O'Brien, T. Ono, P. I. Palmer, N. Pan, D. Pierrot, K. Pocock, B. Poulter, L. Resplandy, E. Robertson, C. Rödenbeck, C. Rodriguez, T. M. Rosan, J. Schwinger, R. Séférian, J. D. Shutler, I. Skjelvan, T. Steinhoff, Q. Sun, A. J. Sutton, C. Sweeney, S. Takao, T. Tanhua, P. P. Tans, X. Tian, H. Tian, B. Tilbrook, H. Tsujino, F. Tubiello, G. R. van der Werf, A. P. Walker, R. Wanninkhof, C. Whitehead, A. Willstrand Wranne, R. Wright, W. Yuan, C. Yue, X. Yue, S. Zaehle, J. Zeng, and B. Zheng. Global carbon budget 2022. *Earth System Science Data*, 14(11):4811–4900, 2022. . URL https://essd.copernicus.org/articles/14/4811/2022/.

J. J. Fürst, H. Goelzer, and P. Huybrechts. Ice-dynamic projections of the greenland ice sheet in response to atmospheric and oceanic warming. *The Cryosphere*, 9(3): 1039–1062, 2015. . URL https://tc.copernicus.org/articles/9/1039/2015/.

Charles Galdies, Richard Bellerby, Donata Canu, Wenting Chen, Enrique Garcia-Luque, Blaženka Gašparović, Jelena Godrijan, Paul J. Lawlor, Frank Maes, Alenka Malej, Dionisios Panagiotaras, Beatriz Martinez Romera, Claire E. Reymond, Julien Rochette, Cosimo Solidoro, Robert Stojanov, Rachel Tiller, Isabel Torres de Noronha, Grzegorz Uścinowicz, Natașa Vaidianu, Cormac Walsh, and Roberta

Guerra. European policies and legislation targeting ocean acidification in european waters - Current state. *Marine Policy*, 118(May):103947, 2020. ISSN 0308597X. .

Natalya D. Gallo, David G. Victor, and Lisa A. Levin. Ocean commitments under the Paris Agreement. *Nature Climate Change*, 7(11):833–838, 2017. ISSN 17586798. .

Yun Gao, Xiang Gao, and Xiaohua Zhang. The 2° c global temperature target and the evolution of the long-term goal of addressing climate change—from the united nations framework convention on climate change to the paris agreement. *Engineering*, 3(2):272–278, 2017. ISSN 2095-8099. . URL https://www.sciencedirect.com/science/article/pii/S2095809917303077.

Julius Garbe, Torsten Albrecht, Anders Levermann, Jonathan F. Donges, and Ricarda Winkelmann. The hysteresis of the Antarctic Ice Sheet. *Nature*, 585(7826):538–544, 2020. ISSN 14764687. . URL http://dx.doi.org/10.1038/s41586-020-2727-5.

Andra J. Garner, Jeremy L. Weiss, Adam Parris, Robert E. Kopp, Radley M. Horton, Jonathan T. Overpeck, and Benjamin P. Horton. Evolution of 21st Century Sea Level Rise Projections. *Earth's Future*, 6(11):1603–1615, 2018. ISSN 23284277. .

Benjamin S. Giese and Sulagna Ray. El niño variability in simple ocean data assimilation (soda), 1871–2008. *Journal of Geophysical Research: Oceans*, 116(C2), 2011. . URL https://agupubs.onlinelibrary.wiley.com/doi/abs/10.1029/2010JC006695.

B.C. Glavovic, R. Dawson, W. Chow, M. Garschagen, M. Haasnoot, C. Singh, and A. Thomas. *Cross-Chapter Paper 2: Cities and Settlements by the Sea*, pages 2163–2194. Cambridge University Press, Cambridge, UK and New York, USA, 2022. ISBN 9781009325844. .

N. R. Golledge, D. E. Kowalewski, T. R. Naish, R. H. Levy, C. J. Fogwill, and E. G. W. Gasson. The multi-millennial antarctic commitment to future sea-level rise. *Nature*, 526(7573):421–425, Oct 2015. ISSN 1476-4687. . URL https://doi.org/10.1038/nature15706.

Peter Good, Alistair Sellar, Yongming Tang, Steve Rumbold, Rich Ellis, Douglas Kelley, and Till Kuhlbrodt. Mohc ukesm1.0-ll model output prepared for cmip6 scenariomip ssp245, 2019. URL https://doi.org/10.22033/ESGF/CMIP6.6339.

Simon A. Good, Matthew J. Martin, and Nick A. Rayner. En4: Quality controlled ocean temperature and salinity profiles and monthly objective analyses with uncertainty estimates. *Journal of Geophysical Research: Oceans*, 118(12):6704–6716, 2013. . URL https://agupubs.onlinelibrary.wiley.com/doi/abs/10.1002/2013JC009067.

Philip Goodwin. How historic simulation–observation discrepancy affects future warming projections in a very large model ensemble. *Climate Dynamics*, 47(7-8): 2219–2233, 2016. ISSN 14320894. .

Philip Goodwin. On the time evolution of climate sensitivity and future warming. *Earth's Future*, 6(9):1336–1348, 2018. . URL https://agupubs.onlinelibrary.wiley.com/doi/abs/10.1029/2018EF000889.

Philip Goodwin. Probabilistic projections of future warming and climate sensitivity trajectories. *Oxford Open Climate Change*, 1(1):kgab007, 07 2021. ISSN 2634-4068. . URL https://doi.org/10.1093/oxfclm/kgab007.

Philip Goodwin, Richard G. Williams, and Andy Ridgwell. Sensitivity of climate to cumulative carbon emissions due to compensation of ocean heat and carbon uptake. *Nature Geoscience*, 8(1):29–34, 2015. ISSN 17520908. .

Philip Goodwin, Ivan D. Haigh, Eelco J. Rohling, and Aimée Slangen. A new approach to projecting 21st century sea-level changes and extremes. *Earth's Future*, 5 (2):240–253, 2017. ISSN 23284277. .

Philip Goodwin, S Brown, I D Haigh, R J Nicholls, and J M Matter. Adjusting Mitigation Pathways to stabilize climate at 1.5 and 2.0 ° C rise in global temperatures to year 2300. *Earth's Future*, 6:0–3, 2018a. .

Philip Goodwin, Anna Katavouta, Vassil M. Roussenov, Gavin L. Foster, Eelco J. Rohling, and Richard G. Williams. Pathways to 1.5°c and 2°c warming based on observational and geological constraints. *Nature Geoscience*, 11(2):102–107, 2018b. ISSN 17520908. . URL http://dx.doi.org/10.1038/s41561-017-0054-8.

Aslak Grinsted and Jens Hesselbjerg Christensen. The transient sensitivity of sea level rise. *Ocean Science*, 17(1):181–186, 2021. ISSN 18120792. .

Aslak Grinsted, J. C. Moore, and S. Jevrejeva. Reconstructing sea level from paleo and projected temperatures 200 to 2100 AD. *Climate Dynamics*, 34(4):461–472, 2010. ISSN 09307575. .

Aslak Grinsted, Jonathan Bamber, Rory Bingham, Sammie Buzzard, Isabel Nias, Kelvin Ng, and Jennifer Weeks. The Transient Sea Level Response to External Forcing in CMIP6 Models. *Earth's Future*, 10(10), 2022. ISSN 23284277. .

Yi Guan, Sönke Hohn, and Agostino Merico. Suitable environmental ranges for potential Coral reef habitats in the tropical ocean. *PLoS ONE*, 10(6):1–17, 2015. ISSN 19326203. .

S.K. Gulev, P.W. Thorne, J. Ahn, F.J. Dentener, C.M. Domingues, S. Gerland, D. Gong, D.S. Kaufman, H.C. Nnamchi, J. Quaas, J.A. Rivera, S. Sathyendranath, S.L. Smith, B. Trewin, K. von Schuckmann, and R.S. Vose. *Changing State of the Climate System*, page 287–422. Cambridge University Press, Cambridge, United Kingdom and New York, NY, USA, 2021. .

E. Hanna, X. Fettweis, and R. J. Hall. Brief communication: Recent changes in summer greenland blocking captured by none of the cmip5 models. *The Cryosphere*, 12(10): 3287–3292, 2018. . URL https://tc.copernicus.org/articles/12/3287/2018/.

J. Hansen, R. Ruedy, M. Sato, and K. Lo. Global surface temperature change. *Reviews of Geophysics*, 48(4), 2010. . URL https://agupubs.onlinelibrary.wiley.com/doi/abs/10.1029/2010RG000345.

Ellycia R. Harrould-Kolieb. Ocean Acidification and the UNFCCC : Finding Legal Clarity in the Twilight Xone. *Washington Journal of Environmental Law and Policy*, 6 (2):612–632, 2016.

Ellycia R. Harrould-Kolieb. (Re)Framing ocean acidification in the context of the United Nations Framework Convention on climate change (UNFCCC) and Paris Agreement. *Climate Policy*, 19(10):1225–1238, 2019. ISSN 17527457. .

Ellycia R. Harrould-Kolieb and Dorothée Herr. Ocean acidification and climate change: Synergies and challenges of addressing both under the UNFCCC. *Climate Policy*, 12(3):378–389, 2012. ISSN 17527457. .

Claudine Hauri, Tobias Friedrich, and Axel Timmermann. Abrupt onset and prolongation of aragonite undersaturation events in the Southern Ocean. *Nature Climate Change*, 6(2):172–176, 2016. ISSN 17586798. .

Tim H. J. Hermans, Jonathan M. Gregory, Matthew D. Palmer, Mark A. Ringer, Caroline A. Katsman, and Aimée B. A. Slangen. Projecting global mean sea-level change using cmip6 models. *Geophysical Research Letters*, 48(5):e2020GL092064, 2021. . URL https://agupubs.onlinelibrary.wiley.com/doi/abs/10.1029/2020GL092064. e2020GL092064 2020GL092064.

Tim H.J. Hermans, Víctor Malagón-Santos, Caroline A. Katsman, Robert A. Jane, D. J. Rasmussen, Marjolijn Haasnoot, Gregory G. Garner, Robert E. Kopp, Michael Oppenheimer, and Aimée B.A. Slangen. The timing of decreasing coastal flood protection due to sea-level rise. *Nature Climate Change*, 13(4):359–366, 2023. ISSN 17586798. .

Jochen Hinkel, John A Church, and Jonathan M Gregory. Meeting User Needs for Sea Level Rise Information : A Decision Analysis Perspective Earth's Future. *Earth's Future*, 7(3):320–337, 2019. .

Ove Hoegh-Guldberg, Daniela Jacob, Michael Taylor, Marco Bindi, Sally Brown, Ines Camilloni, Arona Diedhiou, Riyanti Djalante, Kristie L. Ebi, Francois Engelbrecht, Joel Guiot, Yasuaki Hijioka, Shagun Mehrotra, Antony Payne, Sonia I. Seneviratne, Adelle Thomas, Rachel Warren, and Guangsheng Zhou. *Impacts of 1.5°C Global Warming on Natural and Human Systems*, pages 175–312. Cambridge University

Press, Cambridge, United Kingdom and New York, NY, USA, 2018. ISBN 9781009157940. .

Stefan Hofer, Andrew J. Tedstone, Xavier Fettweis, and Jonathan L. Bamber. Cloud microphysics and circulation anomalies control differences in future Greenland melt. *Nature Climate Change*, 9(7):523–528, 2019. ISSN 17586798. . URL http://dx.doi.org/10.1038/s41558-019-0507-8.

Stefan Hofer, Charlotte Lang, Charles Amory, Christoph Kittel, Alison Delhasse, Andrew Tedstone, and Xavier Fettweis. Greater Greenland Ice Sheet contribution to global sea level rise in CMIP6. *Nature Communications*, 11(1):1–11, 2020. ISSN 20411723. . URL http://dx.doi.org/10.1038/s41467-020-20011-8.

Kimmaree M. Horvath, Karl D. Castillo, Pualani Armstrong, Isaac T. Westfield, Travis Courtney, and Justin B. Ries. Next-century ocean acidification and warming both reduce calcification rate, but only acidification alters skeletal morphology of reef-building coral Siderastrea siderea. *Scientific Reports*, 6(February):1–12, 2016. ISSN 20452322. .

Boyin Huang, Viva F. Banzon, Eric Freeman, Jay Lawrimore, Wei Liu, Thomas C. Peterson, Thomas M. Smith, Peter W. Thorne, Scott D. Woodruff, and Huai-Min Zhang. Extended reconstructed sea surface temperature version 4 (ersst.v4). part i: Upgrades and intercomparisons. *Journal of Climate*, 28(3):911 – 930, 2015. . URL https://journals.ametsoc.org/view/journals/clim/28/3/jcli-d-14-00006.1.xml.

T. P. Hughes, A. H. Baird, D. R. Bellwood, M. Card, S. R. Connolly, C. Folke, R. Grosberg, O. Hoegh-Guldberg, J. B.C. Jackson, J. Kleypas, J. M. Lough, P. Marshall, M. Nyström, S. R. Palumbi, J. M. Pandolfi, B. Rosen, and J. Roughgarden. Climate change, human impacts, and the resilience of coral reefs. *Science*, 301(5635):929–933, 2003. ISSN 00368075. .

Eric V Hull. Ocean acidification: Legal and policy responses to address climate change's evil twin. *New York University Law Journal*, (3):507–544, 2014.

Catriona L. Hurd, Andrew Lenton, Bronte Tilbrook, and Philip W. Boyd. Current understanding and challenges for oceans in a higher-CO2 world. *Nature Climate Change*, 8(8):686–694, 2018. ISSN 17586798. . URL http://dx.doi.org/10.1038/s41558-018-0211-0.

Luke P. Jackson and Svetlana Jevrejeva. A probabilistic approach to 21st century regional sea-level projections using rcp and high-end scenarios. *Global and Planetary Change*, 146:179–189, 2016. ISSN 0921-8181. . URL https://www.sciencedirect.com/science/article/pii/S0921818116300686.

Luke P. Jackson, Aslak Grinsted, and Svetlana Jevrejeva. 21st Century Sea-Level Rise in Line with the Paris Accord. *Earth's Future*, 6(2):213–229, 2018. ISSN 23284277. .

Stanley S. Jacobs, Adrian Jenkins, Claudia F. Giulivi, and Pierre Dutrieux. Stronger ocean circulation and increased melting under Pine Island Glacier ice shelf. *Nature Geoscience*, 4(8):519–523, 2011. ISSN 17520894. .

Aurich Jeltsch-Thömmes, Thomas F. Stocker, and Fortunat Joos. Hysteresis of the Earth system under positive and negative CO2 emissions. *Environmental Research Letters*, 15(12), 2020. ISSN 17489326. .

S. Jevrejeva, J. C. Moore, and A. Grinsted. How will sea level respond to changes in natural and anthropogenic forcings by 2100? *Geophysical Research Letters*, 37(7):1–5, 2010. ISSN 00948276. .

Jiu Jiang, Long Cao, Xiaoyu Jin, Zechen Yu, Han Zhang, Jianjie Fu, and Guibin Jiang. Response of ocean acidification to atmospheric carbon dioxide removal. *Journal of Environmental Sciences*, 2023. ISSN 1001-0742. . URL https://www.sciencedirect.com/science/article/pii/S1001074223001882.

Fortunat Joos and Thomas L Frölicher. Impact of Climate Change Mitigation on Ocean Acidification Projections. In *Ocean Acidification*. Oxford University Press, 09 2011. ISBN 9780199591091. . URL https://doi.org/10.1093/oso/9780199591091.003.0019.

David P. Keller, Andrew Lenton, Emma W. Littleton, Andreas Oschlies, Vivian Scott, and Naomi E. Vaughan. The Effects of Carbon Dioxide Removal on the Carbon Cycle. *Current Climate Change Reports*, 4(3):250–265, 2018. ISSN 21986061. .

J. J. Kennedy, N. A. Rayner, R. O. Smith, D. E. Parker, and M. Saunby. Reassessing biases and other uncertainties in sea surface temperature observations measured in situ since 1850: 2. biases and homogenization. *Journal of Geophysical Research: Atmospheres*, 116(D14), 2011. . URL https://agupubs.onlinelibrary.wiley.com/doi/abs/10.1029/2010JD015220.

J. J. Kennedy, N. A. Rayner, C. P. Atkinson, and R. E. Killick. An ensemble data set of sea surface temperature change from 1850: The met office hadley centre hadsst.4.0.0.0 data set. *Journal of Geophysical Research: Atmospheres*, 124(14): 7719–7763, 2019. . URL https://agupubs.onlinelibrary.wiley.com/doi/abs/10.1029/2018JD029867.

Rakhyun E. Kim. Is a new multilateral environmental agreement on ocean acidification necessary? *Review of European Community and International Environmental Law*, 21(3):243–258, 2012. ISSN 09628797. .

Ebru Kirezci, Ian R. Young, Roshanka Ranasinghe, Daniel Lincke, and Jochen Hinkel. Global-scale analysis of socioeconomic impacts of coastal flooding over the 21st century. *Frontiers in Marine Science*, 9(January):1–21, 2023. .

Joan A. Kleypas, Robert W. Buddemeier, David Archer, Jean Pierre Gattuso, Chris Langdon, and Bradley N. Opdyke. Geochemical consequences of increased atmospheric carbon dioxide on coral reefs. *Science*, 284(5411):118–120, 1999. ISSN 00368075. .

Reto Knutti, Joeri Rogelj, Jan Sedlácek, and Erich M. Fischer. A scientific critique of the two-degree climate change target. *Nature Geoscience*, 9(1):13–18, 2016. ISSN 17520908. .

Robert E. Kopp, Frederik J. Simons, Jerry X. Mitrovica, Adam C. Maloof, and Michael Oppenheimer. Probabilistic assessment of sea level during the last interglacial stage. *Nature*, 462(7275):863–867, 2009. ISSN 00280836. .

Robert E. Kopp, Radley M. Horton, Christopher M. Little, Jerry X. Mitrovica, Michael Oppenheimer, D. J. Rasmussen, Benjamin H. Strauss, and Claudia Tebaldi. Probabilistic 21st and 22nd century sea-level projections at a global network of tide-gauge sites. *Earth's Future*, 2(8):383–406, 2014. ISSN 2328-4277. .

Robert E. Kopp, Andrew C. Kemp, Klaus Bittermann, Benjamin P. Horton, Jeffrey P. Donnelly, W. Roland Gehrels, Carling C. Hay, Jerry X. Mitrovica, Eric D. Morrow, and Stefan Rahmstorf. Temperature-driven global sea-level variability in the common era. *Proceedings of the National Academy of Sciences*, 113(11):E1434–E1441, 2016. . URL https://www.pnas.org/doi/abs/10.1073/pnas.1517056113.

Robert E. Kopp, R. M. DeConto, Daniel A. Bader, Carling C. Hay, Radley M. Horton, Scott Kulp, Michael Oppenheimer, David Pollard, and Benjamin H. Strauss. Evolving Understanding of Antarctic Ice-Sheet Physics and Ambiguity in Probabilistic Sea-Level Projections. *Earth's Future*, 5(12):1217–1233, 2017. ISSN 23284277. .

Scott A. Kulp and Benjamin H. Strauss. New elevation data triple estimates of global vulnerability to sea-level rise and coastal flooding. *Nature Communications*, 10(1), 2019. ISSN 20411723. . URL http://dx.doi.org/10.1038/s41467-019-12808-z.

L. Kwiatkowski, O. Torres, L. Bopp, O. Aumont, M. Chamberlain, J. R. Christian, J. P. Dunne, M. Gehlen, T. Ilyina, J. G. John, A. Lenton, H. Li, N. S. Lovenduski, J. C. Orr, J. Palmieri, Y. Santana-Falcón, J. Schwinger, R. Séférian, C. A. Stock, A. Tagliabue, Y. Takano, J. Tjiputra, K. Toyama, H. Tsujino, M. Watanabe, A. Yamamoto, A. Yool, and T. Ziehn. Twenty-first century ocean warming, acidification, deoxygenation, and upper-ocean nutrient and primary production decline from cmip6 model projections. *Biogeosciences*, 17(13):3439–3470, 2020. . URL https://bg.copernicus.org/articles/17/3439/2020/.

Heidi R. Lamirande. From sea to carbon cesspool: preventing the world's marine ecosystems from falling victim to ocean acidification. *Suffolk Transnational Law Review*, 34, Jan 2011. ISSN 1072-8546. URL http://vlex.com/vid/from-to-carbon-cesspool-634978189.

J.-Y. Lee, J. Marotzke, G. Bala, L. Cao, S. Corti, J.P. Dunne, F. Engelbrecht, E. Fischer, J.C. Fyfe, C. Jones, A. Maycock, J. Mutemi, O. Ndiaye, S. Panickal, and T. Zhou. *Future Global Climate: Scenario-Based Projections and Near-Term Information*, page 553–672. Cambridge University Press, Cambridge, United Kingdom and New York, NY, USA, 2021. .

A. Levermann, R. Winkelmann, S. Nowicki, J. L. Fastook, K. Frieler, R. Greve, H. H. Hellmer, M. A. Martin, M. Meinshausen, M. Mengel, A. J. Payne, D. Pollard, T. Sato, R. Timmermann, W. L. Wang, and R. A. Bindschadler. Projecting Antarctic ice discharge using response functions from SeaRISE ice-sheet models. *Earth System Dynamics*, 5(2):271–293, 2014. ISSN 21904987. .

Anders Levermann, Peter U. Clark, Ben Marzeion, Glenn A. Milne, David Pollard, Valentina Radic, and Alexander Robinson. The multimillennial sea-level commitment of global warming. *Proceedings of the National Academy of Sciences of the United States of America*, 110(34):13745–13750, 2013. ISSN 10916490. .

Anders Levermann, Ricarda Winkelmann, Torsten Albrecht, Heiko Goelzer, Nicholas R. Golledge, Ralf Greve, Philippe Huybrechts, Jim Jordan, Gunter Leguy, Daniel Martin, Mathieu Morlighem, Frank Pattyn, David Pollard, Aurelien Quiquet, Christian Rodehacke, Helene Seroussi, Johannes Sutter, Tong Zhang, Jonas Van Breedam, Reinhard Calov, R. M. Deconto, Christophe Dumas, Julius Garbe, G. Hilmar Gudmundsson, Matthew J. Hoffman, Angelika Humbert, Thomas Kleiner, William H. Lipscomb, Malte Meinshausen, Esmond Ng, Sophie M.J. Nowicki, Mauro Perego, Stephen F. Price, Fuyuki Saito, Nicole Jeanne Schlegel, Sainan Sun, and Roderik S.W. Van De Wal. Projecting Antarctica's contribution to future sea level rise from basal ice shelf melt using linear response functions of 16 ice sheet models (LARMIP-2). *Earth System Dynamics*, 11(1):35–76, 2020. ISSN 21904987. .

S. Levitus, J. I. Antonov, T. P. Boyer, O. K. Baranova, H. E. Garcia, R. A. Locarnini, A. V. Mishonov, J. R. Reagan, D. Seidov, E. S. Yarosh, and M. M. Zweng. World ocean heat content and thermosteric sea level change (0–2000m), 1955–2010. *Geophysical Research Letters*, 39(10), 2012. . URL https://agupubs.onlinelibrary.wiley.com/doi/abs/10.1029/2012GL051106.

Gabriel Lewis, Erich Osterberg, Robert Hawley, Hans Peter Marshall, Tate Meehan, Karina Graeter, Forrest McCarthy, Thomas Overly, Zayta Thundercloud, David Ferris, Bess G. Koffman, and Jack Dibb. Atmospheric Blocking Drives Recent

Albedo Change Across the Western Greenland Ice Sheet Percolation Zone. *Geophysical Research Letters*, 48(10):1–11, 2021. ISSN 19448007. .

Nicholas Lewis. An objective Bayesian Improved Approach for Applying Optimal Fingerprint Techniques to Estimate Climate Sensitivity. *Journal of Climate*, 26(19): 7414–7429, 2013. ISSN 08948755. .

Chao Li, Hermann Held, Sascha Hokamp, and Jochem Marotzke. Optimal temperature overshoot profile found by limiting global sea level rise as a lower-cost climate target. *Science Advances*, 6(2):1–9, 2020. ISSN 23752548. .

Dawei Li, Robert M. DeConto, and David Pollard. Climate model differences contribute deep uncertainty in future Antarctic ice loss. *Science advances*, 9(7):1–14, 2023. ISSN 23752548. .

N. S. Lovenduski, M. C. Long, and K. Lindsay. Natural variability in the surface ocean carbonate ion concentration. *Biogeosciences*, 12(21):6321–6335, 2015. ISSN 17264189. .

Jason Lowe and Jonathan Gregory. A sea of uncertainty. *Nat Rep Clim Change*, 4, 04 2010. .

Daniel P. Lowry, Mario Krapp, Nicholas R. Golledge, and Alanna Alevropoulos-Borrill. The influence of emissions scenarios on future antarctic ice loss is unlikely to emerge this century. *Communications Earth & Environment*, 2(1): 221, Oct 2021. ISSN 2662-4435. . URL https://doi.org/10.1038/s43247-021-00289-2.

Xiao Luo and Ting Lin. A semi-empirical framework for ice sheet response analysis under oceanic forcing in antarctica and greenland. *Climate Dynamics*, 60(1):213–226, Jan 2023. ISSN 1432-0894. . URL https://doi.org/10.1007/s00382-022-06317-x.

Andrew H. MacDougall and Pierre Friedlingstein. The origin and limits of the near proportionality between climate warming and cumulative co2 emissions. *Journal of Climate*, 28(10):4217 – 4230, 2015. . URL https://journals.ametsoc.org/view/journals/clim/28/10/jcli-d-14-00036.1.xml.

Syukuro Manabe and Richard T. Wetherald. Thermal Equilibrium of the Atmosphere with a Given Distribution of Relative Humidity. *Journal of the Atmospheric Sciences*, 24(3):241–259, May 1967. .

Torge Martin, Arne Biastoch, Gerrit Lohmann, Uwe Mikolajewicz, and Xuezhu Wang. On timescales and reversibility of the ocean's response to enhanced greenland ice sheet melting in comprehensive climate models. *Geophysical Research Letters*, 49(5): e2021GL097114, 2022. . URL https://agupubs.onlinelibrary.wiley.com/doi/abs/10.1029/2021GL097114.

Rowan C. Martindale, William M. Berelson, Frank A. Corsetti, David J. Bottjer, and A. Joshua West. Constraining carbonate chemistry at a potential ocean acidification event (the Triassic-Jurassic boundary) using the presence of corals and coral reefs in the fossil record. *Palaeogeography, Palaeoclimatology, Palaeoecology*, 350-352:114–123, 2012. ISSN 00310182. . URL http://dx.doi.org/10.1016/j.palaeo.2012.06.020.

Sabine Mathesius, Matthias Hofmann, Ken Caldeira, and Hans Joachim Schellnhuber. Long-term response of oceans to CO2 removal from the atmosphere. *Nature Climate Change*, 5(12):1107–1113, 2015. ISSN 17586798. .

H. Damon Matthews, Nathan P. Gillett, Peter A. Stott, and Kirsten Zickfeld. The proportionality of global warming to cumulative carbon emissions. *Nature*, 459 (7248):829–832, 2009. ISSN 00280836. . URL http://dx.doi.org/10.1038/nature08047.

Ben I. McNeil and Richard J. Matear. Southern Ocean acidification: A tipping point at 450-ppm atmospheric CO2. *Proceedings of the National Academy of Sciences of the United States of America*, 105(48):18860–18864, 2008. ISSN 00278424. .

Gerald A. Meehl, Aixue Hu, Claudia Tebaldi, Julie M. Arblaster, Warren M. Washington, Haiyan Teng, Benjamin M. Sanderson, Toby Ault, Warren G. Strand, and James B. White. Relative outcomes of climate change mitigation related to global temperature versus sea-level rise. *Nature Climate Change*, 2(8):576–580, 2012. ISSN 1758678X. .

Matthias Mengel, Anders Levermann, Katja Frieler, Alexander Robinson, Ben Marzeion, and Ricarda Winkelmann. Future sea level rise constrained by observations and long-term commitment. *Proceedings of the National Academy of Sciences of the United States of America*, 113(10):2597–2602, 2016. ISSN 10916490. .

Matthias Mengel, Alexander Nauels, Joeri Rogelj, and Carl Friedrich Schleussner. Committed sea-level rise under the Paris Agreement and the legacy of delayed mitigation action. *Nature Communications*, 9(1):1–10, 2018. ISSN 20411723. . URL http://dx.doi.org/10.1038/s41467-018-02985-8.

Dirk Messner, John Schellnhuber, Stefan Rahmstorf, and Daniel Klingenfeld. The budget approach: A framework for a global transformation toward a low-carbon economy. *Journal of Renewable and Sustainable Energy*, 2(3):1–14, 2010. ISSN 19417012. .

Fredrik Moberg and Carl Folke. Ecological goods and services of coral reef ecosystems. *Ecological Economics*, 29(2):215–233, 1999. ISSN 0921-8009. . URL https://www.sciencedirect.com/science/article/pii/S0921800999000099.

C. P. Morice, J. J. Kennedy, N. A. Rayner, J. P. Winn, E. Hogan, R. E. Killick, R. J. H. Dunn, T. J. Osborn, P. D. Jones, and I. R. Simpson. An updated assessment of

near-surface temperature change from 1850: The hadcrut5 data set. *Journal of Geophysical Research: Atmospheres*, 126(3):e2019JD032361, 2021. . URL https://agupubs.onlinelibrary.wiley.com/doi/abs/10.1029/2019JD032361.

Colin P. Morice, John J. Kennedy, Nick A. Rayner, and Phil D. Jones. Quantifying uncertainties in global and regional temperature change using an ensemble of observational estimates: The hadcrut4 data set. *Journal of Geophysical Research: Atmospheres*, 117(D8), 2012. .

Jérémie Mouginot, Eric Rignot, Anders A. Bjørk, Michiel van den Broeke, Romain Millan, Mathieu Morlighem, Brice Noël, Bernd Scheuchl, and Michael Wood. Forty-six years of Greenland Ice Sheet mass balance from 1972 to 2018. *Proceedings of the National Academy of Sciences of the United States of America*, 116(19):9239–9244, 2019. ISSN 10916490. .

A. Nauels, M. Meinshausen, M. Mengel, K. Lorbacher, and T. M. L. Wigley. Synthesizing long-term sea level rise projections – the magicc sea level model v2.0. *Geoscientific Model Development*, 10(6):2495–2524, 2017. . URL https://gmd.copernicus.org/articles/10/2495/2017/.

Alexander Nauels, Johannes Gütschow, Matthias Mengel, Malte Meinshausen, Peter U. Clark, and Carl Friedrich Schleussner. Attributing long-term sea-level rise to Paris Agreement emission pledges. *Proceedings of the National Academy of Sciences of the United States of America*, 116(47):23487–23492, 2019. ISSN 10916490. .

Barbara Neumann, Athanasios T. Vafeidis, Juliane Zimmermann, and Robert J. Nicholls. Future coastal population growth and exposure to sea-level rise and coastal flooding - a global assessment. *PLOS ONE*, 10(3):1–34, 03 2015. . URL https://doi.org/10.1371/journal.pone.0118571.

Isabel J. Nias, Sophie Nowicki, Denis Felikson, and Bryant Loomis. Modeling the greenland ice sheet's committed contribution to sea level during the 21st century. *Journal of Geophysical Research: Earth Surface*, 128(2):e2022JF006914, 2023. . e2022JF006914 2022JF006914.

Robert J. Nicholls, Sally Brown, Philip Goodwin, Thomas Wahl, Jason Lowe, Martin Solan, Jasmin A. Godbold, Ivan D. Haigh, Daniel Lincke, Jochen Hinkel, Claudia Wolf, and Jan Ludolf Merkens. Stabilization of global temperature at 1.5°C and 2.0°C: Implications for coastal areas. *Philosophical Transactions of the Royal Society A: Mathematical, Physical and Engineering Sciences*, 376(2119), 2018. ISSN 1364503X. .

Z. Nicholls, M. Meinshausen, J. Lewis, M. Rojas Corradi, K. Dorheim, T. Gasser, R. Gieseke, A. P. Hope, N. J. Leach, L. A. McBride, Y. Quilcaille, J. Rogelj, R. J. Salawitch, B. H. Samset, M. Sandstad, A. Shiklomanov, R. B. Skeie, C. J. Smith, S. J. Smith, X. Su, J. Tsutsui, B. Vega-Westhoff, and D. L. Woodard. Reduced Complexity

Model Intercomparison Project Phase 2: Synthesizing Earth System Knowledge for Probabilistic Climate Projections. *Earth's Future*, 9(6):1–25, 2021. ISSN 23284277. .

William D. Nordhaus. Economic growth and climate: The carbon dioxide problem. *The American Economic Review*, 67(1):341–346, 1977. ISSN 00028282. URL http://www.jstor.org/stable/1815926.

William D. Nordhaus. To slow or not to slow: The economics of the greenhouse effect. *The Economic Journal*, 101(407):920–937, 1991. ISSN 00130133, 14680297. URL http://www.jstor.org/stable/2233864.

E. Z. Ong, M. Briffa, T. Moens, and C. Van Colen. Physiological responses to ocean acidification and warming synergistically reduce condition of the common cockle Cerastoderma edule. *Marine Environmental Research*, 130:38–47, 2017. ISSN 18790291. . URL http://dx.doi.org/10.1016/j.marenvres.2017.07.001.

Michael Oppenheimer, Bruce Glavovic, Jochen Hinkel, Roderik van de Wal, Alexandre K. Magnan, Amro Abd-Elgawad, Rongshuo Cai, Miguel Cifuentes-Jara, Robert M. Deconto, Tuhin Ghosh, John Hay, Federico Isla, Ben Marzeion, Benoit Meyssignac, and Zita Sebesvari. Chapter 4: Sea Level Rise and Implications for Low Lying Islands, Coasts and Communities. IPCC SR Ocean and Cryosphere. *IPCC Special Report on the Ocean and Cryosphere in a Changing Climate [H.- O. Pörtner, D.C. Roberts, V. Masson-Delmotte, P. Zhai, M. Tignor, E. Poloczanska, K. Mintenbeck, M. Nicolai, A. Okem, J. Petzold, B. Rama, N. Weyer (eds.)]. In press.*, Chapter 4(Final Draft): 1–14, 2019. ISSN 1138-1728.

Nilufer Oral. Ocean acidification: Falling between the legal cracks of UNCLOS and the UNFCCC? *Ecology Law Quarterly*, 45(1):9–30, 2018. ISSN 00461121. .

Mirko Orlić and Zoran Pasarić. Semi-empirical versus process-based sea-level projections for the twenty-first century. *Nature Climate Change*, 3(8):735–738, 2013. ISSN 1758678X. .

Timothée Ourbak and Alexandre K. Magnan. The Paris Agreement and climate change negotiations: Small Islands, big players. *Regional Environmental Change*, 18 (8):2201–2207, 2018. ISSN 1436378X. .

John M. Pandolfi, Sean R. Connolly, Dustin J. Marshall, and Anne L. Cohen. Projecting coral reef futures under global warming and ocean acidification. *Science*, 333(6041): 418–422, 2011. ISSN 00368075. .

B. R. Parizek, K. Christianson, S. Anandakrishnan, R. B. Alley, R. T. Walker, R. A. Edwards, D. S. Wolfe, G. T. Bertini, S. K. Rinehart, R. A. Bindschadler, and S. M.J. Nowicki. Dynamic (in)stability of Thwaites Glacier, West Antarctica. *Journal of Geophysical Research: Earth Surface*, 118(2):638–655, 2013. ISSN 21699011. .

Frank Pattyn, Catherine Ritz, Edward Hanna, Xylar Asay-Davis, R. M. Deconto, Gaël Durand, Lionel Favier, Xavier Fettweis, Heiko Goelzer, Nicholas R. Golledge, Peter Kuipers Munneke, Jan T.M. Lenaerts, Sophie Nowicki, Antony J. Payne, Alexander Robinson, Hélène Seroussi, Luke D. Trusel, and Michiel van den Broeke. The Greenland and Antarctic ice sheets under 1.5 °C global warming. *Nature Climate Change*, 8(12):1053–1061, 2018. ISSN 17586798. . URL http://dx.doi.org/10.1038/s41558-018-0305-8.

A. J. Payne, S. Nowicki, A. Abe-Ouchi, C. Agosta, P. M. Alexander, T. Albrecht, X. S. Asay-Davis, A. Aschwanden, A. Barthel, T. J. Bracegirdle, R. Calov, C. Chambers, Y. Choi, R. I. Cullather, J. K. Cuzzone, C. Dumas, T. Edwards, D. Felikson, X. Fettweis, B. K. Galton-Fenzi, H. Goelzer, R. Gladstone, N. R. Golledge, J. M. Gregory, R. Greve, T. Hattermann, M. J. Hoffman, A. Humbert, P. Huybrechts, N. C. Jourdain, T. Kleiner, P. K. Munneke, E. Y. Larour, S. Le Clec'h, V. Lee, G. Leguy, W. H. Lipscomb, C. M. Little, D. P. Lowry, M. Morlighem, I. Nias, F. Pattyn, T. Pelle, S. Price, A. Quiquet, R. Reese, M. Rückamp, N. J. Schlegel, H. Seroussi, A. Shepherd, E. Simon, D. A. Slater, R. Smith, F. Straneo, S. Sun, L. Tarasov, L. Trusel, J. Van Breedam, R. S. W. van de Wal, M. R. van den Broeke, R. Winkelmann, C. Zhao, and T. Zhang. Future sea level change under cmip5 and cmip6 scenarios from the greenland and antarctic ice sheets. *Geophys. Res. Lett.*, 48(16):e2020GL091741, 2021. .

Carles Pelejero, Eva Calvo, and Ove Hoegh-Guldberg. Paleo-perspectives on ocean acidification. *Trends in Ecology and Evolution*, 25(6):332–344, 2010. ISSN 01695347. . URL http://dx.doi.org/10.1016/j.tree.2010.02.002.

David Pollard and R. M. Deconto. Hysteresis in Cenozoic Antarctic ice-sheet variations. *Global and Planetary Change*, 45(1-3 SPEC. ISS.):9–21, 2005. ISSN 09218181. .

Stefan Rahmstorf. A semi-empirical approach to projecting future sea-level rise. *Science (New York, N.Y.)*, 315:368–70, 02 2007. .

N. Raoult, S. Charbit, C. Dumas, F. Maignan, C. Ottlé, and V. Bastrikov. Improving modelled albedo over the greenland ice sheet through parameter optimisation and modis snow albedo retrievals. *The Cryosphere*, 17(7):2705–2724, 2023. . URL https://tc.copernicus.org/articles/17/2705/2023/.

D. J. Rasmussen, Klaus Bittermann, Maya K. Buchanan, Scott Kulp, Benjamin H. Strauss, Robert E. Kopp, and Michael Oppenheimer. Extreme sea level implications of 1.5°c, 2.0°c, and 2.5°c temperature stabilization targets in the 21st and 22nd centuries. *Environmental Research Letters*, 13(3), 2018. ISSN 17489326. .

Keywan Riahi, Shilpa Rao, Volker Krey, Cheolhung Cho, Vadim Chirkov, Guenther Fischer, Georg Kindermann, Nebojsa Nakicenovic, and Peter Rafaj. Rcp 8.5—a

scenario of comparatively high greenhouse gas emissions. *Climatic Change*, 109(1): 33, 2011. . URL https://doi.org/10.1007/s10584-011-0149-y.

Andy Ridgwell and Richard E. Zeebe. The role of the global carbonate cycle in the regulation and evolution of the Earth system. *Earth and Planetary Science Letters*, 234 (3-4):299–315, 2005. ISSN 0012821X. .

E. Rignot, J. Mouginot, M. Morlighem, H. Seroussi, and B. Scheuchl. Widespread, rapid grounding line retreat of Pine Island, Thwaites, Smith, and Kohler glaciers, West Antarctica, from 1992 to 2011. *Geophysical Research Letters*, 41(10):3502–3509, 2014. ISSN 19448007. .

Catherine Ritz, Tamsin L. Edwards, Gaël Durand, Antony J. Payne, Vincent Peyaud, and Richard C.A. Hindmarsh. Potential sea-level rise from Antarctic ice-sheet instability constrained by observations. *Nature*, 528(7580):115–118, 2015. ISSN 14764687. .

Alexander A. Robel, Hélène Seroussi, and Gerard H. Roe. Marine ice sheet instability amplifies and skews uncertainty in projections of future sea-level rise. *Proceedings of the National Academy of Sciences of the United States of America*, 116(30):14887–14892, 2019. ISSN 10916490. .

Joeri Rogelj, Michiel Schaeffer, Pierre Friedlingstein, Nathan P. Gillett, Detlef P. Van Vuuren, Keywan Riahi, Myles Allen, and Reto Knutti. Differences between carbon budget estimates unravelled. *Nature Climate Change*, 6(3):245–252, 2016. ISSN 17586798. . URL http://dx.doi.org/10.1038/nclimate2868.

Joeri Rogelj, Alexander Popp, Katherine V. Calvin, Gunnar Luderer, Johannes Emmerling, David Gernaat, Shinichiro Fujimori, Jessica Strefler, Tomoko Hasegawa, Giacomo Marangoni, Volker Krey, Elmar Kriegler, Keywan Riahi, Detlef P. Van Vuuren, Jonathan Doelman, Laurent Drouet, Jae Edmonds, Oliver Fricko, Mathijs Harmsen, Petr Havlík, Florian Humpenöder, Elke Stehfest, and Massimo Tavoni. Scenarios towards limiting global mean temperature increase below 1.5°c. *Nature Climate Change*, 8(4):325–332, 2018. ISSN 17586798. . URL http://dx.doi.org/10.1038/s41558-018-0091-3.

Joeri Rogelj, Piers M. Forster, Elmar Kriegler, Christopher J. Smith, and Roland Séférian. Estimating and tracking the remaining carbon budget for stringent climate targets. *Nature*, 571(7765):335–342, 2019. ISSN 14764687. .

Sebastian H.R. Rosier, Ronja Reese, Jonathan F. Donges, Jan De Rydt, G. Hilmar Gudmundsson, and Ricarda Winkelmann. The tipping points and early warning indicators for Pine Island Glacier, West Antarctica. *Cryosphere*, 15(3):1501–1516, 2021. ISSN 19940424. .

Jonathan C. Ryan, Alun Hubbard, Marek Stibal, Tristram D. Irvine-Fynn, Joseph Cook, Laurence C. Smith, Karen Cameron, and Jason Box. Dark zone of the greenland ice sheet controlled by distributed biologically-active impurities. *Nature Communications*, 9(1):1065, Mar 2018. ISSN 2041-1723. . URL https://doi.org/10.1038/s41467-018-03353-2.

Michiel Schaeffer, William Hare, Stefan Rahmstorf, and Martin Vermeer. Long-term sea-level rise implied by 1.5°C and 2 °C warming levels. *Nature Climate Change*, 2 (12):867–870, 2012. ISSN 1758678X. .

Carl Friedrich Schleussner, Tabea K. Lissner, Erich M. Fischer, Jan Wohland, Mahé Perrette, Antonius Golly, Joeri Rogelj, Katelin Childers, Jacob Schewe, Katja Frieler, Matthias Mengel, William Hare, and Michiel Schaeffer. Differential climate impacts for policy-relevant limits to global warming: The case of 1.5°c and 2°c. *Earth System Dynamics*, 7(2):327–351, 2016. ISSN 21904987. .

Carl Friedrich Schleussner, Peter Pfleiderer, and Erich M Fischer. Half a degree makes a difference in the observational record. *Nature Publishing Group*, 7(7):1–5, 2017. ISSN 1758-678X. . URL http://dx.doi.org/10.1038/nclimate3320.

Sonia I. Seneviratne, Markus G. Donat, Andy J. Pitman, Reto Knutti, and Robert L. Wilby. Allowable CO2 emissions based on regional and impact-related climate targets. *Nature*, 529(7587):477–483, 2016. ISSN 14764687. . URL http://dx.doi.org/10.1038/nature16542.

Sonia I. Seneviratne, Joeri Rogelj, Roland Séférian, Richard Wartenburger, Myles R. Allen, Michelle Cain, Richard J. Millar, Kristie L. Ebi, Neville Ellis, Ove Hoegh-Guldberg, Antony J. Payne, Carl Friedrich Schleussner, Petra Tschakert, and Rachel F. Warren. The many possible climates from the Paris Agreement's aim of 1.5°C warming. *Nature*, 558(7708):41–49, 2018. ISSN 14764687. . URL http://dx.doi.org/10.1038/s41586-018-0181-4.

Andrew Shepherd, Erik Ivins, Eric Rignot, Ben Smith, Michiel van den Broeke, Isabella Velicogna, Pippa Whitehouse, Kate Briggs, Ian Joughin, Gerhard Krinner, Sophie Nowicki, Tony Payne, Ted Scambos, Nicole Schlegel, Geruo A, Cécile Agosta, Andreas Ahlstrøm, Greg Babonis, Valentina R. Barletta, Anders A. Bjørk, Alejandro Blazquez, Jennifer Bonin, William Colgan, Beata Csatho, Richard Cullather, Marcus E. Engdahl, Denis Felikson, Xavier Fettweis, Rene Forsberg, Anna E. Hogg, Hubert Gallee, Alex Gardner, Lin Gilbert, Noel Gourmelen, Andreas Groh, Brian Gunter, Edward Hanna, Christopher Harig, Veit Helm, Alexander Horvath, Martin Horwath, Shfaqat Khan, Kristian K. Kjeldsen, Hannes Konrad, Peter L. Langen, Benoit Lecavalier, Bryant Loomis, Scott Luthcke, Malcolm McMillan, Daniele Melini, Sebastian Mernild, Yara Mohajerani, Philip Moore, Ruth Mottram, Jeremie Mouginot, Gorka Moyano, Alan Muir, Thomas Nagler, Grace

Nield, Johan Nilsson, Brice Noël, Ines Otosaka, Mark E. Pattle, W. Richard Peltier, Nadège Pie, Roelof Rietbroek, Helmut Rott, Louise Sandberg Sørensen, Ingo Sasgen, Himanshu Save, Bernd Scheuchl, Ernst Schrama, Ludwig Schröder, Ki-Weon Seo, Sebastian B. Simonsen, Thomas Slater, Giorgio Spada, Tyler Sutterley, Matthieu Talpe, Lev Tarasov, Willem Jan van de Berg, Wouter van der Wal, Melchior van Wessem, Bramha Dutt Vishwakarma, David Wiese, David Wilton, Thomas Wagner, Bert Wouters, Jan Wuite, and The IMBIE Team. Mass balance of the greenland ice sheet from 1992 to 2018. *Nature*, 579(7798):233–239, Mar 2020. ISSN 1476-4687. . URL https://doi.org/10.1038/s41586-019-1855-2.

S. C. Sherwood, M. J. Webb, J. D. Annan, K. C. Armour, P. M. Forster, J. C. Hargreaves, G. Hegerl, S. A. Klein, K. D. Marvel, E. J. Rohling, M. Watanabe, T. Andrews, P. Braconnot, C. S. Bretherton, G. L. Foster, Z. Hausfather, A. S. von der Heydt, R. Knutti, T. Mauritsen, J. R. Norris, C. Proistosescu, M. Rugenstein, G. A. Schmidt, K. B. Tokarska, and M. D. Zelinka. An Assessment of Earth's Climate Sensitivity Using Multiple Lines of Evidence. *Reviews of Geophysics*, 58(4):1–93, 2020. ISSN 19449208. .

Doug M. Smith, Richard P. Allan, Andrew C. Coward, Rosie Eade, Patrick Hyder, Chunlei Liu, Norman G. Loeb, Matthew D. Palmer, Chris D. Roberts, and Adam A. Scaife. Earth's energy imbalance since 1960 in observations and cmip5 models. *Geophysical Research Letters*, 42(4):1205–1213, 2015. . URL https://agupubs.onlinelibrary.wiley.com/doi/abs/10.1002/2014GL062669.

Thomas M. Smith, Richard W. Reynolds, Thomas C. Peterson, and Jay Lawrimore. Improvements to noaa's historical merged land–ocean surface temperature analysis (1880–2006). *Journal of Climate*, 21(10):2283 – 2296, 2008. . URL https://journals.ametsoc.org/view/journals/clim/21/10/2007jcli2100.1.xml.

Susan Solomon, Gian-Kasper Plattner, Reto Knutti, and Pierre Friedlingstein. Irreversible climate change due to carbon dioxide emissions. *Proceedings of the National Academy of Sciences*, 106(6):1704–1709, 2009. . URL https://www.pnas.org/doi/abs/10.1073/pnas.0812721106.

D. Stammer, R S W Van De Wal, R J Nicholls, and J A Church. Framework for High - End Estimates of Sea Level Rise for Stakeholder Applications. *Earth ' s Future*, pages 923–938, 2019. .

M. Steinacher and F. Joos. Transient Earth system responses to cumulative carbon dioxide emissions: Linearities, uncertainties, and probabilities in an observation-constrained model ensemble. *Biogeosciences*, 13(4):1071–1103, 2016. ISSN 17264189. .

M. Steinacher, F. Joos, T. L. Frölicher, G.-K. Plattner, and S. C. Doney. Imminent ocean acidification in the arctic projected with the ncar global coupled carbon

cycle-climate model. *Biogeosciences*, 6(4):515–533, 2009. . URL https://bg.copernicus.org/articles/6/515/2009/.

M. Steinacher, Fortunat Joos, and Thomas F. Stocker. Allowable carbon emissions lowered by multiple climate targets. *Nature*, 499(7457):197–201, 2013. ISSN 00280836. .

Stephanie C. Talmage and Christopher J. Gobler. Effects of elevated temperature and carbon dioxide on the growth and survival of larvae and juveniles of three species of northwest Atlantic bivalves. *PLoS ONE*, 6(10), 2011. ISSN 19326203. .

Claudia Tebaldi, Roshanka Ranasinghe, Michalis Vousdoukas, D. J. Rasmussen, Ben Vega-Westhoff, Ebru Kirezci, Robert E. Kopp, Ryan Sriver, and Lorenzo Mentaschi. Extreme sea levels at different global warming levels. *Nature Climate Change*, 11(9): 746–751, 2021. ISSN 17586798. .

Jens Terhaar, Lester Kwiatkowski, and Laurent Bopp. Emergent constraint on Arctic Ocean acidification in the twenty-first century. *Nature 2020 582:7812*, 582(7812): 379–383, 2020. ISSN 1476-4687. . URL http://www.nature.com/articles/s41586-020-2360-3.

Jens Terhaar, Thomas L. Frölicher, Mathias T. Aschwanden, Pierre Friedlingstein, and Fortunat Joos. Adaptive emission reduction approach to reach any global warming target. *Nature Climate Change*, 12(12):1136–1142, 2022. ISSN 17586798. .

Michelle Tigchelaar, Axel Timmermann, Tobias Friedrich, Malte Heinemann, and David Pollard. Nonlinear response of the Antarctic Ice Sheet to late Quaternary sea level and climate forcing. *Cryosphere*, 13(10):2615–2631, 2019. ISSN 19940424. .

Katarzyna B. Tokarska, Kirsten Zickfeld, and Joeri Rogelj. Path Independence of Carbon Budgets When Meeting a Stringent Global Mean Temperature Target After an Overshoot. *Earth's Future*, 7(12):1283–1295, 2019. ISSN 23284277. .

Katarzyna B. Tokarska, Martin B. Stolpe, Sebastian Sippel, Erich M. Fischer, Christopher J. Smith, Flavio Lehner, and Reto Knutti. Past warming trend constrains future warming in CMIP6 models. *Science Advances*, 6(12):1–14, 2020. ISSN 23752548. .

S. Treu, S. Muis, S. Dangendorf, T. Wahl, J. Oelsmann, S. Heinicke, K. Frieler, and M. Mengel. Reconstruction of hourly coastal water levels and counterfactuals without sea level rise for impact attribution. *Earth System Science Data Discussions*, 2023:1–23, 2023. . URL https://essd.copernicus.org/preprints/essd-2023-112/.

United Nations. Nationally determined contributions under the Paris Agreement. Synthesis report by the Secretariat. United Nations Framework Convention on

Climate Change. Technical Report October, 2022. URL https://unfccc.int/documents/619180.

P. Vaittinada Ayar, L. Bopp, J. R. Christian, T. Ilyina, J. P. Krasting, R. Séférian, H. Tsujino, M. Watanabe, A. Yool, and J. Tjiputra. Contrasting projections of the enso-driven co_2 flux variability in the equatorial pacific under high-warming scenario. *Earth System Dynamics*, 13(3):1097–1118, 2022. . URL https://esd.copernicus.org/articles/13/1097/2022/.

R. S.W. van de Wal, R. J. Nicholls, D. Behar, K. McInnes, D. Stammer, J. A. Lowe, J. A. Church, R. DeConto, X. Fettweis, H. Goelzer, M. Haasnoot, I. D. Haigh, J. Hinkel, B. P. Horton, T. S. James, A. Jenkins, G. LeCozannet, A. Levermann, W. H. Lipscomb, B. Marzeion, F. Pattyn, A. J. Payne, W. T. Pfeffer, S. F. Price, H. Seroussi, S. Sun, W. Veatch, and K. White. A High-End Estimate of Sea Level Rise for Practitioners. *Earth's Future*, 10(11):1–24, 2022. ISSN 23284277. .

Russell S. Vose, Derek Arndt, Viva F. Banzon, David R. Easterling, Byron Gleason, Boyin Huang, Ed Kearns, Jay H. Lawrimore, Matthew J. Menne, Thomas C. Peterson, Richard W. Reynolds, Thomas M. Smith, Claude N. Williams, and David B. Wuertz. Noaa's merged land–ocean surface temperature analysis. *Bulletin of the American Meteorological Society*, 93(11):1677 – 1685, 2012. . URL https://journals.ametsoc.org/view/journals/bams/93/11/bams-d-11-00241.1.xml.

Hylke De Vries, Caroline Katsman, and Sybren Drijfhout. Constructing scenarios of regional sea level change using global temperature pathways. *Environmental Research Letters*, 9(11), 2014. ISSN 17489326. .

Paul S. Wilcox, Charlotte Honiat, Martin Trüssel, R. Lawrence Edwards, and Christoph Spötl. Exceptional warmth and climate instability occurred in the European Alps during the Last Interglacial period. *Communications Earth and Environment*, 1(1), 2020. ISSN 2662-4435. . URL http://dx.doi.org/10.1038/s43247-020-00063-w.

Phillip Williamson and Carol Turley. Ocean acidification in a geoengineering context. *Philosophical Transactions of the Royal Society A: Mathematical, Physical and Engineering Sciences*, 370(1974):4317–4342, 2012. ISSN 1364503X. .

Y. Yara, M. Vogt, M. Fujii, H. Yamano, C. Hauri, M. Steinacher, N. Gruber, and Y. Yamanaka. Ocean acidification limits temperature-induced poleward expansion of coral habitats around Japan. *Biogeosciences*, 9(12):4955–4968, 2012. ISSN 17264170. .

Richard E. Zeebe and Dieter Wolf-Gladrow. Chapter 3 stable isotope fractionation. In *CO2 in seawater: Equilibrium, kinetics, isotopes*, volume 65 of *Elsevier Oceanography Series*, pages 141–250. Elsevier, 2001. . URL https://www.sciencedirect.com/science/article/pii/S0422989401800040.

Zhihua Zhang, John C. Moore, Donald Huisingh, and Yongxin Zhao. Review of geoengineering approaches to mitigating climate change. *Journal of Cleaner Production*, 103:898–907, sep 2015. ISSN 0959-6526. .

Kirsten Zickfeld, Michael Eby, H. Damon Matthews, and Andrew J. Weaver. Setting cumulative emissions targets to reduce the risk of dangerous climate change. *Proceedings of the National Academy of Sciences of the United States of America*, 106(38): 16129–16134, 2009. ISSN 00278424. .

Kirsten Zickfeld, Michael Eby, Andrew J. Weaver, Kaitlin Alexander, Elisabeth Crespin, Neil R. Edwards, Alexey V. Eliseev, Georg Feulner, Thierry Fichefet, Chris E. Forest, Pierre Friedlingstein, Hugues Goosse, Philip B. Holden, Fortunat Joos, Michio Kawamiya, David Kicklighter, Hendrik Kienert, Katsumi Matsumoto, Igor I. Mokhov, Erwan Monier, Steffen M. Olsen, Jens O. P. Pedersen, Mahe Perrette, Gwenaëlle Philippon-Berthier, Andy Ridgwell, Adam Schlosser, Thomas Schneider Von Deimling, Gary Shaffer, Andrei Sokolov, Renato Spahni, Marco Steinacher, Kaoru Tachiiri, Kathy S. Tokos, Masakazu Yoshimori, Ning Zeng, and Fang Zhao. Long-term climate change commitment and reversibility: An emic intercomparison. *Journal of Climate*, 26(16):5782 – 5809, 2013. . URL https://journals.ametsoc.org/view/journals/clim/26/16/jcli-d-12-00584.1.xml.

Kirsten Zickfeld, Andrew H. MacDougall, and H. Damon Matthews. On the proportionality between global temperature change and cumulative CO2 emissions during periods of net negative CO2 emissions. *Environmental Research Letters*, 11(5), 2016. ISSN 17489326. .